

INFLUENCE OF CERTAIN REACTION PARAMETERS  
ON METHANATION OF COAL GAS TO SNG

K.-H. Eisenlohr<sup>+</sup> F. W. Moeller<sup>+</sup> and M. Dry<sup>++</sup>

<sup>+</sup> Lurgi Mineraloeltechnik GmbH., Frankfurt/M., Germany

<sup>++</sup> South African Coal, Oil and Gas Corporation, Sasolburg, South Africa

INTRODUCTION

Converting coal to a gas which has the same characteristics as natural pipeline quality gas and which is known as substitute natural gas (SNG) is one of the promising possibilities to overcome the increasing energy demand in the United States.

Lurgi pressure gasification of coal and treating and purifying processes for the product gas used in 14 commercial plants are planned to be the basis of a process route to convert coal into SNG 1) 2) 3).

Four different process steps are required in the Lurgi process (Fig. 1):

Pressure gasification of coal  
Shift conversion of crude gas  
Gas purification by Rectisol  
Methane synthesis.

As the methane synthesis process has not yet been applied commercially, it has been of significant importance to demonstrate the technical feasibility of this process step. Therefore two semicommercial pilot plants have been operated for 1 1/2 years.

One plant, designed and erected by Lurgi and South African Coal, Oil and Gas Corporation (SASOL), Sasolburg, South Africa, was operated as a sidestream plant to a commercial Fischer-Tropsch Synthesis. Synthesis gas is produced in a commercial coal pressure gasification plant which includes Rectisol gas purification and shift conversion. So the overall process scheme for production of SNG from coal could be demonstrated successfully.

The other plant, a joint effort of Lurgi and El Paso Natural Gas Corporation, was operated at the same time at Petrochemie, Schwechat, near Vienna, Austria. Starting from synthesis gas produced from naphtha different reaction conditions to those of the SASOL plant have been successfully operated.

The results of two long-term test runs in the SASOL plant in view of the catalyst life under design conditions in a commercial methane synthesis have been published already 3). This paper deals with further test results of both demonstration units concerning the influence of certain reaction parameters which are the basis for flexibility and operability of the Lurgi methanation scheme.

## DESIGN OF THE DEMONSTRATION PLANTS

The scheme of a commercial methane synthesis provides a multistage reaction system and hot recycle of product gas. Adiabatic reactors connected with waste heat boilers to remove the heat in form of high pressure steam are used.

In designing the pilot plants major emphasis was placed on the design of the catalytic reactor system. Thermodynamic parameters (composition of feed gas, temperature, temperature rise, pressure, etc.) as well as hydrodynamic parameters (bed depth, linear velocity, catalyst pellet size etc.) are identical to those of a commercial methanation plant. This permits direct upscaling of test results to commercial size reactors, because radial gradients do not exist in an adiabatic shaft reactor.

Arrangement of the semicommercial pilot plants permitted supervision and operation of the plant from a central control panel. The installed safety control system has been successfully tested during several emergency shut-downs with no effect on reactor material and catalyst.

The scheme of the methanation demonstration units can be seen in Fig. 2. Synthesis gas, after being heated in heater E-1, is mixed with recycle gas. Zinc oxide reactor D-1 serves as an emergency catch pot for sulfur breakthrough from the purification plant. The total feed is heated in heater E-2 and charged to main methanation reactor D-2 with additional steam. Effluent gas from reactor D-2 is cooled in heat exchanger E-3 and cooler E-4, thereby condensing the steam. Part of the reactor effluent gas is recycled, while the rest is reheated in E-3 and fed to final or polishing methanation reactor D-3. Product gas from D-3 is cooled in E-5.

All tests reported here are performed with a special methanation catalyst G 1-85 developed by BASF, Ludwigshafen, for this process. The catalyst with a relatively high nickel content on a carrier was changed to reactors D-2 and D-3 in unreduced form and had to be activated by reduction with hydrogen.

## INFLUENCE OF SYNTHESIS GAS COMPOSITION

The influence of synthesis gas composition on conversion, catalyst life, carbon black formation, etc. has been determined in numerous tests. Characteristic parameters for synthesis gas composition are  $H_2/CO$  ratio, residual  $CO_2$  content and content of trace components in form of higher hydrocarbons and catalyst poisons.

### $H_2/CO$ Ratio

In a commercial shift conversion plant a change in throughput and conversion has to be taken into account and will affect the  $H_2/CO$  ratio of the synthesis gas. Therefore the Sasol plant has been operated in three different test runs of more than 1000 hours each with various  $H_2/CO$  ratios in synthesis gas to see if there is any effect on operability of methane synthesis.  $H_2/CO$  ratios of 5.8; 3.7 and 2.0 were adjusted by varying the mixing ratio of shifted and unshifted coal gas. The test results obtained at a synthesis pressure of 18 kp/cm<sup>2</sup> are summarized in Tab. 1. The expected equilibrium conversion was achieved in all test runs. A remarkable result has been that there is no difference in the axial temperature profile while operating with synthesis gas with a  $H_2/CO$  ratio of 3.7 or 5.8. Adiabatic

endtemperature was reached in both cases in 20% of the catalyst bed depth after 500 operating hours respectively 22% bed depth after 1000 operating hours. Corresponding results have been achieved during a long-term test of 4000 operating hours when the  $H_2/CO$  ratio was decreased from 5.8 to 3.8 after 1500 hours and no change in temperature profile and deactivation rate was measurable. 3)

A deviation from these results was measured while operating with a  $H_2/CO$  ratio of 2.0. After 500 hours 23% of the catalyst bed depth are needed to reach adiabatic end temperature. The slower reaction rate might be explained by the higher steam content in reactor feed gas and by the fact that part of the CO has to be converted by the relatively slow shift conversion reaction. The negative value of  $CO_2$  conversion shows that  $CO_2$  is formed and not consumed.

In all three tests there was no sign of carbon black formation. Pressure drop over the reactor stays constant during the whole operating period and there was no accumulation of free carbon on catalyst. Analysis of discharged catalyst for free carbon showed only 80 - 90% of the carbon added to the catalyst as pelletizing aid.

Finally it can be said that variation in  $H_2/CO$  ratio will not affect operability of an SNG plant using a hot recycle system for methanation as demonstrated in the Sasol plant.

#### Residual $CO_2$ Content

The feed gas to Rectisol gas purification will contain 29 - 36 Vol% of  $CO_2$  depending on the rate of shift conversion. The rate of  $CO_2$  to be washed out will be determined by the requirements of methane syntheses and by the need to minimize the cost for Rectisol purification.

For SNG manufacture it is necessary to reduce the hydrogen to a minimum to achieve a high calorific value. This is best realized if synthesis gas, instead of having a stoichiometric composition, contains a surplus of  $CO_2$  which can be utilized to reduce the  $H_2$  content to less than 1 percent according to equilibrium conditions by the  $CO_2$  methanation reaction. The surplus  $CO_2$  has to be removed at the end of the process sequence. It is, of course, also possible to operate a methanation plant with synthesis gas of stoichiometric composition. In this case there is no need for a final  $CO_2$  removal system. The residual  $H_2$  content will be higher and therefore the heating value will be lower, which can be seen by comparing the results of two long-term runs in Tab. 2.

The Sasol plant was operated with a surplus of  $CO_2$  during a long-term test of 4000 hours. 33.4% of the  $CO_2$  in synthesis gas is methanated, while the rest of 66.6%  $CO_2$  leaves the reaction system unconverted. Product gas from final methanation yielded specification grade SNG containing a residual hydrogen of 0.7 Vol% and residual CO of less than 0.1 Vol%. The heating value was 973 BTU/SCF after  $CO_2$  removal to 0.5 Vol% (calc.).

The Schwechat plant was operated in a long-term test of 5000 hours at the same time with a stoichiometric synthesis gas. The residual hydrogen content could be decreased to 2.2 Vol% resulting in a heating value of 950 BTU/SCF when about 1 Vol% nitrogen is present in synthesis gas.

There was no difference in operability and catalyst behaviour (activity and deactivation) recognizable between the two plants. The expected catalyst life time in a commercial plant, calculated from the movement of the temperature profile down the catalyst bed with time, will be in both cases more than 16000 hours at design conditions.

A significant feature of the operation of the two plants was that only a small deviation in feed gas composition is tolerable when using a stoichiometric synthesis gas. Greater deviations in  $H_2/CO$  ratio and residual  $CO_2$  content of the feed gas will cause serious problems regarding SNG specification. The conclusion is only reasonable when there are no high requirements for SNG specification.

#### Higher-Hydrocarbon Content

Coal pressure gasification gas, after purification in a Rectisol unit, will contain higher hydrocarbons in the  $C_2-C_3$  range of 0.2 to 0.6 Vol%. The results of an analytical examination during all test runs showed that the used nickel catalyst has a good gasification or hydrogenation activity. Unsaturated hydrocarbons such as ethylene and propylene are hydrogenated completely while the saturated hydrocarbons such as ethane and propane are converted to methane up to equilibrium concentrations of 50 ppm ethane and 5 ppm propane.

#### Catalyst Poisons

It is well known that sulfur, chlorine etc. are strong poisons for nickel catalyst. Chlorine was not detectable in synthesis gas downstream Rectisol in the Sasol plant. The total sulfur content in the same gas, in form of  $H_2S$ , COS and organic sulfur compounds, has been  $0.08 \text{ mg/Nm}^3$  on the average with maximum values of  $0.12 \text{ mg/Nm}^3$  total sulfur at average  $H_2S$  content of  $0.03 \text{ mg/Nm}^3$ .

The effect of sulfur contamination on catalyst activity was examined in an extra test run in the Sasol plant. The results can be seen from Fig. 3, where conversion in 6.3% and 23.8% of the total catalyst bed as an indirect criterion of catalyst activity is plotted versus operating time.

In the first operating period (750 - 950 h) the plant was run with the ZnO emergency catchpot on line. Sulfur could be decreased to  $0.04 \text{ mg/Nm}^3$  total sulfur and  $0.02 \text{ mg/Nm}^3 H_2S$ . The conversion in the first 6.3% of the catalyst bed decreased from 50% to 46% while no change in conversion was detectable in the first 23.8% of the bed.

No change in deactivation was measured when in the second operating period (950 - 1230 h) ZnO reactor D-1 was by-passed. The conversion in the first 6.3% of the catalyst bed came down from 46% to 42%.

In the third operating period (1230 - 1380 h) a breakthrough of  $4 \text{ mg/Nm}^3 H_2S$  in synthesis gas was simulated, causing an enormous activity loss. The point of reaching adiabatic end temperature in the catalyst bed went down from 22% to 44% bed depth, while the conversion in the first 23.8% of the bed came down from 100% to 78%. Operating 150 hours with  $4 \text{ mg/Nm}^3 H_2S$  corresponds to one year operation with  $0.08 \text{ mg/Nm}^3$  total sulfur in the feed gas to methanation.

These tests permit the simplified conclusion that synthesis gas purified in a Rectisol unit can be charged directly to the methanation plant without severe problems concerning sulfur poisoning of the nickel catalyst. But to cope with a sudden sulfur breakthrough from Rectisol as a result of maloperation a commercial methanation plant should be operated with a ZnO emergency catchpot on line.

### INFLUENCE OF TEMPERATURE AND PRESSURE

The selection of optimal reactor inlet and outlet temperature is influenced by the catalyst activity and catalyst stability and by the need to minimize operating and investment costs.

Using a catalyst like G 1-85 of BASF inlet temperatures in the range of 260°C to 300°C or even lower will be quite acceptable as indicated by the test reported in Tab. 2. The final decision on design inlet temperature is effected by engineering requirements.

The long-term tests in the Sasol plant as well as in the Schwechat plant have been operated with outlet temperatures of 450°C. But both plants also have been operated with higher load causing reactor outlet temperatures of 470°C or even higher. In comparison with the test run at 450°C there was no increase in deactivation rate detectable, which demonstrates the thermostability of the catalyst. From the viewpoint of thermostability outlet temperatures in the range of 450°C - 500°C are acceptable. Further consideration concerning possibility of overload operation, SNG specification to be achieved in final methanation, end of run conditions, cost of reactor material, etc. will affect the selection of optimal outlet temperature.

The influence of total pressure is limited. For reasons of SNG specification a relatively high pressure is preferred but compression of synthesis gas compared with final SNG compression turned out to be uneconomical. The pressure in methanation is governed by the pressure of gasification and the pressure drop across upstream plants.

### INFLUENCE OF STEAM

Apart from actual synthesis tests extensive investigations were made on fresh and used catalyst to determine the effect of steam on catalyst activity and catalyst stability by measurement of surface areas. While the BET area is a measure of the total surface area, the volume of chemisorbed hydrogen is a measure of the amount of exposed metallic nickel area only and therefore should be a truer measure of the catalytically active area.

The test results of H<sub>2</sub> chemisorption measurement are summarized in Tab. 3. For the fresh reduced G 1-85 an activity equivalent to 11.2 ml/gr was determined. When this reduced catalyst is treated with a mixture of hydrogen and steam, it loses 27% of its activity. This activity loss is definitely caused by steam as a catalyst treated 4000 hours in final methanation with a nearly dry gas showed no activity loss. In the first 1000 operating hours the catalyst loses again 33% of its activity in the top section and 16% in the bottom section of the reactor. This should be called loss of start activity. In the next 3000 operating hours the activity loss has been extremely low. Catalyst has achieved its stabilized standard activity.

The activity loss measured here is caused by recrystallisations as proved by nickel crystallite size determination on the same catalyst samples by scanning electron microscopy.

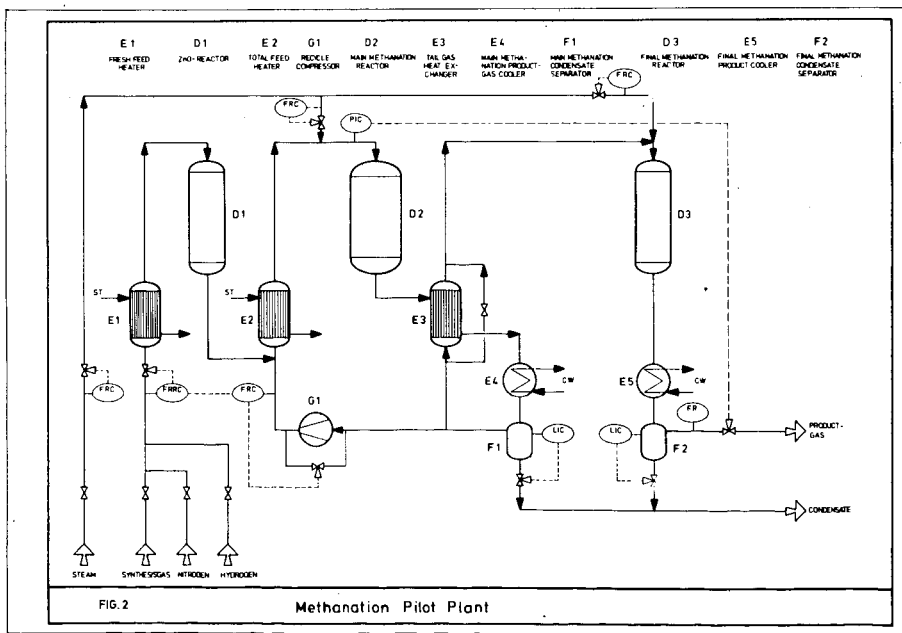
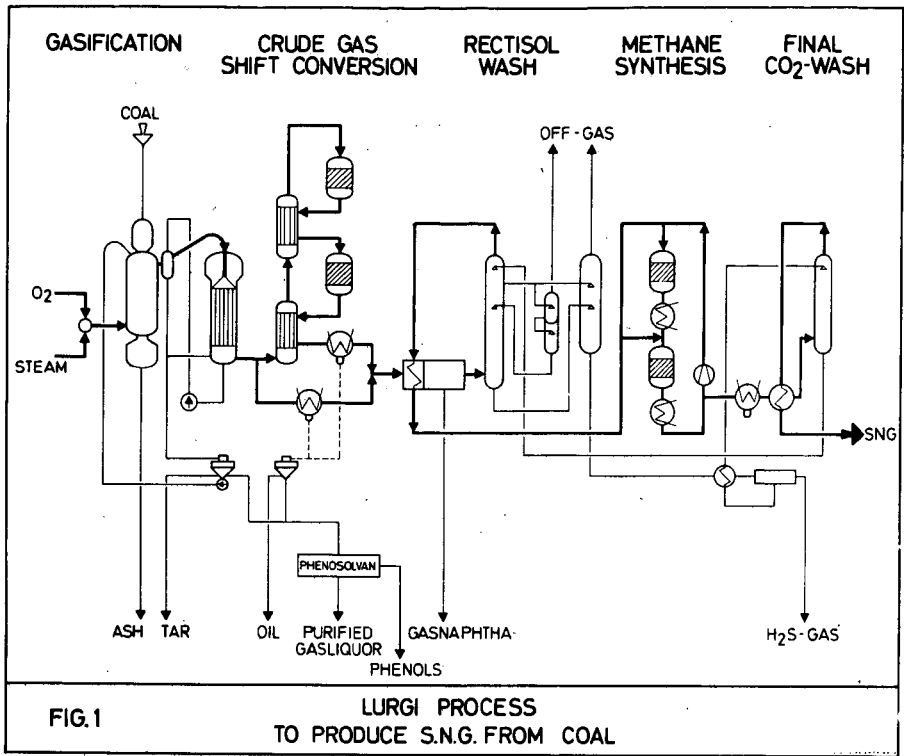
These tests have shown that the catalyst used in demonstration plants has only little tendency to recrystallise or sinter after steam formation and loss of start activity.

### CONCLUSION

These tests have been performed to establish the limits in flexibility and operability of a methanation scheme. The two demonstration plants have been operated to find optimal design parameters as well as the possible variation range which can be handled without affecting catalyst life and SNG specification. Using a hot recycle methanation system the requirement for synthesis gas concerning  $H_2/CO$  ratio,  $CO_2$  content, higher hydrocarbon content are not fixed to a small range, only the content of poisons should be kept to a minimum. The catalyst has proved its chemostability and resistance against high steam contents, resulting into an expected life of more than 16 000 hours.

### Literature:

- (1) Rudolph, P. F. "The Lurgi Route to Substitute Natural Gas from Coal", 4th Synthetic Pipeline Gas Symposium, Chicago, Oct. 1972
- (2) Roger, A. "Supplementing the Natural Gas Supply " Presented to South Texas Section Meeting, American Society of Mechanical Engineers, Houston, April 1973
- (3) Moeller, F.W.,  
Roberts, H. and  
Britz, B. "Methanation of Coal Gas for SNG"  
Hydrocarbon Processing, 53, 4, 69, 1974
- (4) Wallas, S. M. "Reaction Kinetics for Chemical Engineers"  
McGraw Hill NYC, 1959 p. 153



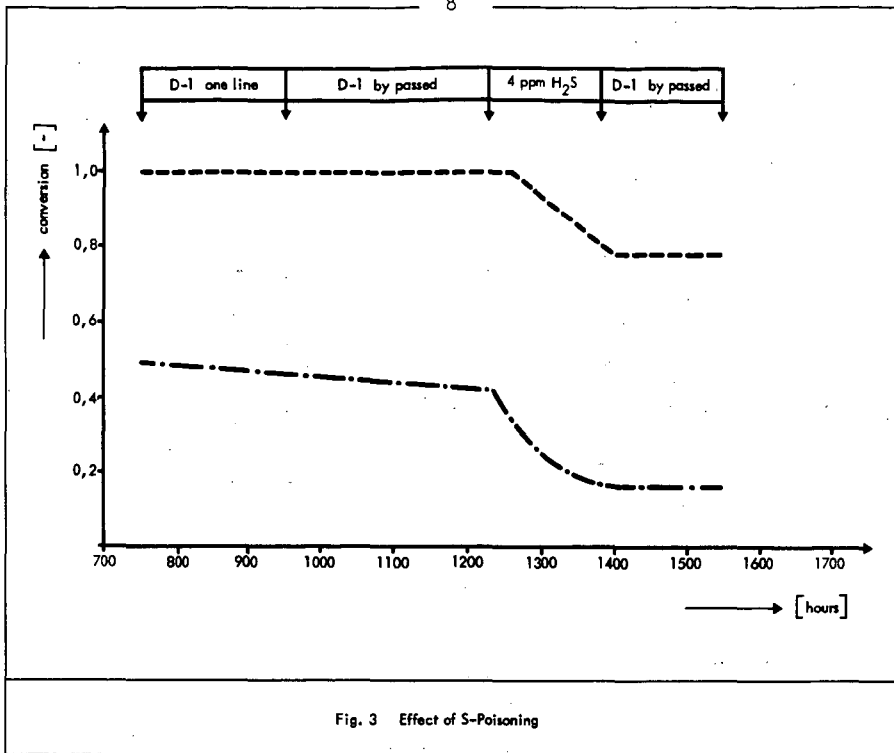


Table 1

	$H_2/CO = 5.8$			$H_2/CO = 3.7$			$H_2/CO = 2.0$		
	Syngas	Feed to D-2	Effluent gas D-2	Syngas	Feed to D-2	Effluent gas D-2	Syngas	Feed to D-2	Effluent gas D-2
Pressure ( $kg/cm^2$ )		18.0			18.0			18.0	
Temperature ( $^{\circ}C$ )	270	300	450	270	300	450	270	300	450
Gas composition									
$CO_2$ Vol%	16.6	20.5	22.1	9.4	15.4	17.2	0.8	14.6	19.0
$CO$ "	10.7	3.4	0.4	16.6	4.1	0.4	28.6	7.2	0.4
$H_2$ "	62.0	23.9	8.7	62.0	20.6	8.4	56.6	22.7	12.0
$CH_4$ "	9.8	50.7	67.0	10.8	57.7	71.6	12.3	52.8	65.5
$C_2+$ "	0.2	0.1	<0.1	0.2	0.1	<0.1	0.2	0.1	<0.1
$N_2$ "	0.7	1.4	1.7	1.0	2.1	2.4	1.5	2.6	3.0
$H_2O$ $Nm^3/Nm^3$	-	0.417	0.584	-	0.387	0.501	-	0.722	0.852
Total conversion									
$U_{CO_2}$ %		48.3			23.7			-1076.3	
$U_{CO}$ %		98.4			99.0			99.3	
$U_{H_2}$ %		94.1			94.3			89.5	
Bed depth needed for total conversion %									
500 hrs		20			20			23	
1000 hrs		22			22			25	

Table 2

	Sasol plant					Schwechat plant					
	Main methanation			Final methanation		Main methanation			Final methanation		
	Syngas	Feed D 2	Effluent gas D 2	Feed D 3	Effluent gas D 3	Syngas	Feed D 2	Effluent gas D 2	Feed D 3	Effluent gas D 3	
Pressure (kp/cm <sup>2</sup> )	-	18.0	-	-	-	-	16.3	-	-	-	
Temperature (°C)	270	300	450	260	315	-	290	440	283	345	
Gascomposition											
CO <sub>2</sub>	Vol%	13.0	19.3	21.5	21.5	21.3	5.1	4.4	4.1	4.1	1.8
CO	Vol%	15.5	4.3	0.4	0.4	<0.1	14.4	4.0	0.1	0.1	<0.1
H <sub>2</sub>	Vol%	60.1	41.3	7.7	7.7	0.7	61.6	25.7	12.1	12.1	2.2
CH <sub>4</sub>	Vol%	10.3	53.3	68.4	68.4	75.9	18.9	65.9	83.7	83.7	96.0
C <sub>2</sub> <sup>+</sup>	Vol%	0.2	0.1	<0.1	<0.1	<0.1	-	-	-	-	-
N <sub>2</sub>	Vol%	0.9	1.7	2.0	2.0	2.0	-	-	-	-	-
H <sub>2</sub> O	(Nm <sup>3</sup> /Nm <sup>3</sup> )	-	0.37	0.50	0.04	0.08	-	0.349	0.481	0.061	0.123
Total Conversion											
U <sub>CO<sub>2</sub></sub>	(%)			33.4						86.1	
U <sub>CO</sub>	(%)			99.9						99.9	
U <sub>H<sub>2</sub></sub>	(%)			99.5						98.6	

Table 3:

	H <sub>2</sub> -Adsorption (ml/gr)
Fresh reduced catalyst G 1-85	11.2
H <sub>2</sub> /H <sub>2</sub> O-Treatment	8.0
Used catalyst out of main methanation	
1000 hrs	4.4 (top bed) 6.4 (bottom bed)
4000 hrs	4.0 (top bed) 6.2 (bottom bed)
Used catalyst out of final methanation	
4000 hrs	11.0 (middle bed)

## SYNTHESIS OF METHANE IN HOT GAS RECYCLE REACTOR--PILOT PLANT TESTS

W. P. Haynes, A. J. Forney, J. J. Elliott, and H. W. Pennline

U.S. Bureau of Mines, 4800 Forbes Avenue, Pittsburgh, Pa.

## INTRODUCTION

Development of large-scale catalytic methanation reactors is necessary to complete the commercialization of plants for converting coal to substitute natural gas. Major objectives in developing a catalytic methanation system are to achieve efficient removal of the heat of reaction so as to minimize thermal deactivation of catalyst and to minimize catalyst deactivation by other causes such as chemical poisoning and structural changes. The hot gas recycle reactor, where large quantities of partially cooled product gas are circulated thru the catalyst bed, affords one satisfactory method of removing large amounts of heat from the catalyst surface. Early Bureau of Mines experiments with the hot gas recycle reactor, however, had short catalyst lives, on the order of 200 hours. (1) <sup>1/</sup> The work described in this report attempts to extend the life of the catalyst in the hot gas recycle reactor system, to determine the effects of some of the process variables, and to compare the performance of a bed of pelleted nickel catalyst against that of a bed of parallel plates coated with Raney nickel.

## PILOT PLANT DESCRIPTION

The reactor in the hot gas recycle pilot plant was constructed of type 304 stainless steel 3 inch schedule 40 pipe, 10 feet long, flanged at each end. In three experiments (HGR-10, 12, and 14), the catalyst bed consisted of grid assemblies of parallel, type 304 stainless steel plates, that had been flame spray coated with Raney nickel. The grid assemblies, each 6 inches long, were stacked to the desired bed height and conformed to the inside diameter of the reactor. Grid plates were aligned perpendicular to the plate alignment of adjacent grids. Prior to assembly, each plate was sand-blasted on both sides, flame sprayed with a bond coat, and finally flame sprayed with the Raney nickel catalyst. Thickness of the Raney nickel coating was approximately 0.02 inches. In experiment HGR-13, the reactor was charged with 1/4" pellets of a commercial grade precipitated nickel catalyst instead of the parallel plates coated with Raney nickel. Physical properties of the catalyst beds are shown in table 1.

The basic hot gas recycle reactor scheme is shown in the simplified flowsheet of figure 1. The main reactor containing the parallel plate grid assemblies is the one under study in this report. The second stage reactor, an adiabatic reactor charged with a precipitated nickel catalyst, was operated at intermittent periods; its operation will be discussed in a later report. Additional heat exchangers, not shown in the flowsheet, were used in the pilot plant to compensate for system heat losses, to achieve a measure of heat recuperation, and to control the gas temperature into the hot gas compressor and into the main reactor. Cooling of the main catalyst bed is achieved by direct transfer of the reaction heat to the slightly cooler gas stream flowing through the bed. Recycle stream is appropriately cooled before returning to the reactor. The hot recycle stream may be cooled either directly without condensation or by cooling a portion of the recycled product gas sufficiently to condense out the water vapor and then returning the resulting cold recycle gas along with the hot recycle gas. After undergoing a final heat exchange, the mixture of the cooled recycle gas and the fresh feed gas comprise a feed to the hot gas recycle

---

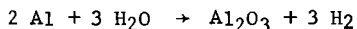
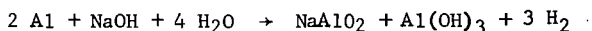
<sup>1/</sup> Underlined numbers in parenthesis refer to references at the end of this paper.

reactor at a controlled temperature that may be 50 to 150° C lower than the reactor outlet temperature, depending upon the total amount of gas recycled and the amount of heat exchange.

Charcoal absorption towers (not shown in the flowsheet) were used to keep the sulfur content in the fresh feed gas to less than 0.1 ppm. in equivalent volume of H<sub>2</sub>S.

#### CATALYST PREPARATION

The metal plates to be coated with Raney nickel were type 304 stainless steel. The surfaces of the plates were prepared by sand-blasting with an iron-free grit and then flame spraying on a light coat of bonding material, about 0.006 inches thick. After the surface was bond coated, the Raney nickel alloy powder (80-100 mesh) was flame sprayed on to the desired thickness. The plates were assembled in parallel, inserted in the reactor, and then activated. Activation of the Raney nickel involved passing a 2 wt. per cent solution of NaOH through the catalyst bed to dissolve away the aluminum phase and leave a spongy surface of highly active free nickel. Activation was stopped after 70 per cent of the aluminum in the Raney alloy was reacted. The remaining unreacted alloy is believed to provide a base upon which the activated nickel remains anchored. The extent of reaction was determined by measuring the hydrogen evolved according to the following three reactions, all of which evolve 3 moles of H<sub>2</sub> for every 2 moles of Al reacted:



After the aluminum was reacted, the catalyst was washed with water which had a pH of about 6.8 until the pH of the effluent water reached about 7.2. After the catalyst was activated and washed, it was always kept under a hydrogen atmosphere until it was put into methanation service at the desired operating pressure and temperature. Before cooling the catalyst to take it out of service, the reactor was purged with hydrogen. It was kept in a hydrogen atmosphere during cooling, depressurizing, and stand-by condition.

In experiment HGR-13, the commercial grade precipitated nickel catalyst was in a reduced and stabilized condition when it was charged into the reactor. No special activation treatment was needed. It was, however, kept under a hydrogen atmosphere at all times until the temperature and pressure of the system was brought to synthesis conditions at which time the synthesis feed gas was gradually fed into the system to start the run.

#### PROCEDURES AND RESULTS

##### General

Experiments HGR-10, 12 and 14 were conducted with the flame sprayed Raney nickel catalyst. Experiment HGR-13 used the pelleted precipitated catalyst to compare its performance with that of catalyst used in HGR-14. Reactor conditions as a function of stream time for experiments HGR-10, 12, 13, and 14 are graphically presented by computer print-out in figures 2, 4, 6, and 8, respectively. Corresponding carbon monoxide concentrations and heating values of the product gases and the yields of methane produced per pound of catalyst used are presented graphically as a function

of stream time in figures 3, 5, 7, and 9. The total recycle ratio was calculated on the basis of stream analyses, and fluctuated widely because of the high sensitivity of the calculated values to small changes in stream analyses. All runs were made at 300 psig.

The major process parameters are presented in tables 2, 3, 4, and 5 at selected periods in experiments HGR-10, 12, 13, and 14, respectively. Carbon recoveries shown for these periods ranged from 63 per cent to 91 per cent. Most of the losses occurred in connection with the recycle compressor system and correspondingly decreased the volume of product gas metered. Such losses, however, did not significantly affect the incoming gas to the main reactor or the performance of the reactor.

#### Experiment HGR-10

Experiment HGR-10 operated at 300 psig with recycle ratios being varied to give temperature rises across the catalyst bed ranging from 50° to 150° C. Temperature control was excellent. Total operating time was relatively short at 910 hours. The initial carbon monoxide concentration in the product gas at 0.3 per cent was higher than the desired value of less than 0.1 per cent. Over the entire experiment, the average rate of catalyst deactivation, expressed as increase in the per cent carbon monoxide in the dry product gas per mscf methane produced per pound of catalyst charged, was 0.23 per cent/mscf/lb. This is a high rate of deactivation compared with the value of about 0.009 per cent/mscf/lb. obtained with Raney nickel catalyst in a tube-wall methanator test (TWR-6). (2) Because the experiment was of short duration, the resulting production of methane per pound of catalyst in HGR-10 was low at about 11.8 mscf/lb. as compared with 177 mscf/lb. in tube-wall reactor test TWR-6.

One probable reason for the relatively poor catalyst performance in experiment HGR-10 was the excessively large deposits of iron and carbon on the catalyst surface. Table 6 shows iron and carbon concentrations of 22.0 and 13.4 weight per cent, respectively, on the catalyst near the gas inlet, and 0.8 and 1.9 weight per cent, respectively, on the catalyst near the gas outlet. It is suspected that the large deposit of iron resulted from the decomposition of iron carbonyl carried in from other parts of the reactor system, and the deposited iron in turn favored the formation of free carbon from the incoming carbon monoxide.

#### Experiment HGR-12

As shown in table 1, the catalyst bed for experiment HGR-12 was the same as that used in experiment HGR-10, except that the coat of Raney nickel used in HGR-12 was slightly thinner than that used in HGR-10. The objective in HGR-12 was to increase catalyst life. The methane produced per pound of catalyst was 39.5 mscf after a total operating time of about 1400 hour (See figure 5). The overall average rate of catalyst deactivation, 0.091 per cent per mscf per lb., was about 40 per cent of that for experiment HGR-10, but still 10 times greater than that of experiment TWR-6. The carbon monoxide concentration in HGR-12 increased from 0.1 per cent at the start of the experiment, to 3.7 per cent at the end of the experiment.

In general, the rate of deactivation was much lower at the lower fresh gas feed rate than at the higher feed rates. For example, during the period between 600 hours and 800 hours stream time, at the lower feed rate of about 206 scfh, the rate of deactivation was 0.022 per cent/mscf/lb. as compared with a deactivation rate of 0.143 per cent/mscf/lb. for the period between 100 hours and 400 hours where the fresh feed rate was about 386 scfh.

The cold gas recycle ratio values shown in figure 4 are metered values and are more consistent than the hot gas recycle and total gas recycle ratio values which, as explained earlier, were calculated from gas analyses. Although the calculated total recycle gas flow rate was erratic, the catalyst bed temperatures were uniform and easily controlled by varying the recycle rate and its temperature level. The uniformity of the catalyst bed temperature, as shown by figure 4, indicates that the actual recycle rate was much more uniform than indicated by the calculated values. The data plotted in figures 4 and 5, indicate that between the stream time of 260 hours and 460 hours, raising the maximum temperature of the catalyst bed from 350° C to 410° C did not significantly change the trend of increasing carbon monoxide concentration in product gas. However, this trend in carbon monoxide concentration was reversed during the subsequent period between 467 and 539 hours when the carbon monoxide concentration in the product gas decreased from 2.0 to 1.7 per cent (dry). This decrease in carbon monoxide concentration is attributed mainly to the ratio of total recycle gas to a fresh gas being decreased from about 20:1 to about 8:1 with an attendant increase in residence time. The decrease in total recycle ratio was achieved by reducing the hot gas recycle ratio to about 5:1 while leaving the cold gas recycle ratio constant at 3:1. The water vapor concentration in the mixed feed to the reactor correspondingly was decreased slightly from 5.5 per cent to 3.7 per cent and the resulting temperature spread across the catalyst bed increased from about 51° C to 112° C. Table 3 shows the wet analyses of the product gas during operation with the lower recycle ratio of 8:1 at 539 hours stream time.

After experiment HGR-12 was ended, samples of the spent catalyst were taken from various locations in the bed, and surface areas (B.E.T.), pore volumes and distribution of pore radii were determined for each sample. The results are shown in table 7 as a function of distance from the gas inlet end of the catalyst bed. Additional catalyst information such as x-ray analysis, chemical analysis, and metal surface area determined by chemisorbed hydrogen are presented in table 8 for spent catalyst at the gas inlet and outlet. The B.E.T. surface areas are about one-half that of freshly activated Raney nickel where the surface area is as high as 64 m<sup>2</sup>/gm.

Special catalyst activities expressed as per cent CO converted to methane were determined in a thermogravimetric analyzer for samples of spent catalyst taken at 0, 6, and 60 inches from the gas inlet; corresponding CO conversions were 0.0, 0.9, and 18 per cent. The catalyst nearest the gas outlet--when compared with catalyst at the gas inlet--was the most active and had the lowest carbon content, the larger pore radii with 96 per cent of its pore volume having radii greater than 60 Å, the lowest B.E.T. surface area (19.5 m<sup>2</sup>/gm) and the largest free metal surface (4.9 m<sup>2</sup>/gm). These observations are all consistent if one assumes that the combination of finer pore structure and higher B.E.T. surface area found at the gas inlet side of the bed is indicative of a higher carbon concentration and that the nickel pore radii are larger than that of the amorphous carbon deposit.

#### Experiment HGR-13

In experiment HGR-13, a two foot bed of commercial catalyst was tested as a packed bed of 1/4 inch pellets. (See table 1 for bed properties). This test was made for comparison with a similar test (HGR-14) using a catalyst bed of parallel plates sprayed with Raney nickel. The experiment also was to show the effect of varying the fresh feed rate from a space velocity of 2000 to 3000 hours<sup>-1</sup>, where space velocity is based on scfh of gas at 1 atm and 32° F per cubic foot of catalyst bed.

Major process conditions for experiment HGR-13 are plotted against stream time in figure 6. The total recycle ratio was held relatively constant at about 10:1 resulting in a constant temperature-rise of about 100° C across the catalyst bed

(300° C at the inlet and 400° C maximum). Near the end of the experiment, the cold recycle ratio was varied between the value of 8:1 and 1:1. The experiment was ended at 1368 hours.

As shown in figure 7, the carbon monoxide concentration in the dry product gas ranged from about 0.02 per cent at the start to 1.2 per cent at 840 hours, and decreased to 0.88 per cent at 1368 hours, at the end of the run. The total methane produced per lb. of catalyst was about 11.5 mscf/lb. Heating value of the product ranged from 885 to about 960 Btu/scf.

The overall deactivation rate expressed as per cent carbon monoxide increase per mscf methane produced per pound of catalyst was about 0.076. During the course of the experiment, as the fresh gas rate was varied from about 210 scfh to 320 scfh and finally back to 210 scfh, deactivation rates corresponding to those feed rates were 0.014, 0.222 and 0.079. Thus, the deactivation rate was increased irreversibly by increasing the fresh gas rate.

Typical operating data from selected periods in experiment HGR-13 are presented in table 4. Period 6, 168 hours stream time, is typical of conditions at the initial part of the experiment while period 54 is representative of conditions at the end of the experiment. Comparison of period 20 with period 6 indicates that very little change in performance occurred over that span of 336 hours of operation; for example, the decrease in conversion of (CO + H<sub>2</sub>) in the fresh feed gas was very slight, decreasing from 98.0 per cent to 97.9 per cent. Comparison of period 20 with period 22, shows typical effects of increasing the fresh feed rate from a space velocity of 2110 hr<sup>-1</sup> to 3020 hr<sup>-1</sup>. Conversion of H<sub>2</sub> + CO in the fresh feed, for example, dropped from 97.9 per cent to 97.1 per cent. Data in period 34 shows a further drop in performance which may be attributed to continued operation at the higher fresh feed rate of 320 scfh or space velocity of 3120 hr<sup>-1</sup>.

After the fresh feed rate was returned to the lower rate of 211 scfh, a comparison of carbon monoxide in the product gas in period 37 (0.4 per cent) with that in period 20 (0.1 per cent) shows that the catalyst had definitely lost activity with time. However, this activity loss is not evident in the respective heating values of 933 and 926 Btu/scf, for periods 37 and 20 because the product gas in period 37 was less diluted with excess hydrogen than was the product gas in period 20. This is confirmed by the H<sub>2</sub>/CO in the fresh feed gas; H<sub>2</sub>/CO=3.01 for period 37 and 3.24 for period 20.

X-ray defraction analysis of the spent catalyst presented in table 8 show the nickel to be present only in the metallic state. Chemical analyses also presented in table 8 indicate very little difference in composition of catalyst at the gas inlet and at the gas outlet.

#### Experiment HGR-14

The reactor was packed with 2 feet of parallel plates sprayed with Raney nickel as described in table 1. Spraying and activation of the catalyst was the same as described under catalyst preparation. Operating conditions were maintained practically the same as they were for experiment HGR-13, except for the periodic changes in the cold gas recycle ratio. Figure 8 shows reactor conditions in experiment HGR-14 as a function of time on stream and figure 9 presents the resulting carbon monoxide concentration, heating values, and methane produced per pound of catalyst.

At the start of the experiment, the carbon monoxide concentration in the product gas was very low, less than 0.01 per cent. The unusually high value (0.71 per cent) shown at 186 hours stream time is due to analytical error. At the end of the experiment, after 2307 hours stream time, carbon monoxide in the product gas had increased

to 0.93 per cent (dry basis) and total methane produced per pound of catalyst was 32 mscf/lb.

The average catalyst deactivation rate over the entire experiment was 0.0291 per cent/mscf/lb. The rate of deactivation during the initial 462 hours operation at a fresh feed space velocity of about 2090 hr<sup>-1</sup> (216 scfh) was very low at 0.0017 per cent/mscf/lb.; from about 500 hours to 841 hours at about 2990 hr<sup>-1</sup> space velocity, the rate of deactivation increased to 0.040 per cent/mscf/lb. Catalyst deactivation rates during HGR-14 are shown below for various operating periods and fresh feed space velocities:

Nominal Fresh Feed Space Velocity, hrs <sup>-1</sup>	Stream Period, hrs		Catalyst Deactivation Rate, per cent/mscf/lb
	From	To	
2000	0	462	0.00166
3000	462	841	0.0396
2000	841	1058	0.0027
2000	1058	1760	0.0187
2000	1760	2180	0.0821

As noted previously in experiment HGR-13, the deactivation rate increased significantly when the fresh feed space velocity was increased from 2000 hr<sup>-1</sup> to 3000 hr<sup>-1</sup>. During the period 841 to 1058 hrs., the fresh feed space velocity was returned to 2000 hr<sup>-1</sup> and the cold gas recycle ratio was increased from about 3:1 to about 9:1 to give a low deactivation rate of 0.0027 per cent/mscf/lb. When the cold recycle ratio was returned to about 3:1 in the period 1058 to 1760 hrs., the rate of catalyst deactivation was increased to 0.0187 per cent/mscf/lb. After 1760 hours, the unit was shut-down and put in standby condition under a hydrogen atmosphere. After the unit was restarted, the deactivation rate had increased greatly to 0.0821 per cent/mscf/lb., indicating that the increase in deactivation rate was associated with this particular shutdown. The fact that this experiment previously had undergone three unscheduled shutdowns at 215, 798, and 894 hours with no adverse effect on performance, indicates that some unknown factor unique to the 1760 hour shutdown was responsible for the subsequent rapid decline in activity.

The operating data shown in table 5 were selected to provide more detailed information on points of special interest in the experiment as follows:

- Period 4.....represents performance at 2000 hr<sup>-1</sup> fresh gas space velocity and 3:1 cold recycle when the catalyst is fresh.
- Period 15.....represents performance at 2000 hr<sup>-1</sup> space velocity before changes to 3000 hr<sup>-1</sup>.
- Periods 17 and 26...represent the beginning and end of the 3000 hr<sup>-1</sup> space velocity operation.
- Period 34.....represents operation at 2000 hr<sup>-1</sup> space velocity and a high value of the cold gas recycle ratio (9.59:1).
- Periods 37 and 62...represent the beginning and end of an operating period later in the experiment with 2000 hr<sup>-1</sup> space velocity and 3:1 cold recycle ratio.
- Periods 62 and 64...provide further comparison of the effect of increasing the cold recycle ratio from 3:1 to 10:1.
- Period 76.....represents performance after a long period of operation, 2207 hours.

X-ray analysis of the spent catalyst (table 8) showed metallic nickel and nickel carbide,  $\text{Ni}_3\text{C}$ , in catalyst near the gas inlet and only metallic nickel in catalyst near the gas outlet.

## DISCUSSION OF RESULTS

### Operability

All four series of experiments have proven that the hot gas recycle methanation system is a usable and operable system. With a total gas recycle ratio of about 10:1 and with CO concentrations as high as 4.3 per cent (wet basis) in the mixed feed entering the catalyst bed, temperature control was excellent; no hot spots developed. It appears likely that lower recycle ratios, although it is not known how much lower, could be used successfully with an attendant increase in inlet CO concentration and an increase in temperature rise across the bed. Further testing is required to determine the limit in decreasing the total recycle ratio and the effect of such a decrease on the catalyst life.

### Flame Sprayed Raney Nickel Plates vs Pellets of Precipitated Catalyst in a Packed Bed

Results of experiment HGR-13 and HGR-14 have shown that the performance of the plates sprayed with Raney nickel catalyst was significantly better than that of the precipitated nickel catalyst pellets. The sprayed plates were better in that they yielded the higher production of methane per pound of catalyst, the longer catalyst life or lower rate of deactivation, the lower carbon monoxide concentration in the product gas, and the lower pressure drop across the catalyst bed.

One of the reasons for developing the parallel plate catalyst was to reduce the pressure drop across the catalyst bed and consequently reduce power costs for circulating the recycle gas. Pressure drop measurements across the 2 foot long catalyst beds are listed below:

Nominal Space Velocity, $\text{hr}^{-1}$	Fresh Feed	Total Feed	Pressure Drop	Inches Water
			Exp. HGR-14 (Parallel plates)	Exp. HGR-13 (1/4" pellets)
2000		22,000	2.0	28
3000		33,000	2.7	49

The above data show that the pressure drop across the parallel plates is in the order of  $1/15^{\text{th}}$  that across the bed of pelleted catalyst.

The bed of parallel plates coated with Raney nickel catalyst was much more reactive than the bed of precipitated nickel. This was shown by the generally lower carbon monoxide concentration in the product gas during operation with the parallel plate bed; for example, after about 450 hours stream time, carbon monoxide in the product was 0.01 per cent for the bed of sprayed Raney nickel (HGR 14) and 0.05 per cent for the bed of precipitated nickel catalyst (HGR 13).

The higher reactivity of the plates coated with Raney nickel is further illustrated by the plots of catalyst temperature vs bed length shown in figure 10. The maximum bed temperature (indicating near completion of methanation) is consistently reached within a shorter distance from the gas inlet and the slope of the curves are correspondingly steeper for the more reactive bed of parallel plates coated with Raney nickel than for the bed of precipitated nickel.

The initial reactivities of the catalyst beds in experiments HGR-13 and 14 are considered to be satisfactorily high; however, the overall rate of deactivation of the bed of Raney nickel catalyst (0.029 per cent/mscf/lb) was much lower than that of the precipitated catalyst (0.076 per cent/mscf/lb). This, consequently, has resulted in a longer catalyst life (2307 vs 1368 hours) and a higher yield of methane per pound of catalyst (32.0 vs 11.5 mscf/lb) for the Raney nickel catalyst over that for the precipitated nickel catalyst.

Other precipitated nickel catalysts have been developed recently that reputedly are superior to that used in experiment HGR-13. These catalysts will be evaluated in the near future, as well as other forms of Raney nickel.

#### Effects of Cold Gas Recycle and Approach to Equilibrium

Product gases resulting from various cold recycle ratios are shown in table 9. For the experiments shown, a decrease in the cold recycle ratio resulted consistently in an increase in concentration in the product gas of water vapor, hydrogen, and carbon dioxide and a decrease in methane. These trends may be noted in experiment HGR-12 as the cold recycle ratio decreased from 8.7:1 to 1.2:1, in experiment HGR-13 as the cold recycle ratio increased from 1.0:1 to 9.1:1, and in experiment HGR-14 as the cold gas recycle ratio decreased from 3.0:1 to 1.0:1. The above-mentioned trends indicate that the water gas shift reaction  $\text{CO} + \text{H}_2\text{O} \rightarrow \text{CO}_2 + \text{H}_2$  was sustained to some degree. Except for the 462 hour period of experiment HGR-14, the apparent mass action constants for the water gas shift reaction based on the product gas compositions shown in table 9 remained fairly constant and ranged between 0.57 and 1.6. These values are much lower than the value of 11.7 for equilibrium conversion at 400° C. At 462 hours in experiment HGR-14, the apparent mass action constant for the shift reaction was 0.075, which represents a much greater departure from equilibrium than that encountered in the other periods shown in table 9. The apparent mass action constant for the methanation reaction  $3\text{H}_2 + \text{CO} \rightarrow \text{CH}_4 + \text{H}_2\text{O}$  at 462 hours in experiment HGR-14 was 2650 which was a much closer approach to the 400° C equilibrium value of  $1.7 \times 10^4$  than was achieved by the other test periods shown in table 9. This greater dominance by the methanation reaction while the catalyst is still relatively fresh probably caused the greater departure from equilibrium observed in the shift reaction during the early part of the experiment, at the 462 hour period.

#### Catalyst Deactivation

In this series of hot gas recycle experiments, the sulfur content in the feed gas was held very low, generally less than 0.1 ppm. Catalyst deactivation caused by sulfur poisoning is, therefore, considered negligible. On the other hand, the iron deposited on the catalyst in experiments HGR-10 and to a lesser extent in experiments HGR-12 and 14, is suspected of promoting carbon formation and subsequent fouling and deactivation of the catalyst. Iron concentrations of 5 mg/mscf have been determined in the recycle stream indicating the presence of iron carbonyl. Iron to nickel ratio in the fresh Raney nickel is about 2.4 Fe:1000 Ni, but the ratios are significantly higher for the spent Raney nickel catalyst. Based on analyses shown in table 8, Fe:Ni ratios for the spent Raney nickel catalysts of experiments HGR-12 and 14 ranged from 5.2 Fe:1000 Ni to 14.8 Fe:1000 Ni with the higher iron concentrations generally resulting in greater carbon deposition. The same trend was observed in experiment HGR-10.

Nickel carbide was detected on the catalyst in experiment HGR-14 and is another compound suspected of deactivating Raney nickel catalyst. However, inasmuch as the shutdown involved purging with hydrogen while the catalyst was hot, the presence of nickel carbide is contrary to Steffgen's (3) findings on a TGA apparatus that nickel

carbide is not stable under hydrogen at temperatures above 280° C. More information on nickel carbide formation is needed.

The metal surface area at the inlet end of the catalyst bed of experiment HGR-12 being smaller than at the outlet end indicates that a decrease in nickel metal sites is part of the deactivation process. Sintering of the nickel is one possible mechanism, but carbon and carbide formation are suspected major causes. The loss of active Raney nickel sites could also conceivably result from diffusion and subsequent alloying of residual free aluminum from unleached catalyst with the free nickel to form an inactive material.

As already noted in the experimental results of experiments HGR-12, 13, and 14, the ratio of catalyst deactivation increased as the fresh gas feed rate increased. It is possible that higher rates of carbon deposition and metal sintering occur at the higher feed rates to result in higher deactivation rates.

In comparing catalyst performance in an adiabatic hot gas recycle reactor vs an isothermal tube-wall reactor, the catalyst in the tube-wall reactor in experiment TWR-6 deactivated much slower than did the catalyst in the best gas recycle test, HGR-14, (0.009 vs 0.0291 per cent/mscf/lb) and produced much more methane per pound of catalyst (177 mscf/lb vs 32 mscf/lb). This indicates that adiabatic operation of a methanation catalyst between 300 and 400° C is not as efficient as operating isothermally at a higher temperature level of about 400° C.

Another factor that may account for the relatively higher rate of deactivation for the hot gas recycle reactor system is the entrainment of oil vapors from the hot recycle gas compressor into the catalyst bed. Evidence of this occurrence was shown by traces of heavy oil collected downstream of the hot gas recycle reactor. Such oil vapors would tend to decompose thermally and subsequently foul the catalyst surface with carbon. In future hot gas recycle tests, efforts will be made to eliminate the deposition of oil on the catalyst bed.

References

- 1) Forney, A. J., Demski, R. J., Bienstock, D., and Field, J. H.,  
"Recent Catalyst Developments in the Hot-Gas-Recycle Process",  
Bureau of Mines Report of Inv. 6609, 1965, 32 pp.
- 2) Haynes, W. P., Elliott, J. J., and Forney, A. J.,  
"Experience with Methanation Catalysts", ACS Fuels Div. Preprint,  
Apr. 10-14, 1972, Vol. 16, no. 2, pp 47-63.
- 3) Steffgen, F. W., and Hobbs, A. P.,  
"Methanation of Synthesis Gas and the Nickel Carbide System",  
Oral presentation at the Pittsburgh Catalysis Society,  
1973 Spring Symposium.

TABLE 1. - Catalyst bed data from hot gas recycle reactor tests

Experiment Nos.	10	12	13	14
Type catalyst.....	Flame-sprayed Raney nickel	Flame-sprayed Raney nickel	Supported nickel	Flame-sprayed Raney nickel
Wt pct nickel.....	42 70	42 70	25	42 70
Pct activated.....	a/ b/	a/ b/	100% reduced	.046 .135
Plate thickness, .....inches	1/4	1/4	--	.006 .022
Space between bare plates,-in.	.224	.224	--	3.07 x 24
AV. bond coat thickness,inches	.006	.006	(1/4" x 1/4" cylindrical pellets)	.103
AV. catalyst thickness, inches	.026	.022	3.07 x 24	
Bed diameter x length, inches	3.07 x 60	3.07 x 60	.103	
Bed volume, .....ft <sup>3</sup>	.257	.257		
Weight of unactivated catalyst.....	3.72	2.86	6.80	3.84
Superficial area of cat., ft <sup>2</sup>	12.7	12.7	18.6	11.4
Void fraction.....	0.421	0.436	0.370	0.515

a/ Before leaching

b/ Leaching of aluminum stopped when 70% of the theoretical amount of hydrogen had evolved.

TABLE 2. - Operating data from selected periods in Experiment HGR-10

Period number.....	5	15	26
Hours on stream .....	168	527	887
Fresh gas:			
Rate.....scfh	200	204	204
H <sub>2</sub> .....vol pct	75.3	75.3	75.6
CO .....vol pct	24.3	24.6	24.2
CO <sub>2</sub> .....vol pct	0.2	0.1	0.1
N <sub>2</sub> .....vol pct	0.0	0.0	0.0
CH <sub>4</sub> .....vol pct	0.2	0.1	0.2
H <sub>2</sub> O .....vol pct	0.0	0.0	0.0
H <sub>2</sub> /CO.....	3.10	3.06	3.09
Exposure vel..... scfh/ft <sup>2</sup>	15.7	16.0	16.1
Space vel..... hr <sup>-1</sup>	779	795	796
Mixed feed gas (wet):			
Rate.....scfh	9138	3744	2401
H <sub>2</sub> .....vol pct	6.0	13.2	17.7
CO .....vol pct	1.2	2.9	4.3
CO <sub>2</sub> .....vol pct	1.3	0.7	0.8
N <sub>2</sub> .....vol pct	0.6	1.4	1.7
CH <sub>4</sub> .....vol pct	83.1	76.7	71.4
H <sub>2</sub> O .....vol pct	7.8	5.0	4.1
H <sub>2</sub> /CO .....	5.06	4.61	4.08
Inlet superficial vel.... f/s	5.44	2.18	1.44
Inlet Reynolds No. ....	5,000	1,960	1,180
Exposure vel.....scfh/ft <sup>2</sup>	51.9	47.5	41.6
Space vel.....hr <sup>-1</sup>	35,600	14,600	9,360
Vol. total recycle/vol. fresh gas	44.7	17.4	10.8
Vol. cold recycle/vol. fresh gas	3.1	2.99	3.05

continued:

TABLE 2. Operating data from selected periods in Experiment HGR-10

Period number.....	5	15	26
<b>Temperatures:</b>			
Gas inlet..... ° C	370	355	375
Maximum catalyst..... ° C	400	425	475
Pressure..... psig	300	300	300
<b>Product gas (wet):</b>			
Rate..... scfh	48.8	55.5	58.3
H <sub>2</sub> ..... vol pct	4.4	9.6	12.1
CO..... vol pct	.7	1.6	2.4
CO <sub>2</sub> ..... vol pct	1.3	.8	.2
N <sub>2</sub> ..... vol pct	.7	1.5	1.8
CH <sub>4</sub> ..... vol pct	84.3	80.0	76.6
H <sub>2</sub> O..... vol pct	8.6	6.4	6.3
H <sub>2</sub> /CO.....	6.2	6.0	5.05
<b>Conversion:</b>			
H <sub>2</sub> ..... pct fresh feed	98.6	96.5	95.4
CO..... pct fresh feed	99.3	98.2	97.2
(H <sub>2</sub> + CO)..... pct fresh feed	98.7	96.9	95.9
H <sub>2</sub> ..... pct mixed feed	27.0	29.9	34.6
CO..... pct mixed feed	44.4	45.8	46.5
(H <sub>2</sub> + CO)..... pct mixed feed	29.8	32.7	37.0
Usage ratio.....	3.07	3.01	3.07
Heating value ..... Btu/scf	952	908	878
Carbon recovery..... pct	87	91	90

TABLE 3. - Operating data from selected periods in Experiment HCR-12

	7	20	31	52	55	56
Period number.....	200	539	803	1307	1379	1403
Hours on stream.....						
Fresh gas:						
Rate.....scfh	388	383	206	386	386	393
H <sub>2</sub> .....vol pct	75.5	75.1	75.1	75.6	75.2	75.3
CO.....vol pct	24.4	24.7	24.7	24.4	24.7	24.6
CO <sub>2</sub> .....vol pct	0.1	0.1	0.1	0	0.1	0
N <sub>2</sub> .....vol pct	0	0	0	0	0	0
CH <sub>4</sub> .....vol pct	0	0.1	0.1	0	0	0.1
H <sub>2</sub> O.....vol pct	0	0	0	0	0	0
H <sub>2</sub> /CO.....	3.09	3.04	3.04	3.10	3.04	3.06
Exposure vel.....scfh/ft <sup>2</sup>	30.6	30.1	16.2	30.4	30.4	30.9
Space vel.....hr <sup>-1</sup>	1510	1490	804	1500	1500	1530
Mixed feed gas (wet):						
Rate.....scfh	7380	3450	5820	7760	9670	15,100
H <sub>2</sub> .....vol pct	14.4	20.2	14.9	20.7	22.3	21.9
CO.....vol pct	2.0	4.2	1.6	4.4	4.2	3.8
CO <sub>2</sub> .....vol pct	0.5	0.4	0.3	0.6	0.8	1.5
N <sub>2</sub> .....vol pct	1.3	0.8	1.2	0.3	0.6	0.8
CH <sub>4</sub> .....vol pct	76.4	70.7	76.6	72.6	66.8	60.8
H <sub>2</sub> O.....vol pct	5.4	3.7	5.4	1.4	5.3	11.2
H <sub>2</sub> /CO.....	7.04	4.82	9.20	4.71	5.34	5.70
Inlet superficial vel.....f/s	3.88	1.86	3.41	4.61	5.73	8.93
Inlet Reynolds No.....	4,270	1,870	3,060	3,910	4,810	7,510
Exposure vel.....scfh/ft <sup>2</sup>	95.6	66.3	75.8	153.0	201.0	306.0
Space vel.....hr <sup>-1</sup>	28,800	13,400	22,700	30,200	37,700	58,900
Vol. total recycle/vol. fresh gas	18.0	7.99	27.2	19.1	24.1	37.4
Vol. cold recycle/vol. fresh gas	3.01	2.99	3.04	8.71	3.01	1.20

continued:

TABLE 3. - Operating data from selected periods in Experiment HCR-12

Period Number	7	20	31	52	55	56
<b>Temperatures:</b>						
Gas inlet..... ° C	294	310	360	368	366	365
Maximum catalyst..... ° C	353	422	412	420	422	420
Pressure..... Psig	300	300	300	300	300	300
<b>Product gas (wet):</b>						
Rate.....scfh	94.6	97.6	45.9	98.8	105.5	127.7
H <sub>2</sub> .....vol pct	10.9	13.0	12.6	17.6	19.9	20.3
CO.....vol pct	0.8	1.6	0.8	3.3	3.3	3.3
CO <sub>2</sub> .....vol pct	0.5	0.5	0.3	0.6	0.9	1.5
N <sub>2</sub> .....vol pct	1.3	0.8	1.2	0.3	0.6	0.8
CH <sub>4</sub> .....vol pct	79.7	77.5	78.8	75.6	69.0	62.2
H <sub>2</sub> O.....vol pct	6.8	6.6	6.3	2.6	6.3	11.9
H <sub>2</sub> /CO.....	13.6	8.13	15.8	5.33	6.03	6.15
<b>Conversion:</b>						
H <sub>2</sub> .....pct fresh feed	96.5	95.6	96.3	94.0	92.8	91.2
CO.....pct fresh feed	99.2	98.4	99.3	96.5	96.3	95.6
(H <sub>2</sub> + CO).....pct fresh feed	97.1	96.3	97.0	94.6	93.6	92.3
H <sub>2</sub> .....pct mixed feed	26.6	39.5	17.2	17.1	12.5	8.18
CO.....pct mixed feed	62.3	64.4	53.6	26.6	22.8	16.0
(H <sub>2</sub> + CO).....pct mixed feed	31.1	43.8	20.7	18.7	14.1	9.34
Usage ratio.....	3.01	2.95	2.95	3.02	2.93	2.92
Heating value.....Btu/scf	908	892	899	857	828	802
Carbon recovery.....pct	80	81	72	83	81	87

TABLE 4. - Operating data from selected periods in Experiment HGR-13

Period number.....	6	20	22	34	37	50	54
Hours on stream .....	168	504	552	840	912	1224	1320
Fresh gas:							
Rate.....scfh	211	216	310	320	211	205	210
H <sub>2</sub> .....vol pct	75.3	76.4	75.5	74.9	74.9	76.1	75.8
CO.....vol pct	24.6	23.6	24.5	24.9	24.9	23.7	24.1
CO <sub>2</sub> .....vol pct	0	0	0	0.1	0.1	0.1	0.1
N <sub>2</sub> .....vol pct	0	0	0	0	0	0	0
CH <sub>4</sub> .....vol pct	0.1	0	0	0.1	0.1	0.1	0
H <sub>2</sub> O.....vol pct	0	0	0	0	0	0	0
H <sub>2</sub> /CO.....	3.06	3.24	3.08	3.01	3.01	3.21	3.15
Exposure vel.....scfh/ft <sup>2</sup>	11.3	11.6	16.7	17.2	11.3	11.0	11.3
Space vel.....hr <sup>-1</sup>	2050	2110	3020	3120	2060	2000	2050
Mixed feed gas (wet):							
Rate.....scfh	2260	2090	3400	3430	2040	2800	3010
H <sub>2</sub> .....vol pct	15.2	16.1	16.9	19.1	15.2	17.9	14.0
CO.....vol pct	2.3	2.5	2.6	3.4	2.9	2.3	2.5
CO <sub>2</sub> .....vol pct	0.2	0.3	0.6	0.7	0.6	0.7	0.4
N <sub>2</sub> .....vol pct	0.9	1.4	1.0	0.9	0.9	0.5	1.2
CH <sub>4</sub> .....vol pct	76.9	75.6	74.5	71.9	76.7	66.8	81.0
H <sub>2</sub> O.....vol pct	4.5	4.1	4.4	4.0	3.7	11.8	0.9
H <sub>2</sub> /CO.....	6.54	6.43	6.41	5.69	5.21	7.72	5.69
Inlet superficial vel.....f/s	1.20	1.11	1.81	1.82	1.09	1.49	1.60
Inlet Reynolds No.....	835	772	1240	1220	753	1010	1120
Exposure vel.....scfh/ft <sup>2</sup>	21.3	21.0	35.8	41.5	19.9	30.5	26.6
Space vel.....hr <sup>-1</sup>	22,000	20,400	33,100	33,400	19,900	27,300	29,400
Vol. total recycle/vol. fresh gas	9.73	8.68	9.98	9.73	8.68	12.7	13.3
Vol. cold recycle/vol. fresh gas	2.98	2.99	3.00	2.96	2.98	1.01	9.05

continued:

TABLE 4. - Operating data from selected periods in Experiment HGR-13

Period number	6	20	22	34	37	50	54
<b>Temperatures:</b>							
Gas inlet..... ° C	301	300	301	301	302	301	301
Maximum catalyst..... ° C	401	400	401	400	401	401	400
Pressure .....	300	300	300	300	300	300	300
<b>Product gas (wet):</b>							
Rate.....scfh	48.1	50.9	79.3	81.1	49.0	47.4	38.4
H <sub>2</sub> .....vol pct	8.8	9.0	10.8	13.1	8.2	13.1	9.2
CO.....vol pct	0	0.1	0.4	1.1	0.4	0.6	0.8
CO <sub>2</sub> .....vol pct	0.3	0.3	0.7	0.8	0.6	0.8	0.4
N <sub>2</sub> .....vol pct	0.9	1.5	1.0	0.9	1.0	0.5	1.3
CH <sub>4</sub> .....vol pct	83.0	82.2	80.3	77.8	83.6	71.0	85.7
H <sub>2</sub> O.....vol pct	7.0	6.9	6.8	6.3	6.2	14.0	2.6
H <sub>2</sub> /CO.....	-	90	27	11.9	20.5	21.8	11.5
<b>Conversion:</b>							
H <sub>2</sub> .....pct fresh feed	97.3	97.2	96.3	95.6	97.5	96.0	97.8
CO.....pct fresh feed	100	99.9	99.6	98.9	99.6	99.4	99.4
(H <sub>2</sub> + CO).....pct fresh feed	98.0	97.9	97.1	96.4	98.0	96.8	98.2
H <sub>2</sub> .....pct mixed feed	45.0	47.2	39.1	34.9	49.6	29.9	37.0
CO.....pct mixed feed	100	96.2	85.3	68.2	87.9	74.4	68.0
(H <sub>2</sub> + CO).....pct mixed feed	52.3	53.8	45.3	39.8	55.7	35.0	41.6
Usage ratio.....	2.71	2.95	2.73	2.91	2.94	3.10	3.09
Heating value.....Btu/scf	935	926	911	890	933	888	925
Carbon recovery.....pct	82	87	90	80	78	70	63

TABLE 5. - Experiment HCR 14 - Selected Test Data

Period number.....	4	15	17	26	34	37	62	64	76
Hours on stream.....	139	462	534	750	1058	1130	1732	1803	2091
<b>Fresh Gas:</b>									
Rate.....scfh	207	214	306	307	207	207	210	203.5	213
H <sub>2</sub> .....vol pct	75.8	75.4	75.3	74.6	75.1	75.4	75.1	74.7	75.4
CO.....vol pct	23.7	23.6	23.6	24.4	22.9	23.6	24.0	24.8	24.1
CO <sub>2</sub> .....vol pct	0.1	0.1	0.3	0.2	0.1	0.1	0.1	0.1	0.1
N <sub>2</sub> .....vol pct	0.4	0.9	0.7	0.8	1.8	0.8	0.8	0.3	0.4
CH <sub>4</sub> .....vol pct	0	0	0.1	0	0.1	0.1	0	0.1	0
H <sub>2</sub> O.....vol pct	0	0	0	0	0	0	0	0	0
H <sub>2</sub> /CO.....	3.20	3.19	3.19	3.06	3.28	3.19	3.13	3.01	3.13
Exposure vel..... scfh/ft <sup>2</sup>	18.0	18.6	26.5	26.6	17.8	17.9	18.2	17.7	18.6
Space vel..... hr <sup>-1</sup>	2010	2090	2980	2990	2020	2020	2050	1980	2080
<b>Mixed feed gas (wet):</b>									
Rate.....scfh	2360	2400	3710	3720	2240	2430	2760	2120	2430
H <sub>2</sub> .....vol pct	15.9	14.0	11.7	8.8	11.8	11.1	10.1	10.4	13.8
CO.....vol pct	2.1	2.1	2.0	2.2	2.2	2.2	2.1	2.9	2.9
CO <sub>2</sub> .....vol pct	0.1	0.1	0.2	1.5	0.2	0.4	0.7	0.4	0.7
N <sub>2</sub> .....vol pct	0.7	1.1	0.9	1.1	1.3	0.9	1.1	1.1	1.2
CH <sub>4</sub> .....vol pct	76.4	78.0	80.6	81.9	84.3	80.7	81.4	85.2	76.9
H <sub>2</sub> O.....vol pct	4.8	4.6	4.6	4.5	0.2	4.7	4.6	0	4.5
H <sub>2</sub> /CO.....	7.68	6.63	5.88	4.00	5.38	5.10	4.84	3.64	4.77
Inlet superficial vel.....f/s	1.25	1.27	1.97	1.97	1.19	1.29	1.46	1.12	1.29
Inlet Reynolds No.....	546	563	882	898	532	582	666	512	570
Exposure vel.....scfh/ft <sup>2</sup>	37.2	34.0	44.5	35.8	27.5	28.2	29.6	24.8	35.6
Space vel.....hr <sup>-1</sup>	23,000	23,400	36,100	36,200	21,800	23,700	26,900	20,700	23,700
Vol. total recycle/vol.fresh gas	10.7	10.4	11.3	11.3	10.1	11.0	12.4	9.66	10.6
Vol. cold recycle/vol.fresh gas	2.95	2.93	3.12	3.01	9.59	2.93	3.13	10.2	2.94

continued:

TABLE 5. - Experiment HGR 14 - Selected Test Data

Period number.....	4	15	17	26	34	37	62	64	76
<b>Temperatures:</b>									
Gas inlet..... °C	299	299	301	300	300	300	300	299	299
Maximum catalyst..... °C	400	400	400	400	401	400	395	397	398
Pressure.....psig	300	300	300	300	300	300	300	300	300
<b>Product gas (wet):</b>									
Rate.....scfh	32.9	28.4	44.2	45.4	27.3	27.6	43.9	44.7	40.6
H <sub>2</sub> .....vol pct	10.0	7.9	5.8	2.8	5.3	5.0	4.7	3.5	7.8
CO.....vol pct	0	0	0.1	0.2	0.1	0.2	0.3	0.5	0.9
CO <sub>2</sub> .....vol pct	0.1	0.1	0.2	1.6	0.2	0.5	0.7	0.5	0.7
N <sub>2</sub> .....vol pct	0.7	1.1	0.9	1.1	1.2	0.9	1.1	1.2	1.3
CH <sub>4</sub> .....vol pct	81.9	83.9	86.1	87.6	90.7	86.3	86.5	91.8	82.5
H <sub>2</sub> O.....vol pct	7.3	7.0	6.9	6.7	2.5	7.1	6.7	2.5	6.8
H <sub>2</sub> /CO.....	-	785	117	14.1	58.3	27.7	16.2	6.68	9.14
<b>Conversion:</b>									
H <sub>2</sub> .....pct fresh feed	97.9	98.6	98.9	99.4	99.1	99.1	98.7	99.0	97.9
CO.....pct fresh feed	100	100	100	99.9	99.9	99.9	99.7	99.5	99.2
(H <sub>2</sub> + CO).....pct fresh feed	98.4	98.9	99.1	99.5	99.3	99.3	98.9	99.1	98.2
H <sub>2</sub> .....pct mixed feed	40.4	47.0	52.2	69.5	57.7	57.0	55.4	67.8	46.5
CO.....pct mixed feed	100	99.6	97.8	91.5	96.2	92.2	86.8	82.6	72.1
(H <sub>2</sub> + CO).....pct mixed feed	47.3	53.9	58.9	73.9	63.7	62.7	60.8	71.0	50.9
Usage ratio.....	3.10	3.13	3.14	3.04	3.23	3.15	3.09	2.99	3.08
Heating value.....Btu/scf	930	941	957	962	961	960	956	967	927
Carbon recovery.....pct	83.1	74.2	79.0	78.5	94.5	98.3	94.4	89.4	86.5

TABLE 6. IRON AND CARBON CONTENT OF RANEY NICKEL CATALYST GRIDS  
AFTER EXPERIMENT HGR-10

GRID	Weight Percent	
	Fe	C
A <sup>1/</sup>	22.0	13.4
B	17.2	9.1
C	3.5	3.9
D	2.7	3.3
E	2.0	2.5
F	2.1	2.0
G	.9	1.5
H	.8	1.6
I	.8	1.6
TOP <sup>2/</sup>	.8	1.9

---

<sup>1/</sup> GAS IN

<sup>2/</sup> GAS OUT

TABLE 7. SURFACE AREAS, PORE VOLUMES, AND PORE RADII  
OF SPENT RANEY NICKEL CATALYST

EXPERIMENT HGR-12

<u>DISTANCE FROM GAS INLET, INCHES</u>	<u>B. E. T. SURFACE AREA, m<sup>2</sup>/gm</u>	<u>AV. PORE RADIUS, A</u>	<u>PORE VOL. cm<sup>3</sup></u>	<u>PERCENT PORE VOLUME WITH THE FOLLOWING RADII</u>				
				<u>&lt; 30Å</u>	<u>30-40Å</u>	<u>40-50Å</u>	<u>50-60Å</u>	<u>&gt; 60Å</u>
0	34.7	47.1	0.083	19.7	11.9	10.8	10.0	47.6
18	31.7	90.6	.146	8.8	6.2	4.9	6.4	73.6
30	34.4	58.6	.101	15.7	9.2	11.6	9.5	54.0
36	32.9	82.0	.135	10.4	7.4	8.0	6.0	68.2
48	24.2	139.0	.168	.5	3.7	7.5	4.7	83.6
60	19.5	109.5	.107	0	0	0	4	96.0

TABLE 8. - Properties of spent methanation catalysts

	Exp. HGR-12 Catalyst		Exp. HGR-13 Catalyst		Exp. HGR-14 Catalyst	
	At Inlet	At Outlet	At Inlet	At Outlet	At Inlet	At Outlet
X-Ray analysis	-	-	Ni	Ni	Ni, Ni <sub>3</sub> C	Ni
Chemical analysis, per cent:						
Ni	67.6	80.4	24.0	25.3	83.4	81.9
Al	13.1	9.6	-	-	6.23	7.90
C	1.74	0.8	5.1	5.2	3.53	0.81
Fe	0.35	0.45	0.12	0.20	1.18	1.21
Na	0.08	0.06	0.23	0.20	-	-
S	0.24	0.13	0.1	0.1	0.19	0.07
Surface area (B.E.T.), m <sup>2</sup> /gm	34.67	19.50	-	-	30.95	29.7
Metal surface area (chemisorbed hydrogen), m <sup>2</sup> /gm	1.3	4.9	-	-	-	-
Average pore radius, Å	47.07	109.53	-	-	48.01	56.69
Percent pore volume > 60Å <sup>0</sup>	47.56	95.97	-	-	42.3	64.2

TABLE 9. - Effect of cold recycle upon product gas

Exp. No.	Stream time, hours	Cold recycle ratio	H <sub>2</sub> O in mixed feed, %	Product gas analysis, per cent, wet basis				Apparent mass action constants, kp		Max temp, °C	
				H <sub>2</sub> O	H <sub>2</sub>	CO	CO <sub>2</sub>	CH <sub>4</sub>	shift reaction		methanation reaction
HGR-12	1307	8.7:1	1.4	2.6	17.6	3.3	0.6	75.6	.78	.24	420
HGR-12	1379	3.0:1	5.3	6.3	19.9	3.3	0.9	69.0	.86	.37	422
HGR-12	1403	1.2:1	11.2	11.9	20.3	3.3	1.5	62.2	1.2	.59	420
HGR-12	539	3.0:1	5.4	6.6	13.0	1.6	0.5	77.5	1.6	3.2	422
HGR-13	1224	1.0:1	11.8	14.0	13.1	0.6	0.8	71.0	.79	16.0	401
HGR-13	1320	9.1:1	0.9	2.6	9.2	0.8	0.4	85.7	.57	7.8	400
HGR-14	462	2.9:1	4.6	7.0	7.9	0.01	0.1	83.9	.075	2650	400
HGR-14	2091	3.0:1	4.5	6.8	7.8	0.9	0.7	82.5	1.02	30.8	398
HGR-14	2307	1.0:1	10.5	13.2	10.1	0.8	1.4	73.0	.75	25.3	398

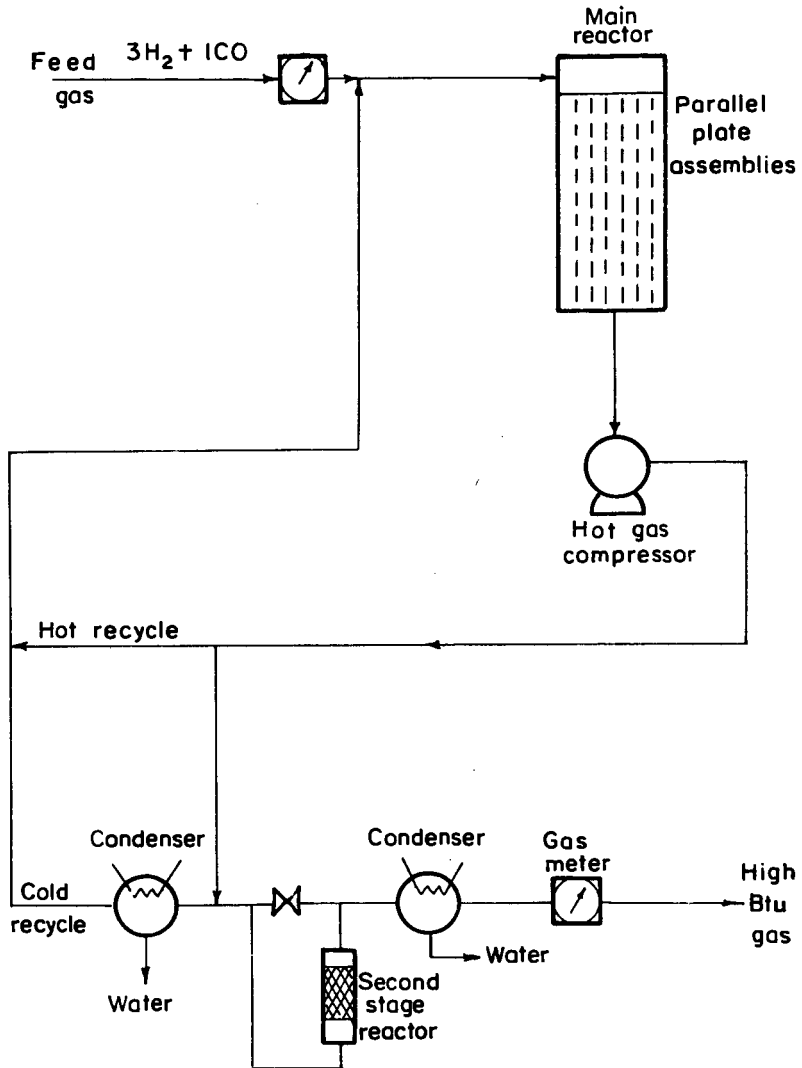


Figure 1 — Flowsheet of hot-gas recycle process

L-13681

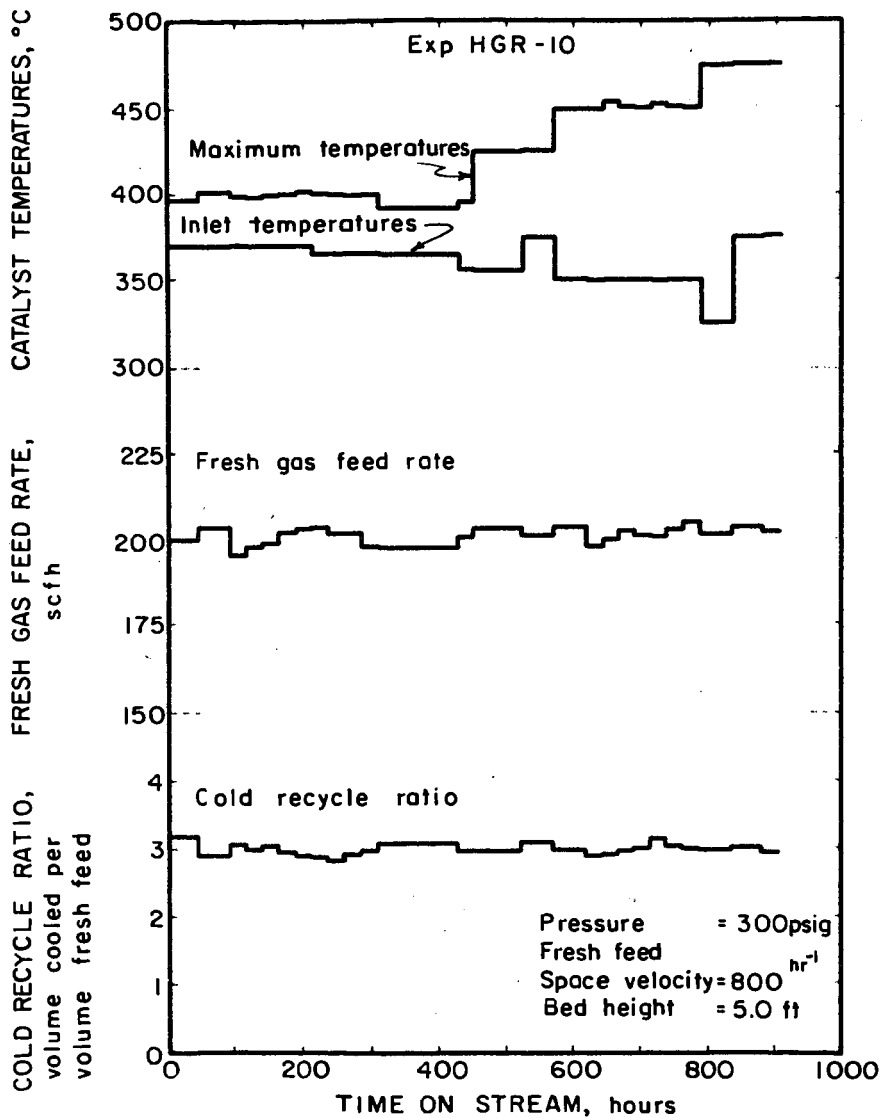


Figure 2 — Reactor conditions.

L-13676

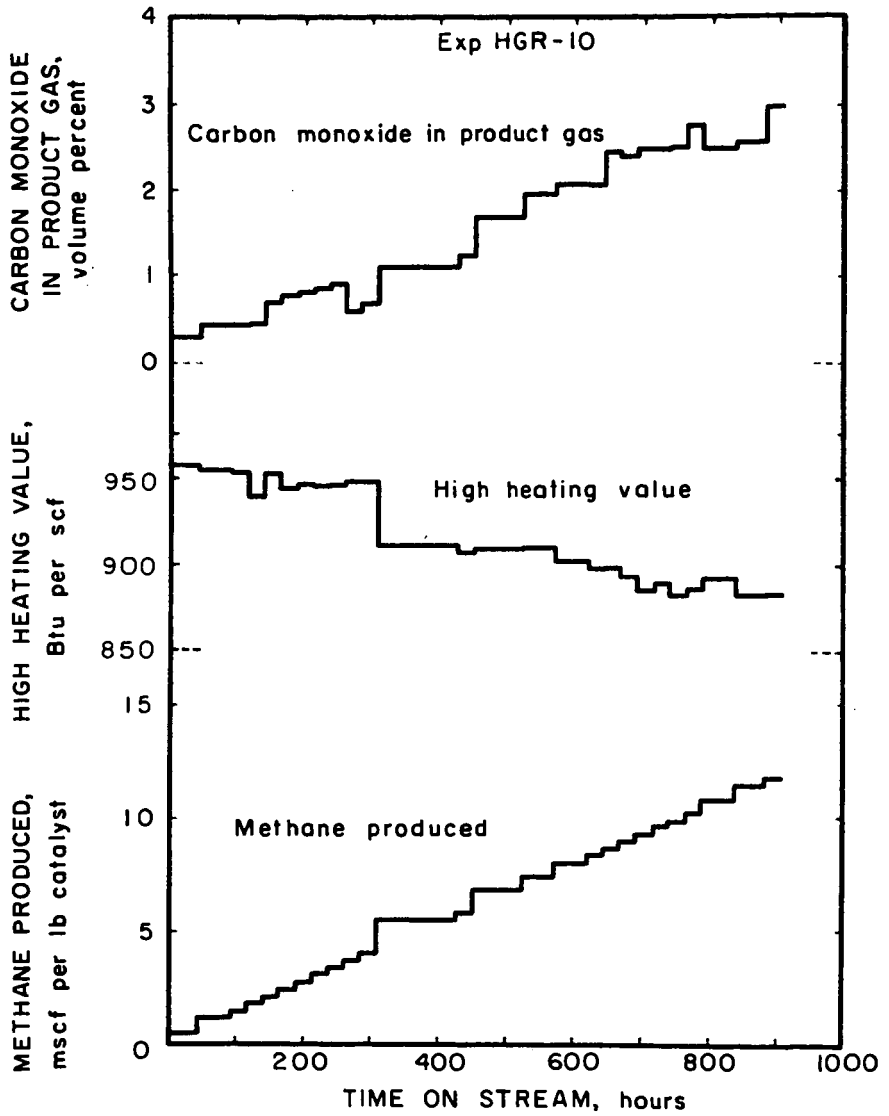


Figure 3—Product gas characteristics

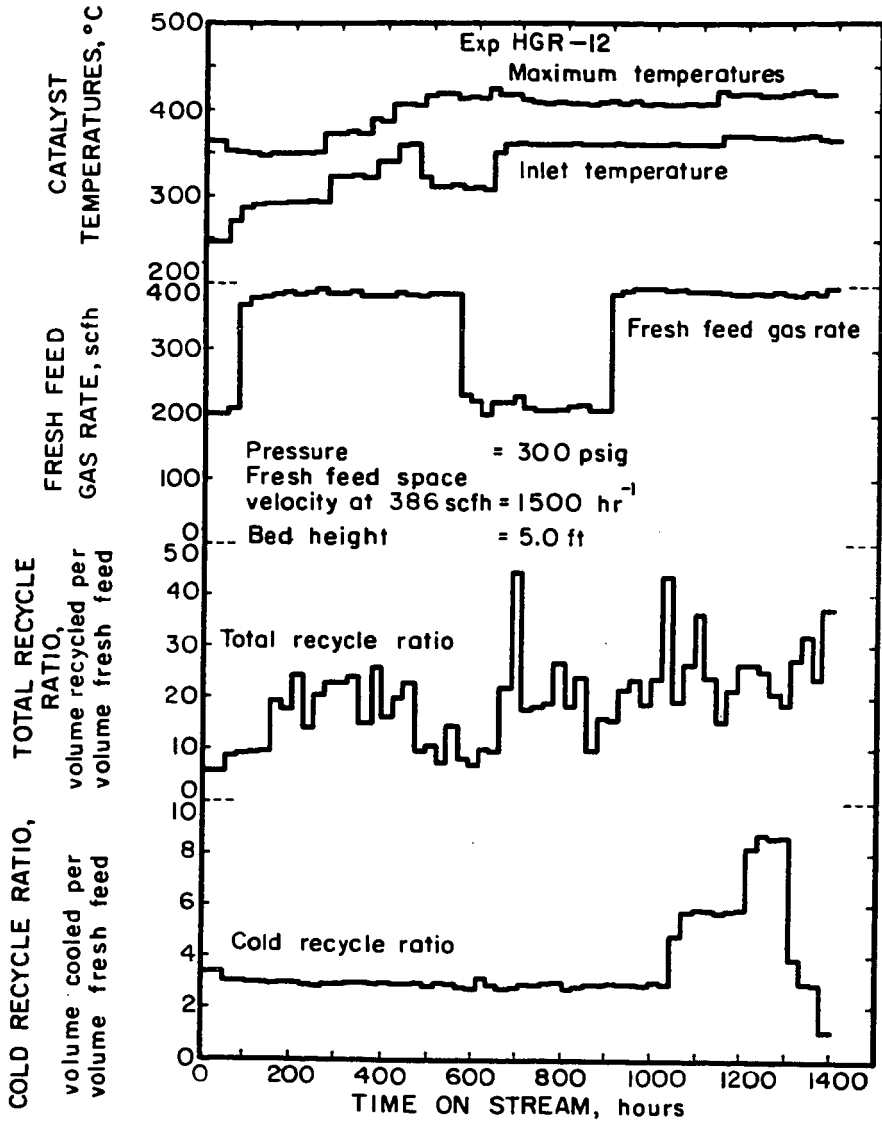


Figure 4 - Reactor conditions

L-13678

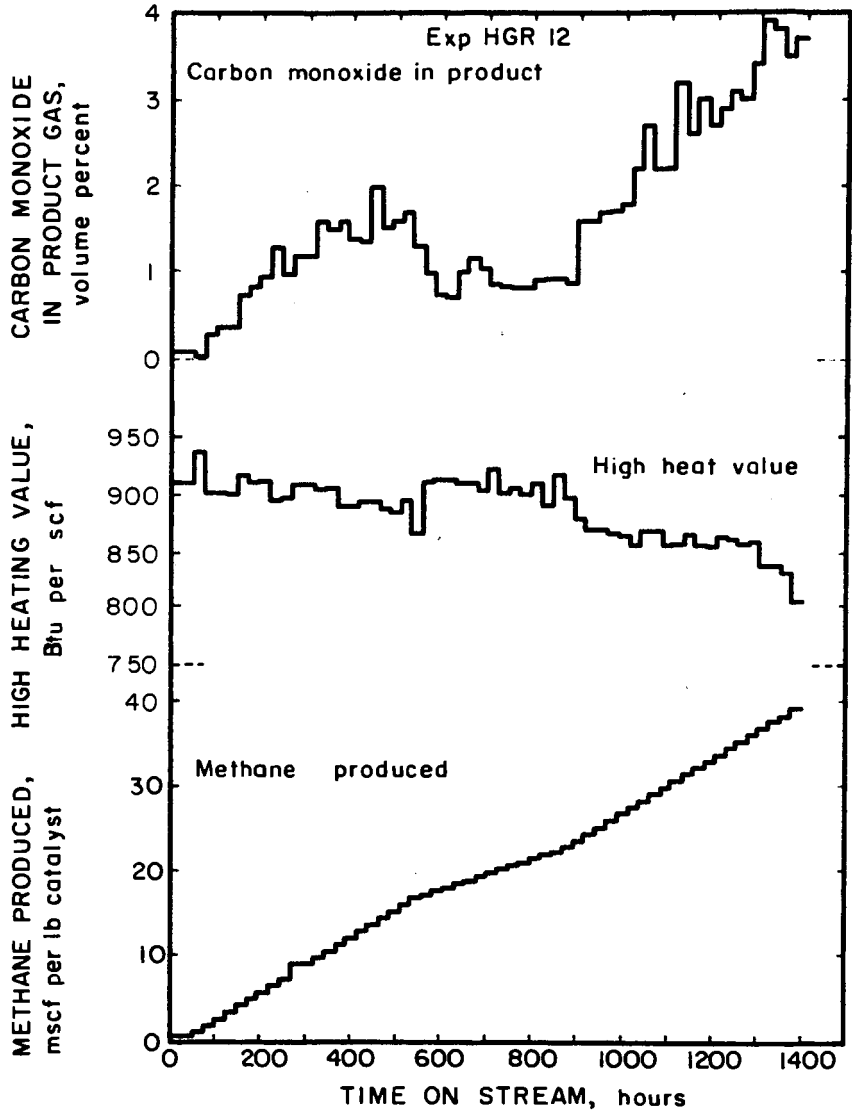


Figure 5 - Product gas characteristics

L-13674

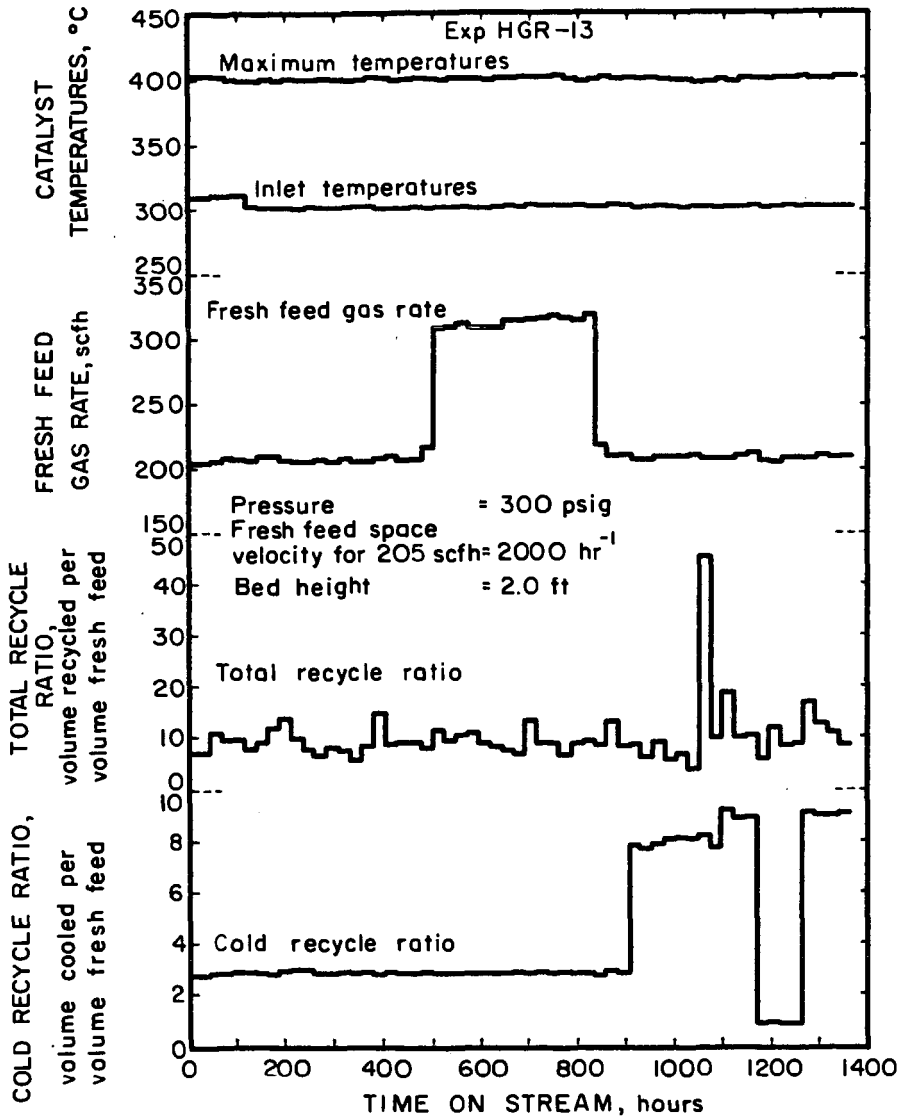


Figure 6 - Reactor conditions

L-13677

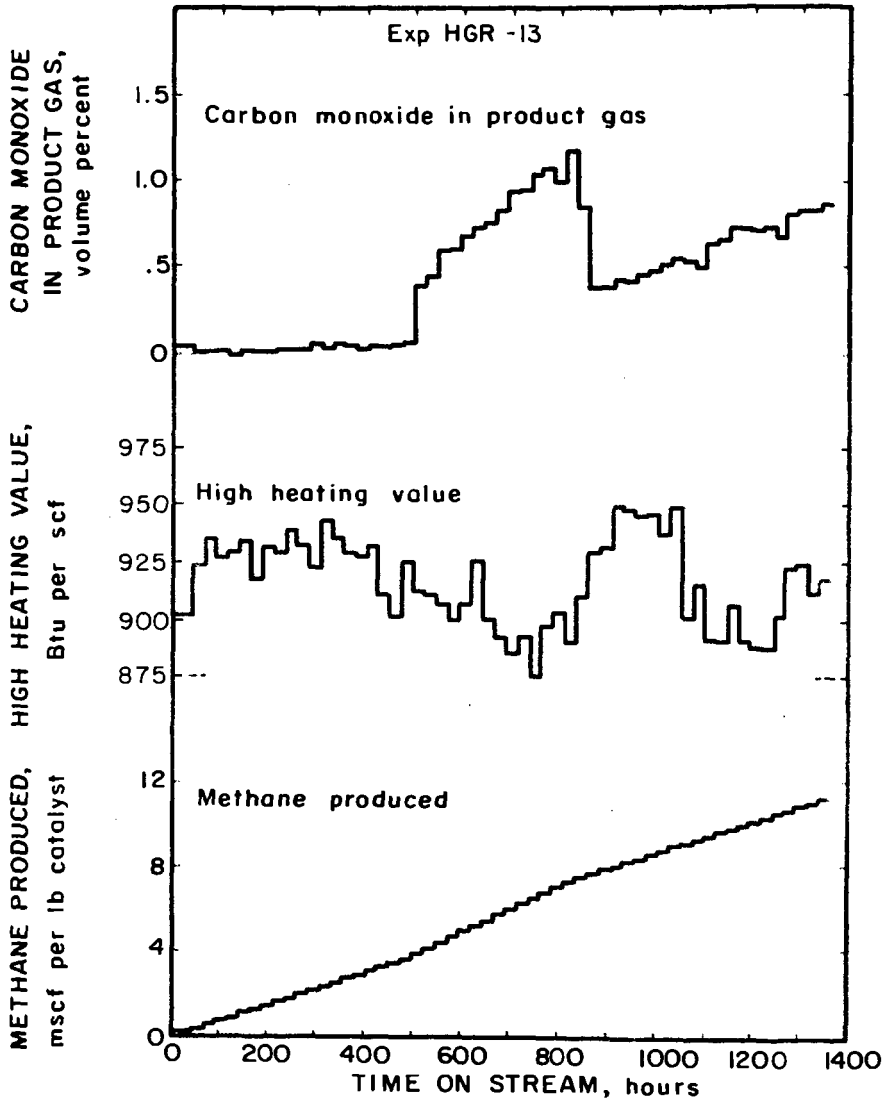


Figure 7 - Product gas characteristics

L-13675

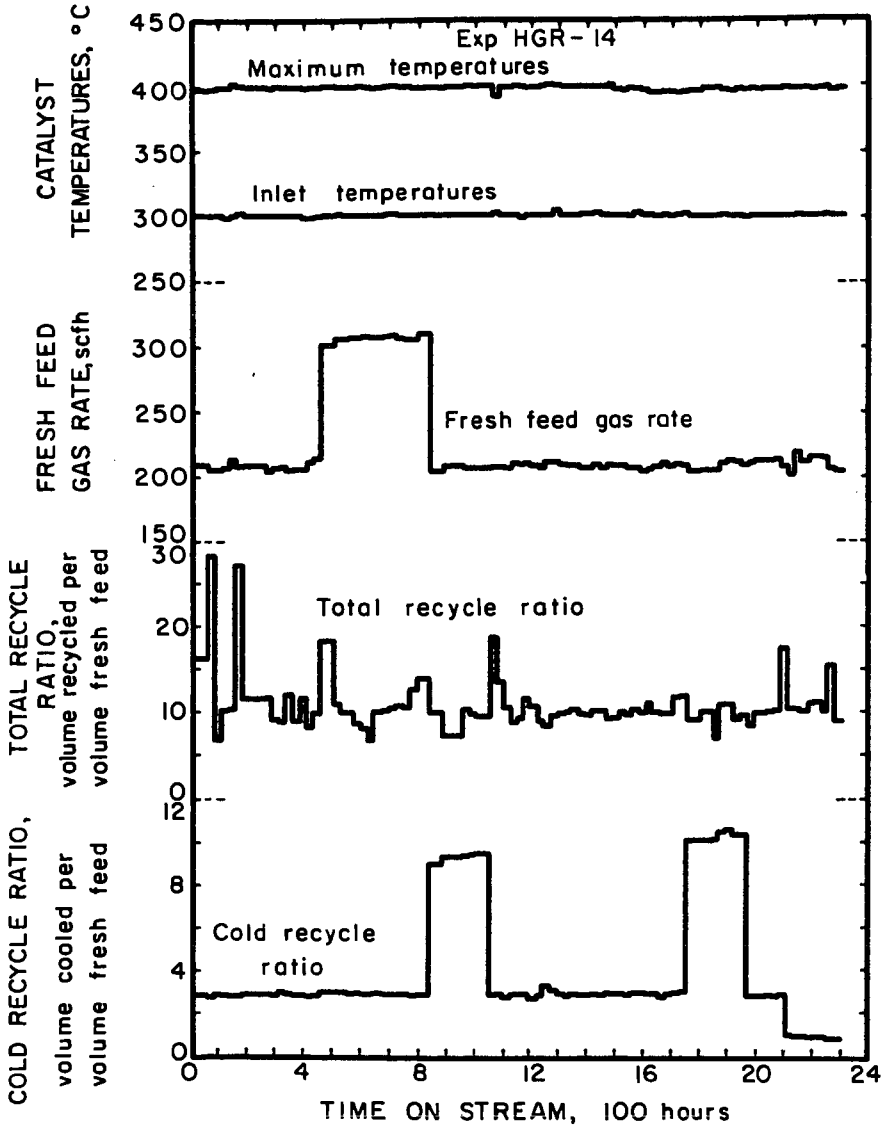


Figure 8 — Reactor conditions

L-13680

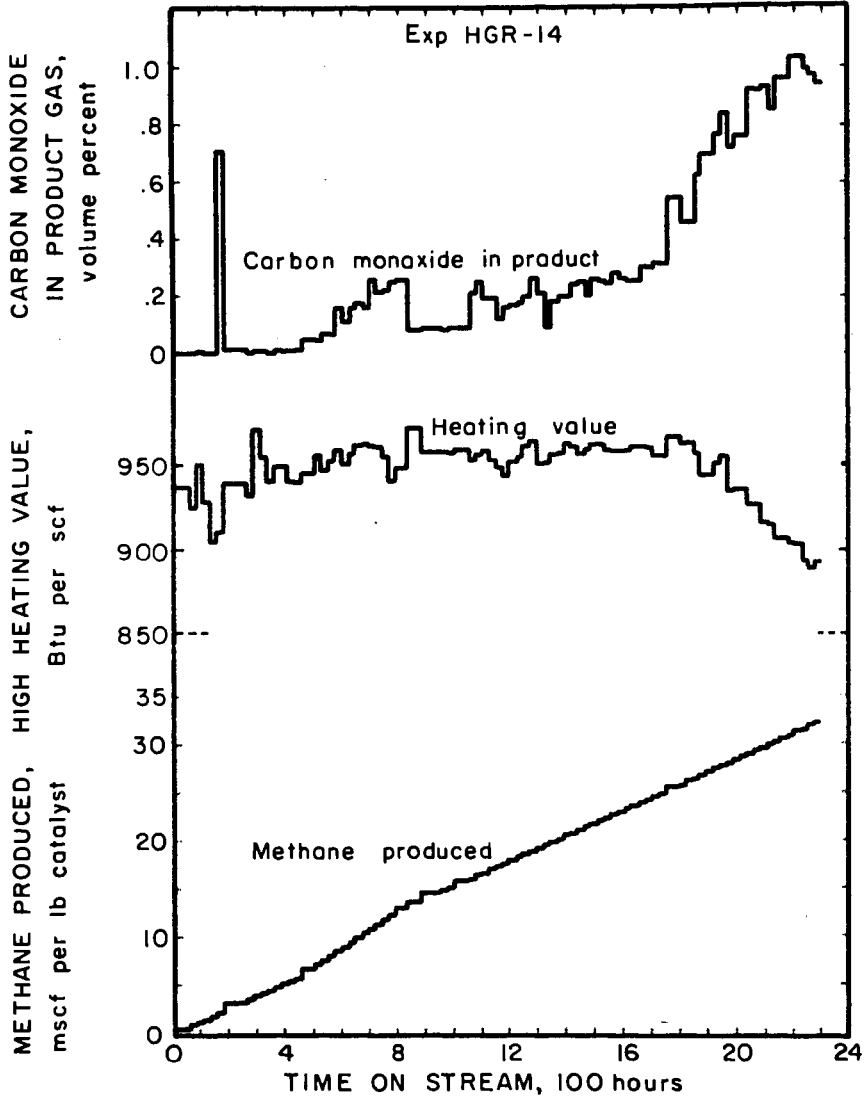


Figure 9 — Product gas characteristics

L-13679

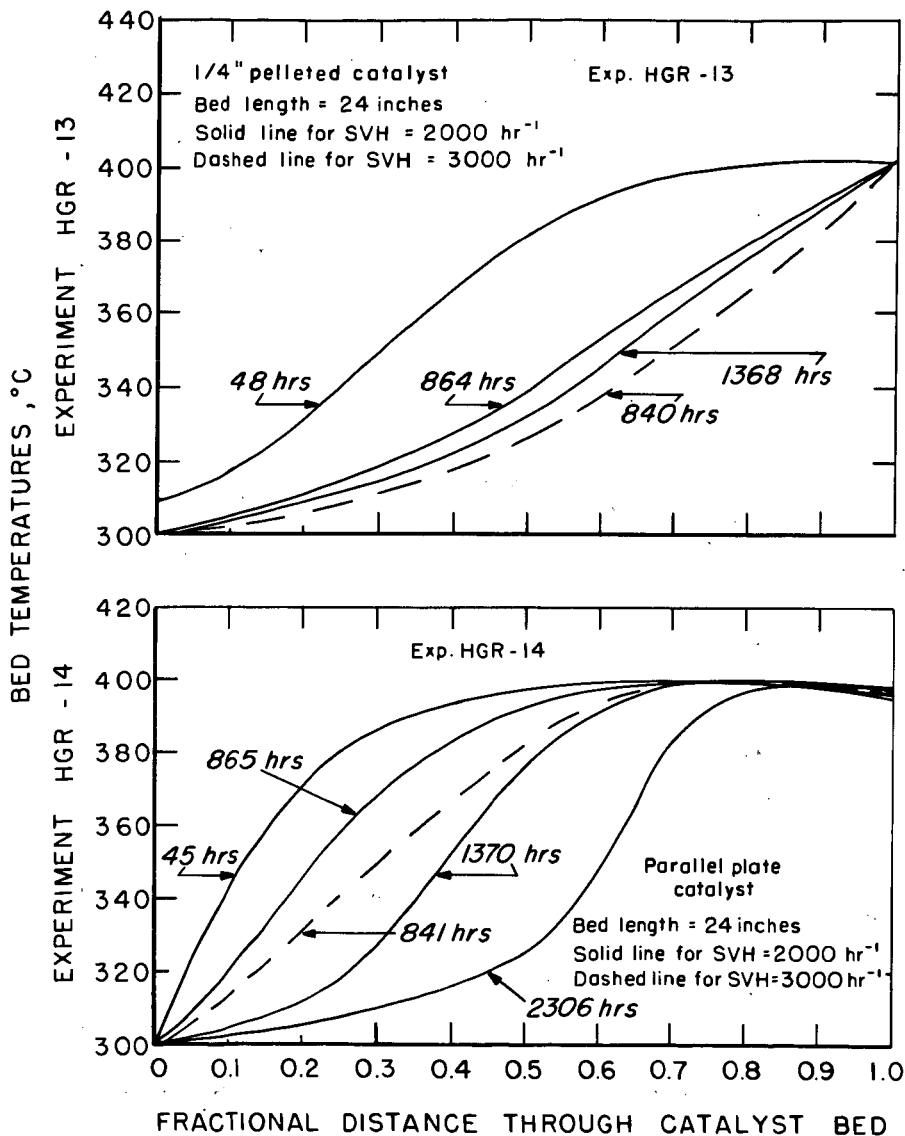


FIGURE 10-Axial temperature profiles, methanation Exp. HGR 13 and 14.

OPERATING EXPERIENCE WITH THE METHANATION UNITS IN THE HYGAS  
PILOT PLANT, W. G. Bair, Institute of Gas Technology, 4201 West 36th Street,  
Chicago, Illinois 60632

The HYGAS process includes a methanation section utilizing a fixed bed catalyst, multiple reactor stages and cold, product gas recycle for temperature control. To date about 550 hours of operation have been obtained on this unit with a wide range of  $H_2/CO$  ratio feed gases. Complete conversion (less than 10 ppm in the product gas) of CO has been obtained in all operation to date.

This paper describes the equipment, process controls, catalyst, and instrumentation of the system and gives operating conditions and results.

# LIQUID PHASE METHANATION OF HIGH CONCENTRATION CO SYNTHESIS GAS

44

Dr. David B. Blum  
Dr. Martin B. Sherwin  
Mr. Marshall E. Frank

American Chemical Society  
Division of Fuel Chemistry  
Atlantic City, New Jersey  
September 1974

## I INTRODUCTION

Development work on the Liquid Phase Methanation process commenced on April 25, 1972 and was first reviewed in October, 1972 at the 4th Annual Pipeline Gas Symposium. The development has proceeded in a very successful manner. Prior to reviewing these recent accomplishments, the basic Process and Program background will be briefly reviewed for those attendees who are not familiar with the technology.

### A. Process Background

The Liquid Phase Methanation Process is ideally suited to the safe and reliable conversion of high concentration carbon monoxide streams to methane. The exothermic heat of reaction, which under adiabatic conditions could theoretically cause temperature rises of about 1700°F in a non-recycle situation is easily removed by the inert fluidizing liquid in a near isothermal system. This is achievable by effecting the heterogeneously catalyzed reaction of the feed gases in the presence of an inert liquid phase which absorbs the large exothermic heat of reaction. The reaction proceeds to near completion in a single pass and economic studies will dictate whether a single stage reactor will be used or if a polishing reactor should be utilized in the final design.

Figure 1 illustrates the process in more detail. The inert liquid is pumped upflow through the reactor at a velocity sufficient to both fluidize the catalyst and remove the reaction heat. The low BTU feed gas is passed cocurrently up the reactor where it is catalytically converted to a high concentration methane stream. The exothermic reaction heat is taken up by the liquid mainly as sensible heat and partly by vaporization (depending upon the volatility of the liquid). The overhead product gases are condensed to remove the product water and to recover any vaporized liquid for recycle. The main liquid flow is circulated through a heat exchanger where the heat of reaction is removed by generating high pressure steam. This also provides excellent temperature control for the system.

### B. Project Background

Development of the Liquid Phase Methanation Process is included within the AGA/OCR joint program on synthetic natural gas production from coal. The development program is divided into three phases which have been proceeding in an overlapping manner. These are reviewed below:

<u>Phase</u>	<u>Object</u>	<u>Percent Completion</u>
I	Exploratory Research and Development	100
II	Construction and Operation of a Larger Scale Process Development Unit (PDU)	90
III	Construction and Operation of a Full Scale Integrated Pilot Plant	40

Completion of the program is scheduled for June 30, 1975.

## II DESCRIPTION OF EQUIPMENT

### A. Bench Scale

The bench scale reactor is 0.81" I.D. x 48" long. The nominal feed gas rate for this unit is 30 SCFH, and is supplied from premixed high pressure gas cylinders. Except for reaction temperature, the bench scale unit is substantially manually operated and controlled. The catalysts used in these studies were standard commercial methanation catalysts, ground to a 16-20 mesh size, which is compatible with the small reactor diameter.

### B. Process Development Unit (PDU)

The nominal feed gas rate for the unit is 1500 SCFH which is a scale-up of 50-100 times the bench scale unit. The methanation reactor is 4" O.D. x 84" high and the catalyst bed height can be varied from 2 to 7 feet. The basic design and flow scheme of the PDU is similar to the bench scale unit. The product gases, following analysis, are sent to an incinerator where they are thermally oxidized to carbon dioxide and water prior to discharge to the atmosphere. Sufficient instrumentation is provided for complete automatic control and monitoring from a remote control room. The reactor is fitted with movable gamma ray detector which is used to measure density differences between the source (radioactive material) and the detector. In this manner we are able to accurately determine the height of the fluidized catalyst bed under varying reaction conditions.

The overall objectives of this phase of the program are:

- Determine effect of all process variables for optimum performance.
- Determine data needed for reliable engineering design and cost estimates of larger plants.
- Determine catalyst life, recovery and regeneration methods.
- Determine liquid life and effectiveness.
- Determine whether reaction model correlation is valid for PDU performance.

### C. Pilot Plant

The third phase of the liquid phase methanation project is the design, construction and operation of a large pilot plant. The basic objectives are to demonstrate the process on a synthesis gas actually produced in a coal gasification process and obtain the necessary design and performance data such that detailed design and engineering can be accomplished for a full size (ca. 250 MM SCFD) coal gasification plant. The reactor design in the pilot plant is 2' diameter by 15' long. This we feel is large enough to provide adequate scale-up information for commercial sized reactors. Again, the design is basically the same as for the PDU and bench scale unit, but obviously modified and adapted for the larger capacity. The scheduled start-up of the pilot plant is June, 1975.

The pilot plant will be located at the site of an existing coal gasification process. At this time, the two most logical places are the IGT plant in Chicago or the CO<sub>2</sub> Acceptor plant in Rapid City, South Dakota. The design concept is to build a skid-mounted unit that could be located at either place or at other locations where coal gasification processes are under construction. With a skid-mounted unit, it could be operated at one site for a period of time and then moved to another location for testing with synthesis gas from another coal gasification process.

The design of the unit is such that it can accommodate synthesis gas feed from any one of a number of processes. The unit will be designed to handle a maximum feed gas of 2 MM SCFD at 1100 psig. This is the maximum output of the IGT Hygas plant. The LPM process can also operate at lower pressure and, hence, Rapid City would handle the lower pressure feed gas. The synthesis gas feed there is only 0.6 MM SCFD and is available at 100 psig.

### III REACTION CORRELATING MODEL

One of the goals of our experimental program in the bench scale unit was to develop the necessary correlations for use in the ultimate design of large commercial plants. With the complexity inherent in the three phase, gas-liquid-solid reaction systems, many models can be postulated. As a background to how a reaction model was finally selected, the physical situation in the three phase system is briefly reviewed.

1. The gas bubbles, after entering the reactor, rise due to convection and buoyancy. On the other hand, the presence of a solid phase retards the upward bubble motion according to its void spacing and particle size.
2. The reactants are transferred from the gas bubbles to the bulk liquid through the gas-liquid interface. Consideration of the relative resistances shows that the liquid film coefficient at the gas-liquid interface should be the least efficient mass transfer step and that the liquid phase concentration at the gas-liquid interface is governed by Henry's Law.
3. The reactants, after diffusing from the gas-liquid interface to the bulk liquid, are convected by the fluid motion to the liquid-catalyst interface.
4. Mass transfer of the reactants from the bulk liquid across the liquid catalyst interface should again be governed by the liquid film coefficient.
5. After absorbing on the catalyst surface, the reactants undergo a catalytic surface reaction.
6. The reaction products desorb and are transferred back to the gas bubbles according to Steps 4 to 1.

As our first approach to the model we considered the controlling step to be one of the following:

- The mass transfer from gas to liquid.
- The mass transfer from liquid to catalyst.
- The catalytic surface reaction step.

The other steps were eliminated since convective transport with small catalyst particles and high local mixing should offer virtually no resistance to the overall reaction scheme. Mathematical models were constructed for each of these three steps.

Our initial experimental results indicated that the kinetic model — first order in liquid phase CO concentration — was the leading candidate. We designed an experimental program then with this reaction model specifically in mind. The integrated rate expression (1) can be written as:

(1) See Appendix for nomenclature.

$$\ln \left( \frac{1}{1-X_T} \right) = \frac{k(P_T - P^*)}{K_{H_{CO}} (M/p_L) (1-2Y_{CO}^0)} \frac{W}{F^0}$$

Therefore a plot of:

$$\ln \left( \frac{1}{1-X_T} \right) \text{ as } \frac{(P_T - P^*)}{F^0} \frac{W}{(1-2Y_{CO}^0)}$$

should result in a straight line through the origin, where the slope  $k/K_{H_{CO}} (M/p_L)$  is a direct measure of the catalyst-liquid pair productivity.

### Bench Scale Results

We performed this type of process variable scan for several sets of catalyst-liquid pairs. A representative example is shown in Figure 2. In all cases, the data supported the proposed mechanism. In addition, we examined the effect of temperature on the kinetic rate constant, and a typical Arrhenius plot is shown in Figure 3. The activation energy calculated for all of the systems run in the bench scale unit fell within 18,000 to 24,000 cal/gm mole.

Data collected (see Figure 4) during these process variable scans indicated that a larger than expected amount of  $CO_2$  was also being formed. Selectivity to  $CO_2$  reached a maximum of 5-10% at about 90-95% CO conversion. At higher conversions, the  $CO_2$  level is reduced either by reverse shift and subsequent methanation of  $CO$ , or by direct methanation of  $CO_2$ . This selectivity to  $CO_2$  can be eliminated by cofeeding small amounts of  $CO_2$  (3-5%). Since multiple  $CO_2$  absorbers are required in the commercial SNG plant, one or more could be relocated downstream of the methanation step. This could offer some economic advantages since  $CO_2$  absorption would now occur at higher concentration and pressure and lower total gas flow.

### Process Development Unit Results

Work in the PDU largely paralleled the bench scale reactor tests, with one important addition - extensive three-phase fluidization studies. As we have previously mentioned, the PDU is equipped with a traversing gamma ray density detector, capable of measuring the bed density within  $\pm 0.01$  specific gravity units. In this manner we were not only able to measure and correlate fluidized bed expansion as a function of liquid and gas velocities and physical properties but we were also able to determine the individual phase volume fractions. The two major findings of this work were (see Figure 5); (1) the absolute values for the gas holdup are 3-4 times greater than the incremental porosity increase due to the gas flow at constant liquid flow, and (2) the gas holdup is essentially independent of liquid velocity for  $1.3 U_{mf} < U_L < 2.5 U_{mf}$ . In addition, the data for all the catalysts indicated that the maximum gas volume fraction obtainable was on the order of 0.5-0.6.

Reaction studies were carried out in the PDU in order to verify the correlating model developed in the bench scale unit. This provides data applicable to the scale-up design required for the pilot plant, and ultimately, the commercial unit. The initial work in the PDU was performed with particles much larger ( $1/8"$ - $3/16"$ ) than those used in the bench scale unit ( $< 1/32"$ ), and the reaction rates for

these larger particles were about one-third the rates obtained with the smaller size particles (compare Figures 2 and 6). In addition, the activation energy obtained with this data was on the order of 11,000 cal/gm mole; just about one-half the value obtained in the bench unit (compare Figures 3 and 7). These results suggested that we were encountering pore diffusion limitations, and we attempted to verify this result by investigating still smaller particles (1/16"). While the reaction rates increased significantly, as they should, the activation energy remained essentially unchanged, indicating that we were still in the pore diffusion regime. Therefore, we can still further increase productivity by simply reducing particle size. This should not be too difficult since 1/32" particles are already being used in analogous commercial systems. The ultimate productivity obtainable has not yet been accurately defined, although we are confident that a vapor hourly space velocity of 4000 hr<sup>-1</sup> at 1000 psig and 650°F with a feed containing 20% CO, 60% H<sub>2</sub>, and 20% CH<sub>4</sub> should result in a CO conversion of 95-98%. One should bear in mind that these results do in fact confirm the first order reaction rate model proposed as a result of the earlier bench scale results. Future work will concentrate on the effect of axial dispersion arising from the varying geometries encountered during scale-up and on determining the optimum particle size for the commercial unit.

In an attempt to define useful catalyst life, we have conducted continuous runs of 2 and 4 weeks duration. These results have been encouraging in that after an initial period of deactivation over the first 50-100 hours (common with nickel hydrogenation catalysts), the catalyst reaches an equilibrium productivity in excess of our original design basis of a VHSV equal to 4000 hr<sup>-1</sup> at 1000 psig and 650°F. Considering these results, and our substantial experience with all types of catalysts, we have every reason to believe that a catalyst life in excess of one year can be achieved at which point catalyst replacement costs are insignificant on overall SNG economics.

#### IV CONCLUSIONS

Based on this past work and ongoing experiments, we feel that the Liquid Phase Methanation process promises to become an economic, reliable and versatile means of converting synthesis gas mixtures to high BTU gas. Chem Systems believes this technology to be a key step in the transformation of fossil feeds to pipeline gas and we look forward to its successful application in commercial coal gasification plants.

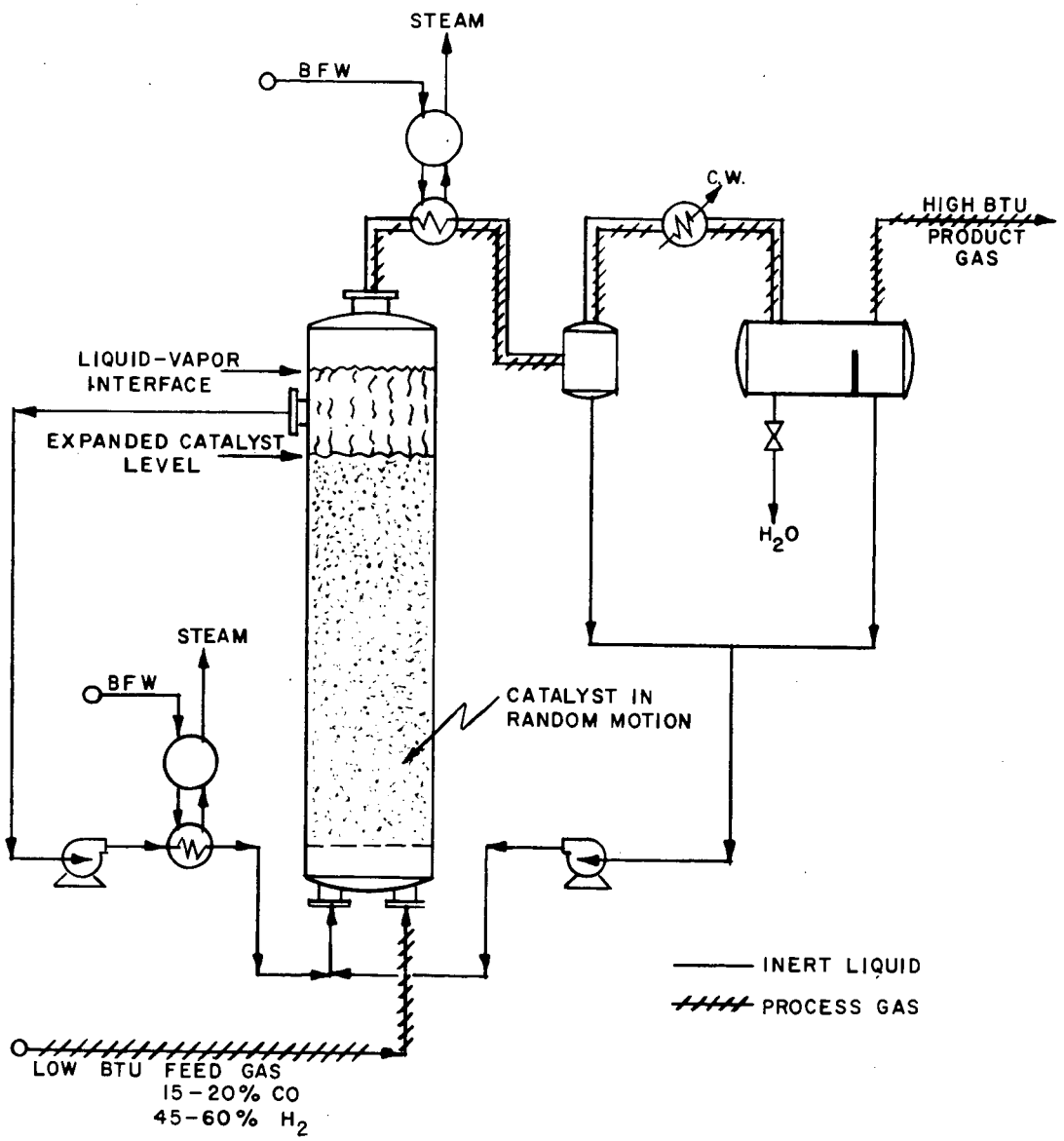
$e_G$	= Gas Phase Volume Fraction
$e_L$	= Bed Porosity; Liquid Only Fluidizing
$e_{LG}$	= Bed Porosity; Liquid and Gas Fluidizing
$F$	= Gas Flow Rate at any Position; g moles/sec
$k$	= Reaction Rate Constant; g moles/sec-gm catalyst-(g mole/cm <sup>3</sup> )
$K_H$	= Henry's Law Coefficient; atm/mole fraction
$M$	= Liquid Phase Molecular Weight; gm/g mole
$\rho_L$	= Liquid Phase Density; gm/cm <sup>3</sup>
$P_T$	= Total Pressure; atm
$P^*$	= Liquid Phase Vapor Pressure; atm
$T$	= Temperature, °K
$U_{mf}$	= Minimum Fluidization Velocity; cm/sec
$U_{OG}$	= Superficial Gas Velocity at Reactor T and $P_T$ ; cm/sec
$W$	= Weight of Catalyst; gms
$X_T$	= Fraction of CO Converted

Super Script

$^0$  = Initial Condition

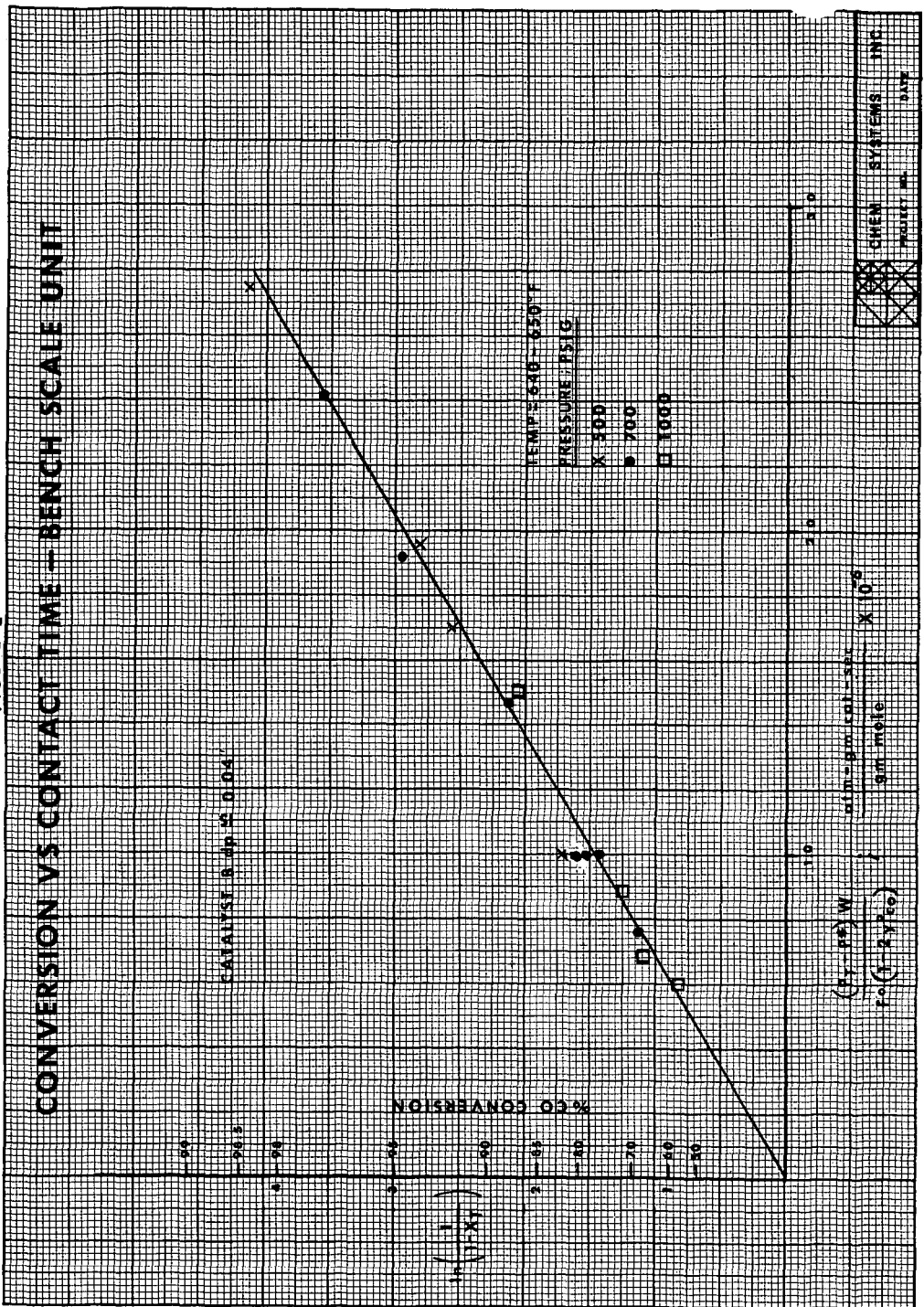
**FIGURE 1**

**LIQUID PHASE METHANATION PROCESS SCHEMATIC**



	CHEM SYSTEMS INC.
	PROJECT NO.      DATE

FIGURE 2



CHEN SYSTEMS, INC.  
PROJECT NO. \_\_\_\_\_ DATE \_\_\_\_\_

FIGURE 3

TEMPERATURE EFFECT ON KINETIC RATE CONSTANT  
BENCH SCALE UNIT

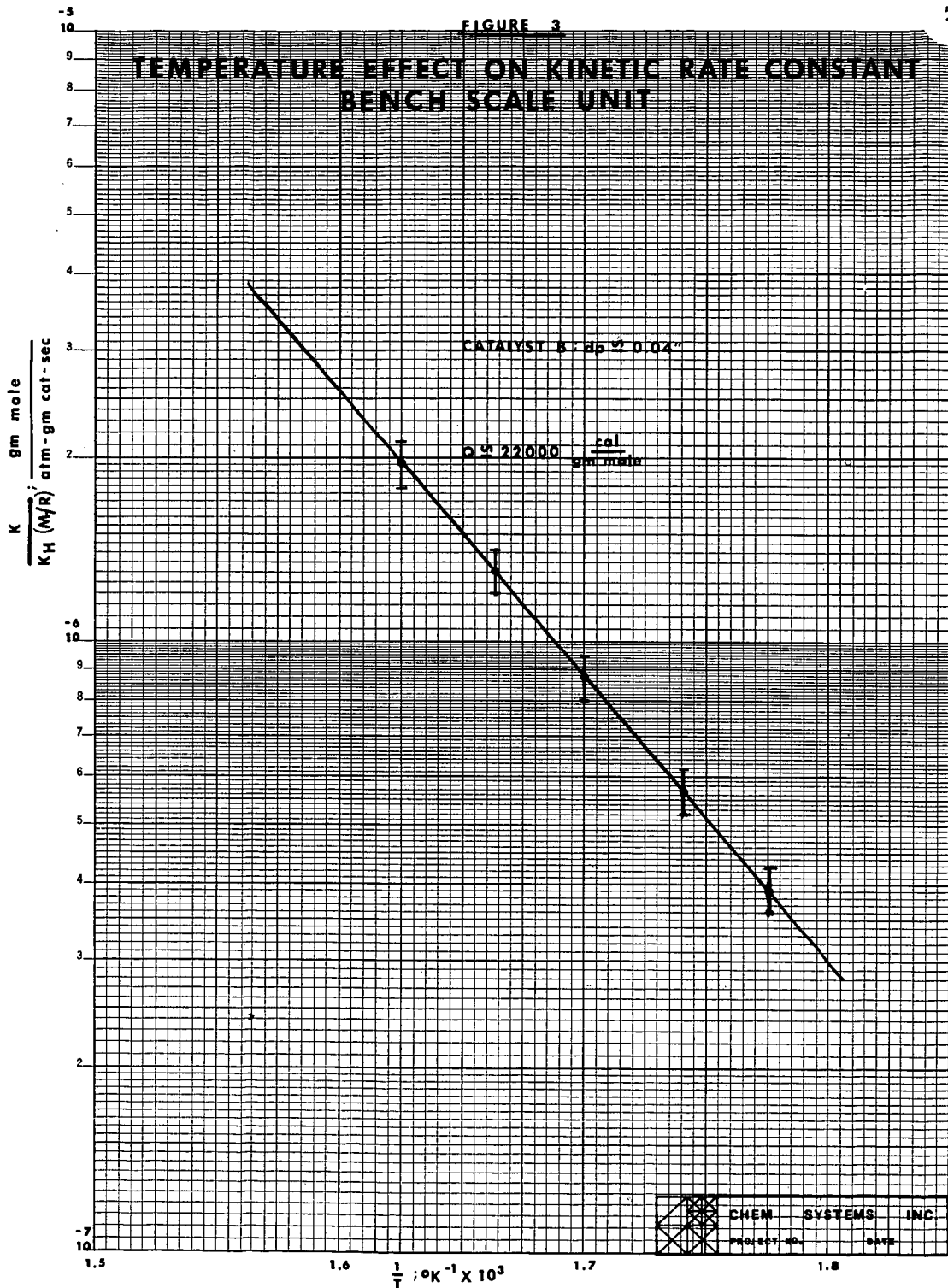


FIGURE 4

# CO<sub>2</sub> SELECTIVITY VS CO CONVERSION

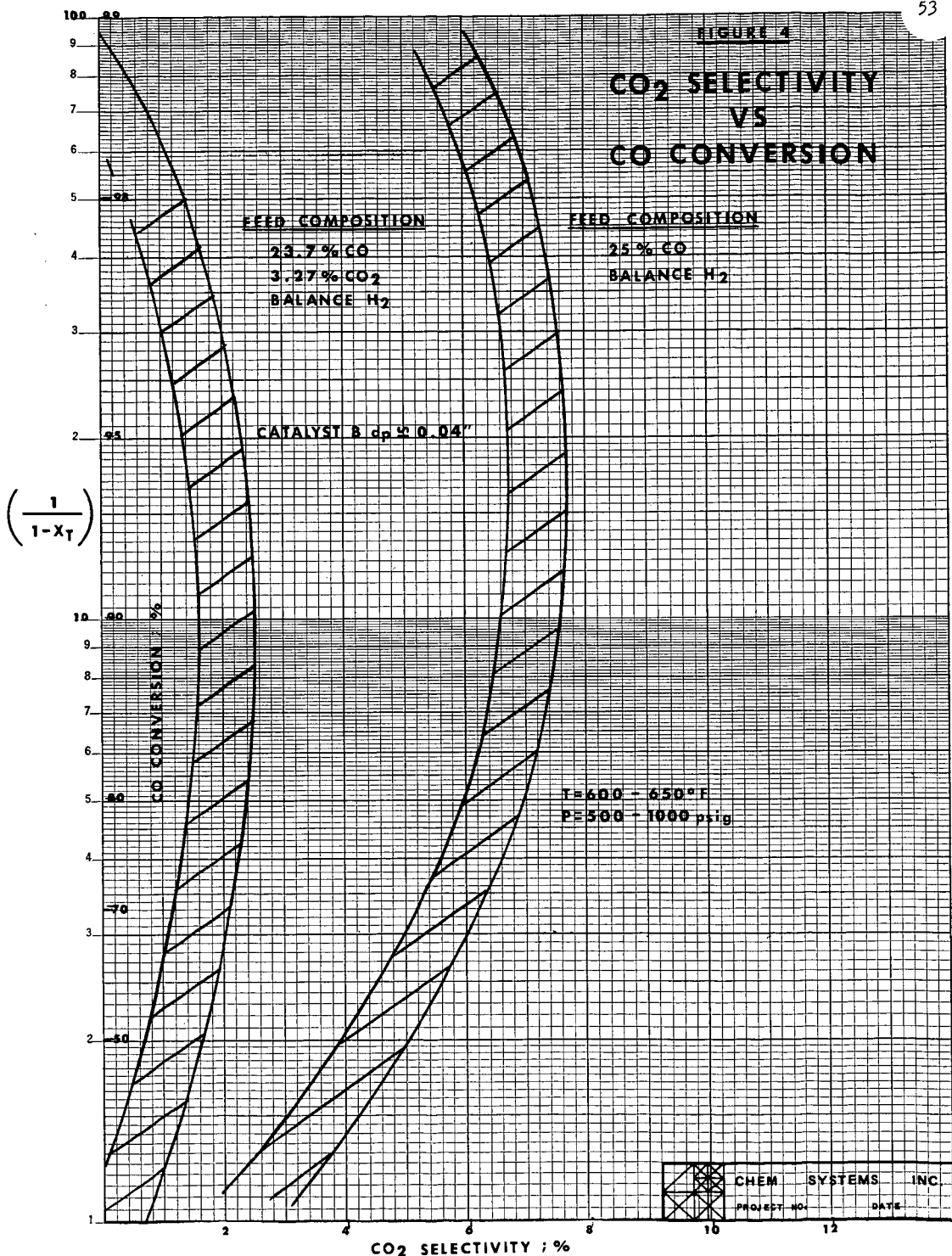
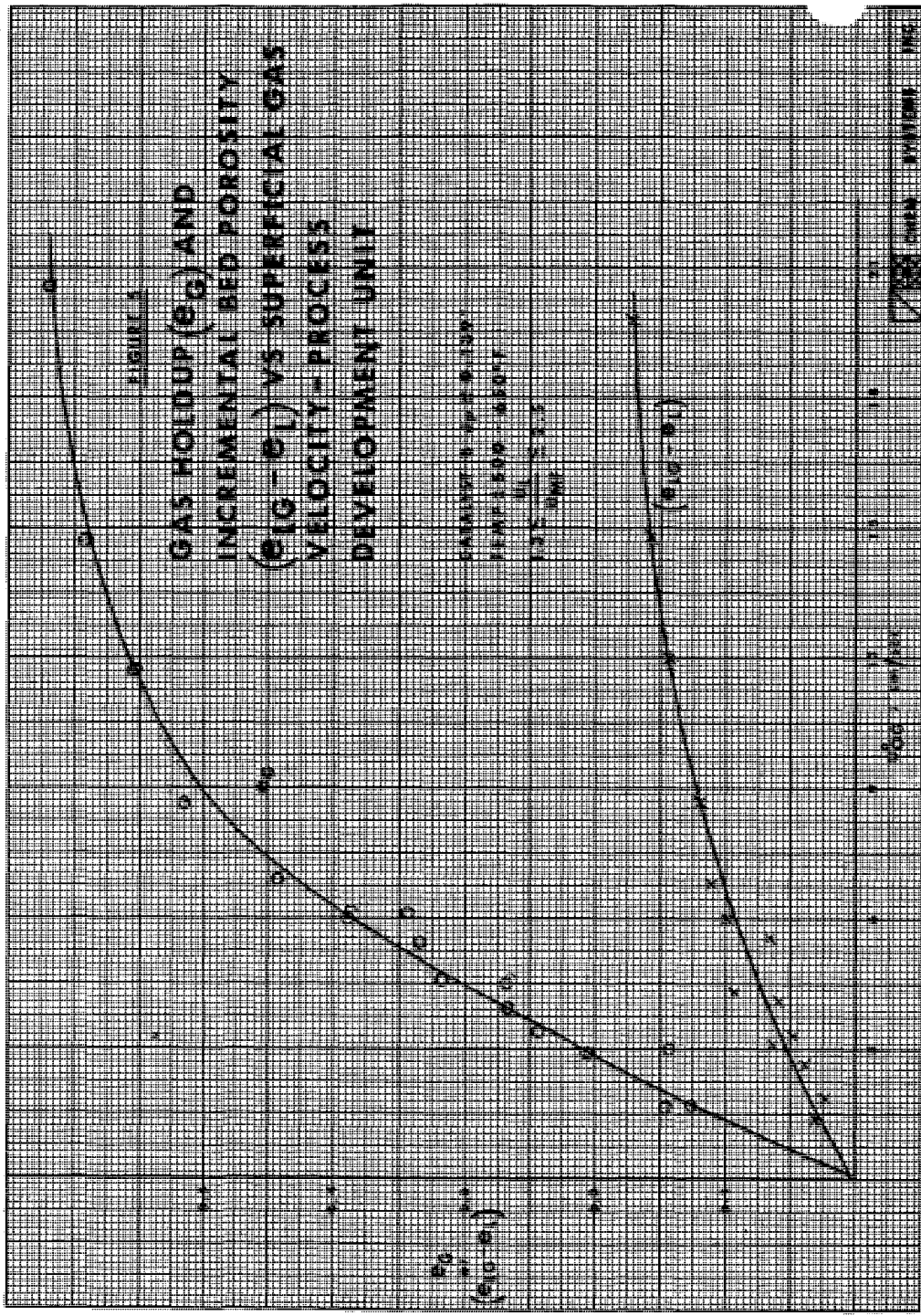


FIGURE A  
 GAS HOLDUP ( $\epsilon_G$ ) AND  
 INCREMENTAL BED POROSITY  
 ( $\epsilon_G - \epsilon_L$ ) VS SUPERFICIAL GAS  
 VELOCITY - PROCESS  
 DEVELOPMENT UNIT

DATA FROM A. J. W. B. J. VAN  
 DER WERF, 1967  
 P. 105-106



PROJECT NO. \_\_\_\_\_

DATE \_\_\_\_\_

FIGURE 3

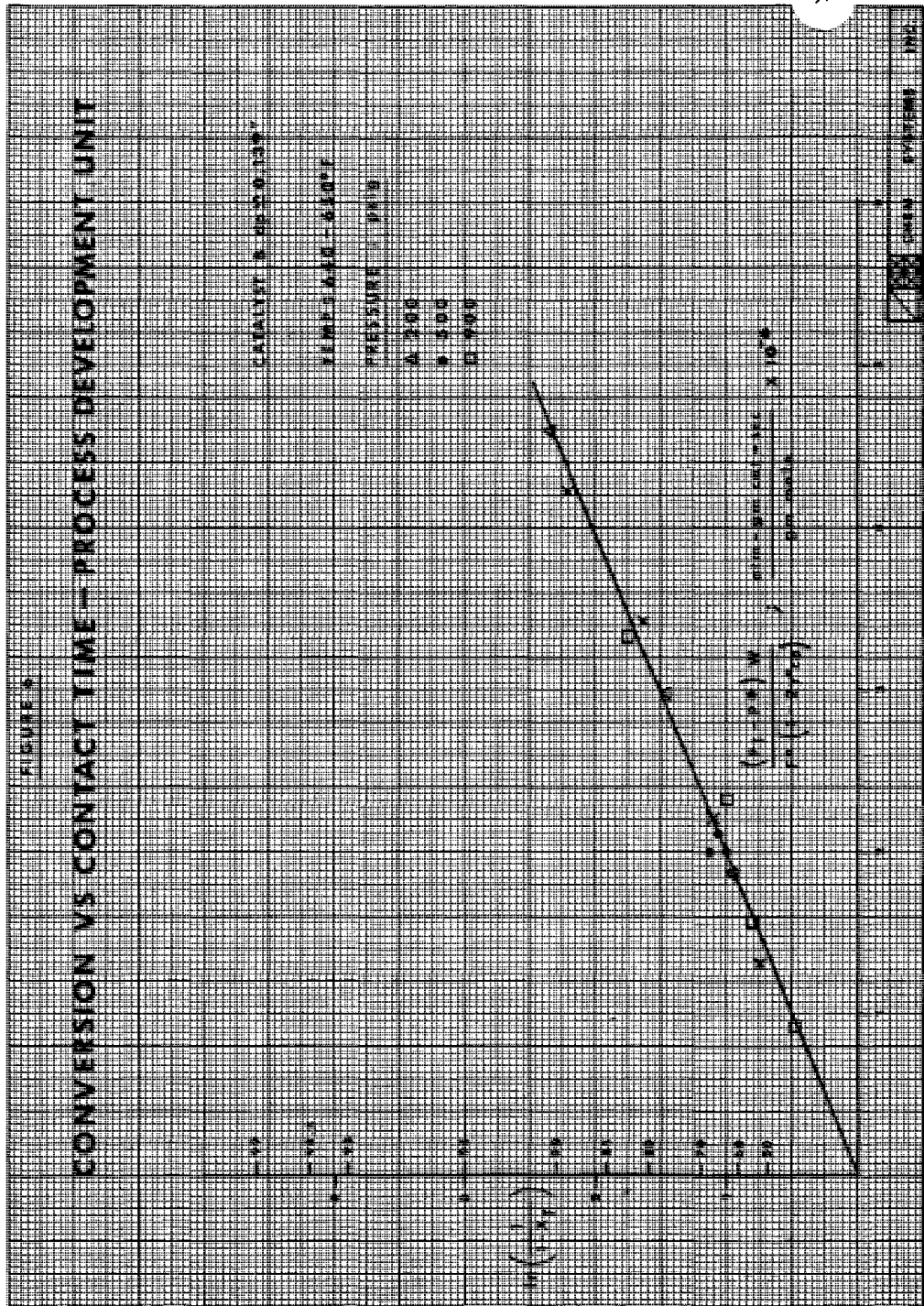
CONVERSION VS CONTACT TIME - PROCESS DEVELOPMENT UNIT

CATALYST: R-28350-1367

TEMPERATURE: 530°F

PRESSURE: 100 PSIG

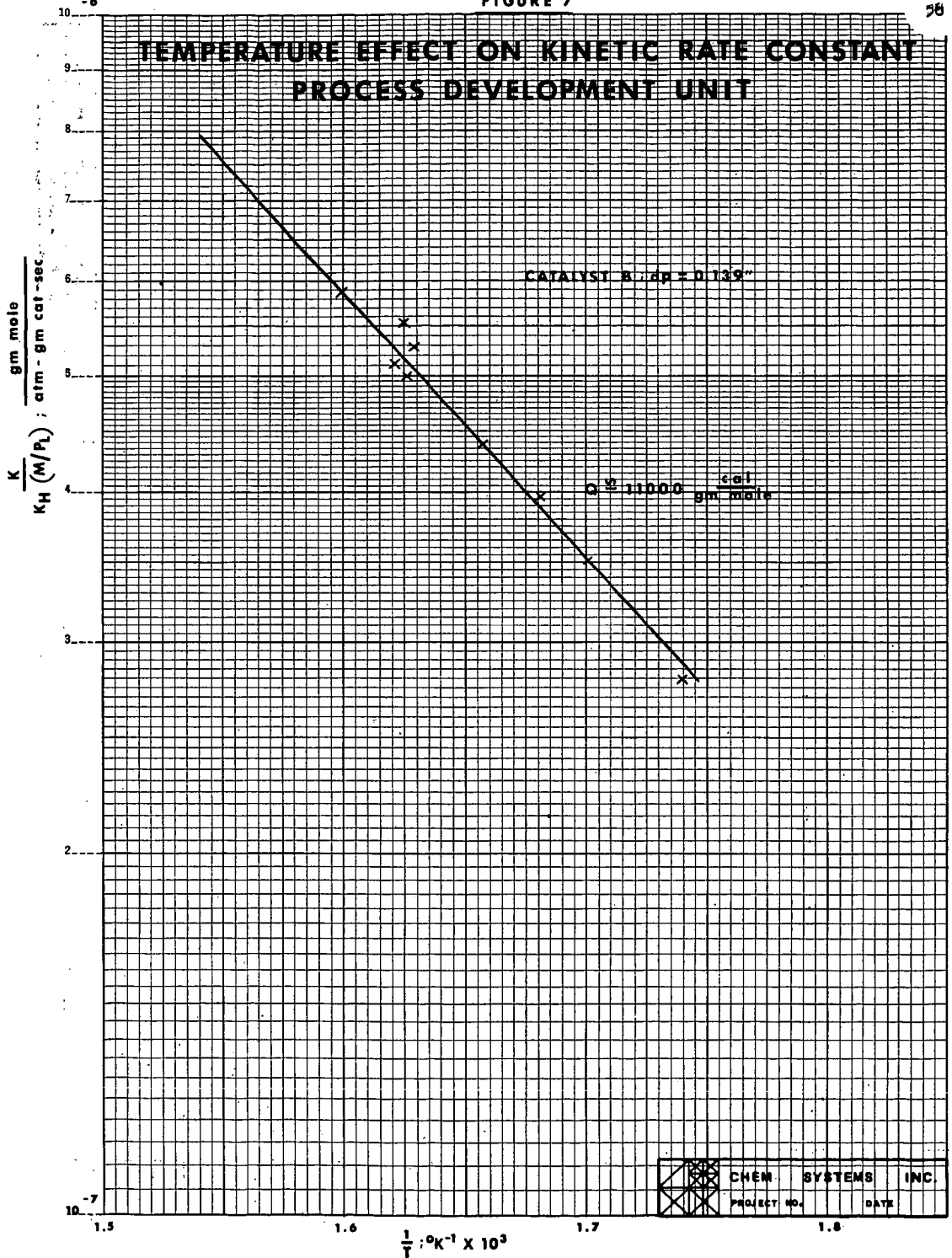
- A: 200
- B: 300
- C: 400
- D: 500



DESIGN  
 CHECKED  
 PROJECT NO. \_\_\_\_\_  
 DATE \_\_\_\_\_

FIGURE 7

TEMPERATURE EFFECT ON KINETIC RATE CONSTANT  
PROCESS DEVELOPMENT UNIT



## THE RMPROCESS

G. A. WHITE, T. R. ROSZKOWSKI, D. W. STANBRIDGE

THE RALPH M. PARSONS COMPANY

PASADENA, CALIFORNIA 91124

## INTRODUCTION

Current specifications for pipeline gas dictate that most gasification processes require an upgrading of their crude syngas by a stage of methanation. The upgrading reduces the concentration of hydrogen and carbon monoxide while increasing the heating value of each cubic foot of gas. The RMP process has demonstrated an unusual upgrading capability by methanating, without recycle, a crude syngas of approximately 50 percent hydrogen and 50 percent carbon monoxide and containing less than 1 percent methane. The process has exceptionally wide applicability for gases produced by any coal gasification system from near atmospheric pressure to over 1000 psig.

## PROCESS DESCRIPTION

In the process, desulfurized syngas flows through a series of fixed-bed adiabatic catalytic reactors. Between reactors, heat is removed from the system by the generation of high pressure steam in conventional heat exchange equipment. As the flow progresses through the series of reactors and exchangers and the bulk of the syngas is methanated, the temperature of the process gas is progressively lowered, finally resulting in an adequately reduced temperature favorable for achieving a high conversion efficiency of hydrogen and carbon oxides to methane.

The series of reactors and exchangers which methanates a raw syngas without pretreatment other than desulfurization, is collectively termed bulk-methanation. The chemical reactions which occur in bulk methanation, including both shift conversion and methanation are moderated by the addition of steam which establishes the thermodynamic limits for these reactions thereby controlling operating temperatures. The flow sequence through bulk methanation is shown in Figure 1.

## EXAMPLE AT 400 PSIA

The conditions selected for illustration here include desulfurized syngas available at 700°F and 400 psia, consisting of 49.8 percent hydrogen, 49.8 percent carbon monoxide, 0.1 percent carbon dioxide and 0.3 percent methane. As shown in Figure 1, 40 percent of this syngas is mixed with superheated steam and the mixture enters the first bulk methanator at 900°F. The principal reaction occurring in this reactor is shift conversion with only a minor degree of methanation. The first reactor effluent is cooled and mixed with an additional 30 percent of the syngas to give a mixed temperature of 1000°F into the second bulk-methanation reactor. Again the second reactor effluent is cooled by the generation of steam, mixed with the remaining 30 percent of the syngas to give a mixed temperature of 1000°F as feed to the third reactor.

In the fourth, fifth and sixth reactors, the inlet temperatures are controlled at 1000°F, 600°F and 500°F respectively which results in a bulk methanated product-gas whose composition is shown in Figure 2. The operating temperatures and pressures for each reactor in bulk-methanation are also shown in Figure 2. The residual hydrogen content leaving the sixth reactor is less than 10 volume percent on a dry basis. Such a gas can then be methanated in a final "dry" stage following carbon dioxide removal, to reduce the hydrogen content to below 3 percent, and leaving less than 0.1 percent carbon monoxide.

#### EXAMPLE AT LOW PRESSURE

A similar set of design numbers are shown in Figure 3 when operating at near atmospheric pressure. Inlet pressure to the first bulk-methanator reactor is 65 psia and the outlet pressure from the sixth reactor is 22 psia. In this case, the total syngas is introduced into the first bulk-methanation reactor together with the total steam. Because the driving force for methanation is proportionately lower at the lower pressure, the outlet temperature even from the first reactor is below 1400°F. Significantly, leaving the sixth reactor, the hydrogen content of the effluent gas on a dry basis is only 12.1 percent at 22 psia compared to 9.3 percent when operating at 312 psia. This relatively small difference is not entirely surprising in view of the lower operating temperature and the large excess of carbon dioxide present in each case which tends to mask the difference in operating pressure.

#### DESIGN FEATURES

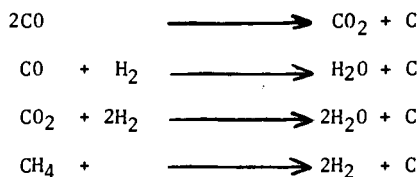
Whether operating at high pressures or low, reactor outlet and inlet temperatures are all conveniently high for the economical generation of 1500 psig steam in conventional heat exchange equipment. Of the total steam produced, approximately one-third is used in the RMP process to accomplish shift conversion, methanation and carbon dioxide regeneration. The mechanical energy of even that portion of the produced steam needed for the operation of the process, will provide a part of the total power requirement of a coal gasification complex by using back pressure turbines. The bulk of the steam produced, approximately two-thirds of the methanation heat, is available as export steam at 1500 psig for any services within a complex.

Now referring back to Figure 1, it is to be noted that there is no separate shift conversion system and no recycle of a product gas for temperature control. Rather, this system is designed to operate adiabatically at elevated temperatures with sufficient steam addition to cause the shift reaction to occur over a nickel catalyst while avoiding carbon formation. The refractory lined reactors contain fixed beds of catalysts and are of conventional designs. The reactors can be a minimum diameter for a given plant capacity since the process gas is once-through only with no recycle, employing less steam than is conventional for shift conversion alone and using a catalyst of a standard ring size of 5/8 x 1/4 inches.

#### AVOIDING ZONES OF CARBON FORMATION

Before proceeding further with methanation into the cleanup stage, it would be well to review some of the design and operating problems which have been experienced by most developers of methanation systems. Specifically, carbon formation and catalyst sintering are two of the more common problems confronting methanation processes. When considering carbon formation, reference is made to its

potential production from carbon oxides and methane as illustrated by the following equations.



The prediction of conditions favorable for the formation of carbon from these sources can be made by straightforward thermodynamic calculations. However, because a number of other chemical reactions can occur simultaneously and since relative reaction rates are not well known, it is useful to know whether a specified mixture of syngas and steam would have a thermodynamic potential for carbon formation when at chemical equilibrium.

To assist in the proper visualization of multiple chemical reactions occurring simultaneously, we have developed a ternary diagram simplified by considering only the concentration levels of the principal chemical elements present in mixtures of syngas and steam. Carbon, hydrogen and oxygen are used as the identifying elements in our system; these elements are located at the three apexes of the ternary diagram shown in Figure 4. A number of chemical compounds are shown on this figure when the elements are appropriately balanced with one another. Hydrocarbons such as methane and butane are on the left of the figure, carbon oxides on the right and water on the base line connecting hydrogen and oxygen.

Figure 5 has superimposed on the ternary, carbon isotherms for a pressure of 30 psia. Interpretation of the isotherms shows that mixtures of the elements which fall above the curves are in the carbon forming region when at chemical equilibrium. Mixtures of the elements which fall below the curves are outside the carbon forming region at equilibrium. Gas mixtures falling within the family of curves should be at an operating temperature that will carry the specified concentration of carbon in the vapor phase.

Figure 6, which represents a family of carbon isotherms at 400 psia, shows that in certain areas of the diagram, elevated temperatures support higher concentrations of carbon in the vapor phase, but in other areas, lower temperatures favor higher concentrations of carbon. So depending upon the element-mix of gases feeding a methanation reactor, an increase in temperature could cause a mixture to approach a condition where carbon could theoretically be formed. Since these figures are based on equilibrium concentrations of chemical compounds, temperature excursions into the carbon formation region may not result automatically in the formation of solid carbon since such reactions may occur at such a slow rate as to be negligible. On the other hand, it is not good practice to design a system that is normally operating under conditions that are theoretically favorable for carbon formation and depend upon kinetics to keep the operation out of trouble.

The mathematical properties of the set of equations describing chemical equilibrium in the synthesis gas system indicate that the carbon producing regions are defined solely by pressure, temperature and elemental analysis. Once a safe blend of reactants has been determined by use of the ternary, the same set of equations which was used to derive the ternary may be used to determine the gas composition.

Figure 2, gives gas compositions which represent proposed operating conditions at the pilot plant. Figure 7 shows where two compositions are located on the ternary diagram relative to the potential for carbon formation: (1) the feed gas composition to the first bulk-methanation reactor and (2) the product composition from the third reactor which then remains a fixed point throughout the remaining reactors since no addition of gas is made beyond the third reactor. From this figure, it can be seen clearly that sufficient steam has been added to move the mixture well outside the carbon formation region. Even after adding the total syngas to the system, it is not theoretically possible to form carbon when the system is at chemical equilibrium.

It will be quickly recognized that feed-gases to most, if not all, methanation systems for SNG production, are theoretically capable of forming carbon. This potential also exists for feed-gases to all first stage shift converters operating in ammonia plants and in hydrogen production plants. However, it has been commercially demonstrated over a period of many years that carbon formation at inlet temperatures to shift converters is a relatively slow reaction and that once shifted, the gas loses its potential for carbon formation. Carbon formation has not been a common problem at the inlet to shift converters and it has been no problem at all in our bench-scale work and it is not anticipated that it will be a problem in our pilot plant operations.

For a clearer understanding of the behavior of syngases in a shift converter, we have established another set of carbon isotherms when considering the shift reaction only (without methanation) in addition to the carbon forming reactions. Figure 8 shows isotherms at a partial pressure of 270 psia for all components of a gas mixture but excluding methane. Figures such as this are helpful when establishing inlet conditions to reactors since operating data from commercial plants can be used as points of reference.

#### CLEAN-UP METHANATION

Returning now to the cleanup stage of methanation, Figure 9 shows a system wherein final methanation occurs following gas cooling and removal of steam, and a reduction of carbon dioxide down to approximately 4 percent. Under these conditions, and at a pressure of 300 psia, residual hydrogen is less than 3 percent and carbon dioxide is less than 2 volume percent of the dry product gas following methanation. When operating at near atmospheric pressure, reduction of steam and carbon dioxide are followed by compression to either an interstage level or to delivery pressure for the final stage of methanation. For all pressure levels, the final stage of methanation is outside the region of carbon formation.

Carbon dioxide can be removed from the effluent gas from bulk methanation by any one of several conventional absorption systems. At this point in the process, the gas that must be treated for carbon dioxide removal is less than half of the volume of a shifted gas from which carbon dioxide is normally removed when preparing a syngas to approach stoichiometric concentrations of reactants for methanation. Finally, the gas would be dried to a nominal 7 pounds of water per million scf of gas.

## CONCLUSION

Advantages of the RMPProcess are related particularly to cost savings in both capital equipment and operating requirements.

1. Shift conversion. The shift reaction and methanation proceed concurrently without interference over bulk-methanation catalyst thereby eliminating the need for a separate shift conversion operation.
2. Steam utilization. Less steam is employed in the RMPProcess than is required for conventional shift conversion even though in other methanation processes as little as one-half of the total syngas is processed through shift conversion to achieve a near-stoichiometric balance of hydrogen and carbon monoxide for methanation.
3. Temperature control. Temperature control is by steam addition. There is no gas recycle and therefore no recycle compressor.
4. Steam production. The RMPProcess operates at temperatures generally above 1000°F providing a large temperature difference for the production of high pressure steam. Because of this, we can produce more steam and produce it at a higher pressure with less heat transfer surface than other processes.
5. Carbon dioxide removal. Aside from contained carbon dioxide which is removed from syngas when absorbing hydrogen sulfide, the total carbon dioxide produced in the methanation system is removed by conventional absorption in a single stage operation where the volume of gas to be treated is a minimum and the partial pressure of the carbon dioxide is a maximum.
6. Low pressure operation. By using the driving force of a large excess of carbon dioxide for methanation when operating at low pressures, bulk methanation can accomplish a high degree of syngas conversion thereby requiring only a single stage of final methanation following compression to meet pipeline SNG specifications. Such an operation reduces the compression duty by reducing the volume of syngas to a fraction of its original volume while still at low pressure.
7. Space velocity. Most of our experimental data has been developed when operating at a wet outlet space velocity of approximately 10,000 volumes per volume per hour. However, we have data at space velocities up to 25,000. The pilot plant will operate in the range of 5,000 when processing 1 million scfd of raw syngas. Operating on a once-through basis without recycle and at the indicated space velocities, catalyst volumes are a minimum compared with other processes when identical over-design factors are used.

Acknowledgement is sincerely made to Catalyst Consulting Services, Inc. of Louisville, Kentucky, in particular to Dr. Harold W. Fleming, for unusual services of the highest quality while directing the bench-scale experimental program which provides the technical basis and support for the RMPProcess.

FIGURE 1 - BULK METHANATION

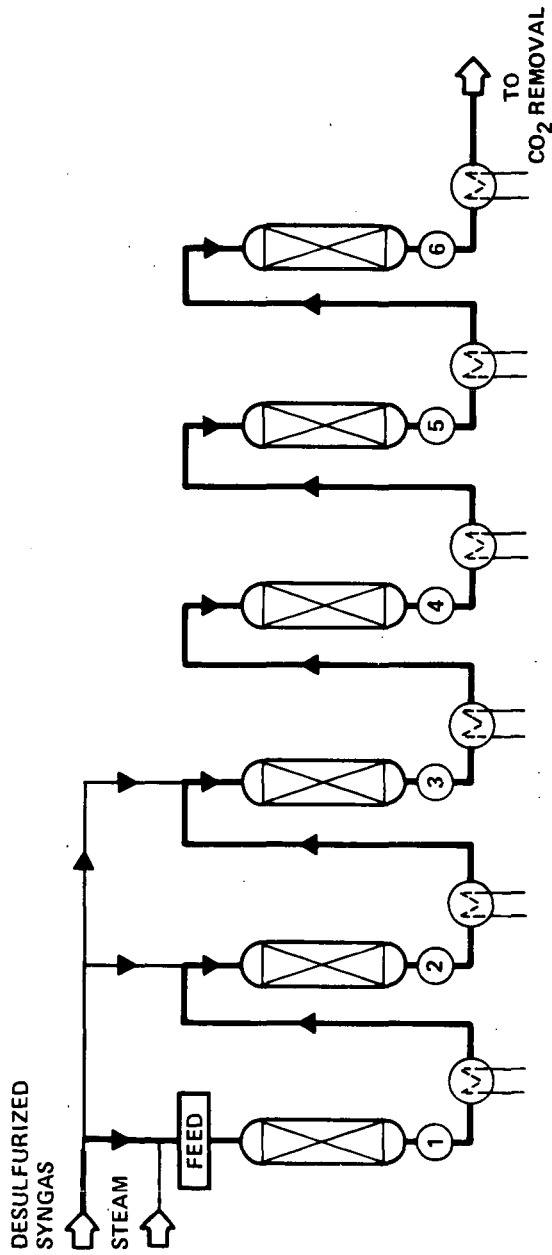


FIGURE 2 - METHANE PRODUCTION @ 400 PSIA

Reactor No.	Feed		-----Outlet-----					
	<u>1</u>	<u>1</u>	<u>2</u>	<u>3</u>	<u>4</u>	<u>5</u>	<u>6</u>	
Composition, Vol %								
H <sub>2</sub>	49.80	54.53	48.07	43.09	36.90	22.86	9.29	
CO	49.80	13.97	18.46	20.63	15.25	5.64	.87	
CO <sub>2</sub>	0.10	25.80	24.04	23.64	29.21	39.90	46.84	
CH <sub>4</sub>	<u>0.30</u>	<u>5.70</u>	<u>9.43</u>	<u>12.64</u>	<u>18.64</u>	<u>31.60</u>	<u>43.00</u>	
	100.00	100.00	100.00	100.00	100.00	100.00	100.00	
Steam/Gas	1.20	0.88	0.56	0.43	0.50	0.65	0.83	
Pressure, psia	397	387	372	357	342	327	312	
Temperature °F	900	1424	1434	1423	1322	1119	881	

FIGURE 3 - METHANE PRODUCTION @ 65 PSIA

Reactor No.	Feed		-----Outlet-----					
	<u>1</u>	<u>1</u>	<u>2</u>	<u>3</u>	<u>4</u>	<u>5</u>	<u>6</u>	
Composition, Vol %								
H <sub>2</sub>	49.80	54.38	50.36	46.50	36.29	24.00	12.05	
CO	49.80	25.37	20.42	16.27	8.24	2.69	0.49	
CO <sub>2</sub>	0.10	17.29	21.99	26.06	34.62	41.83	46.45	
CH <sub>4</sub>	<u>0.30</u>	<u>2.96</u>	<u>7.23</u>	<u>11.17</u>	<u>20.85</u>	<u>31.48</u>	<u>41.01</u>	
	100.00	100.00	100.00	100.00	100.00	100.00	100.00	
Steam/Gas	0.48	0.29	0.33	0.36	0.47	0.62	0.78	
Pressure, psia	62	57	50	43	36	29	22	
Temperature °F	900	1373	1259	1180	1037	884	718	

**FIGURE 4**  
Element Coordinates  
Raw Materials, Intermediates and Products

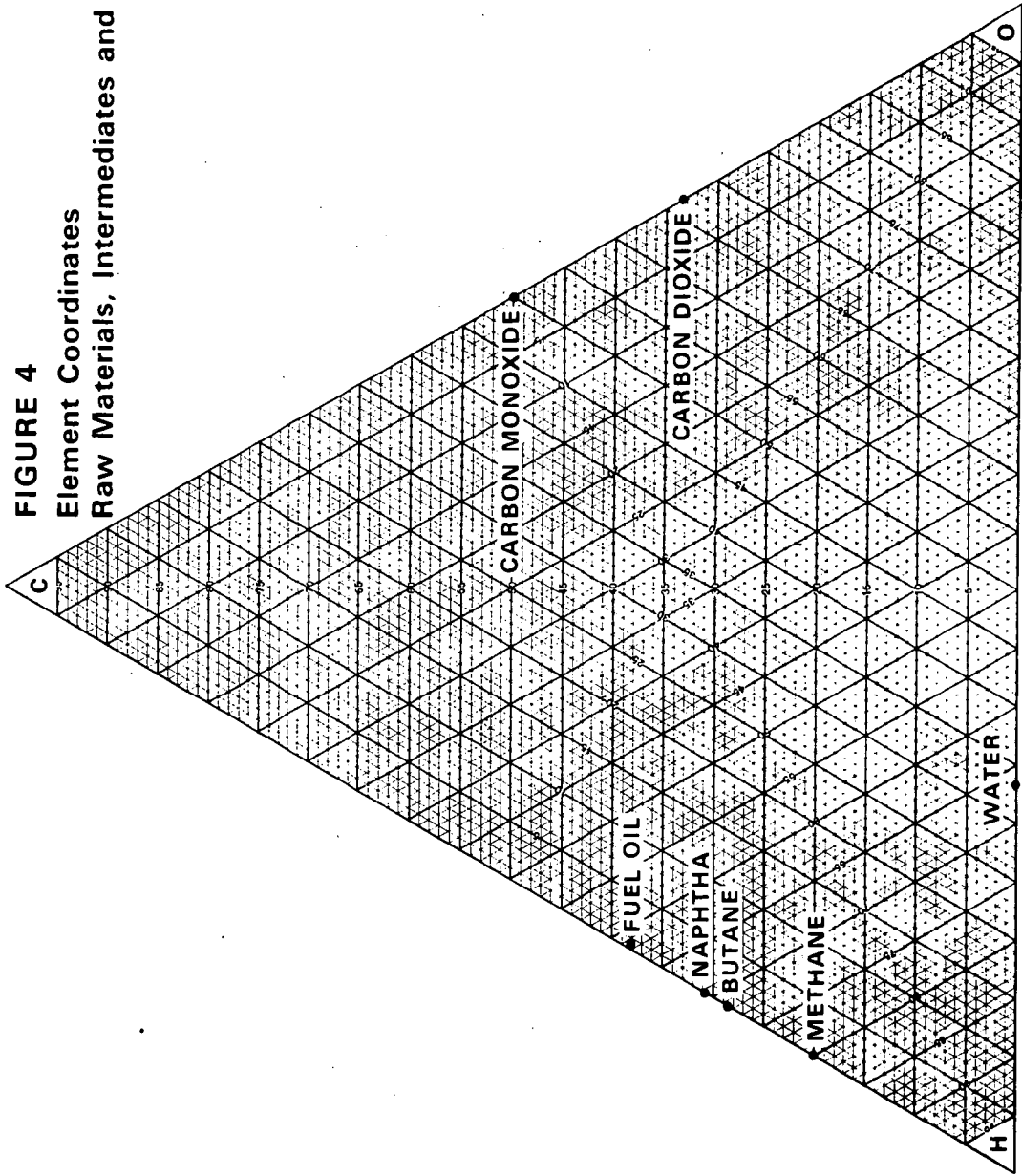


**FIGURE 5**  
Carbon Formation  
Equilibrium Isotherms at 30 psia, °F

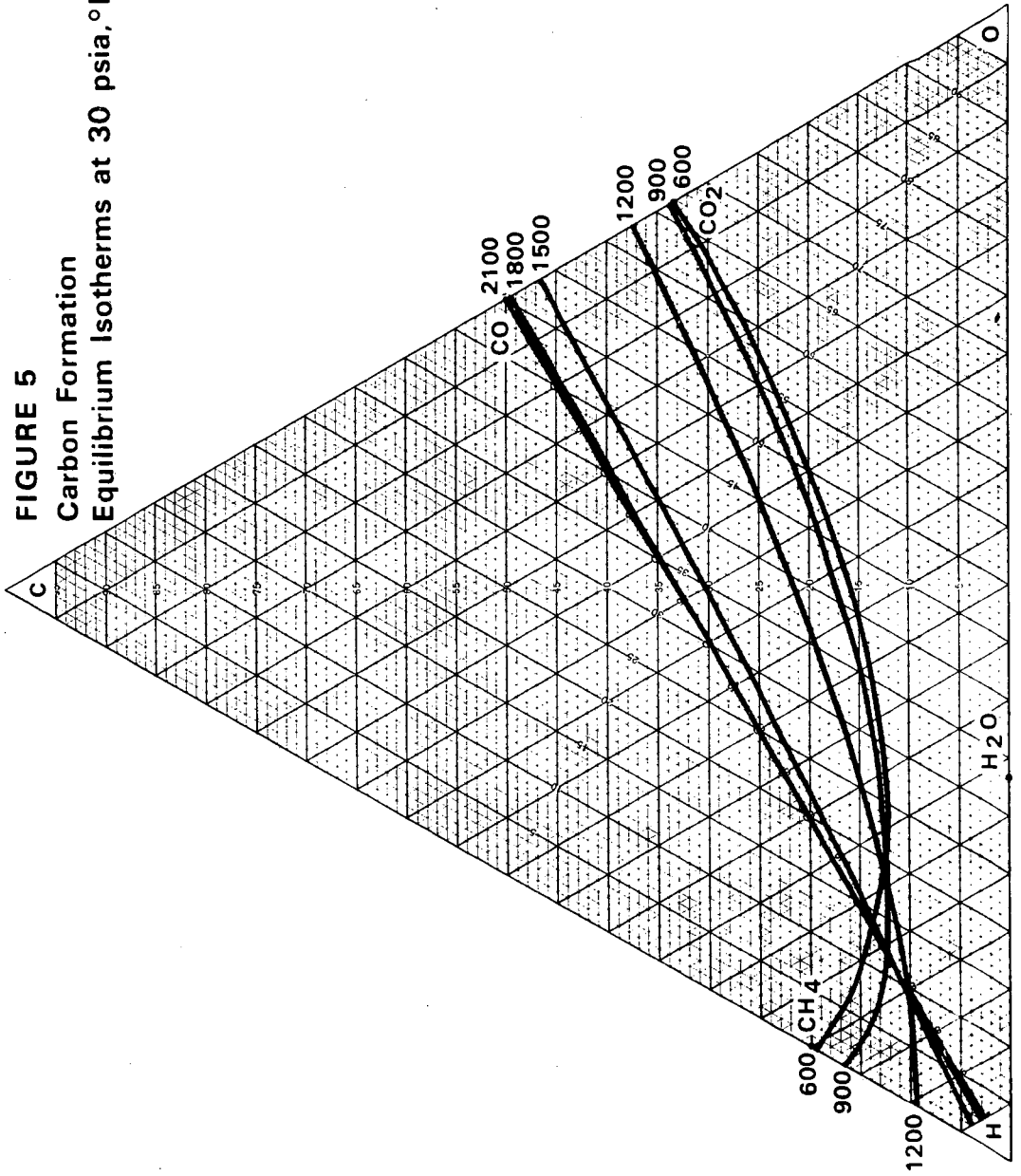


**FIGURE 6.**  
**Carbon Formation**  
**Equilibrium Isotherms at**  
**400 psia Total Pressure and °F**

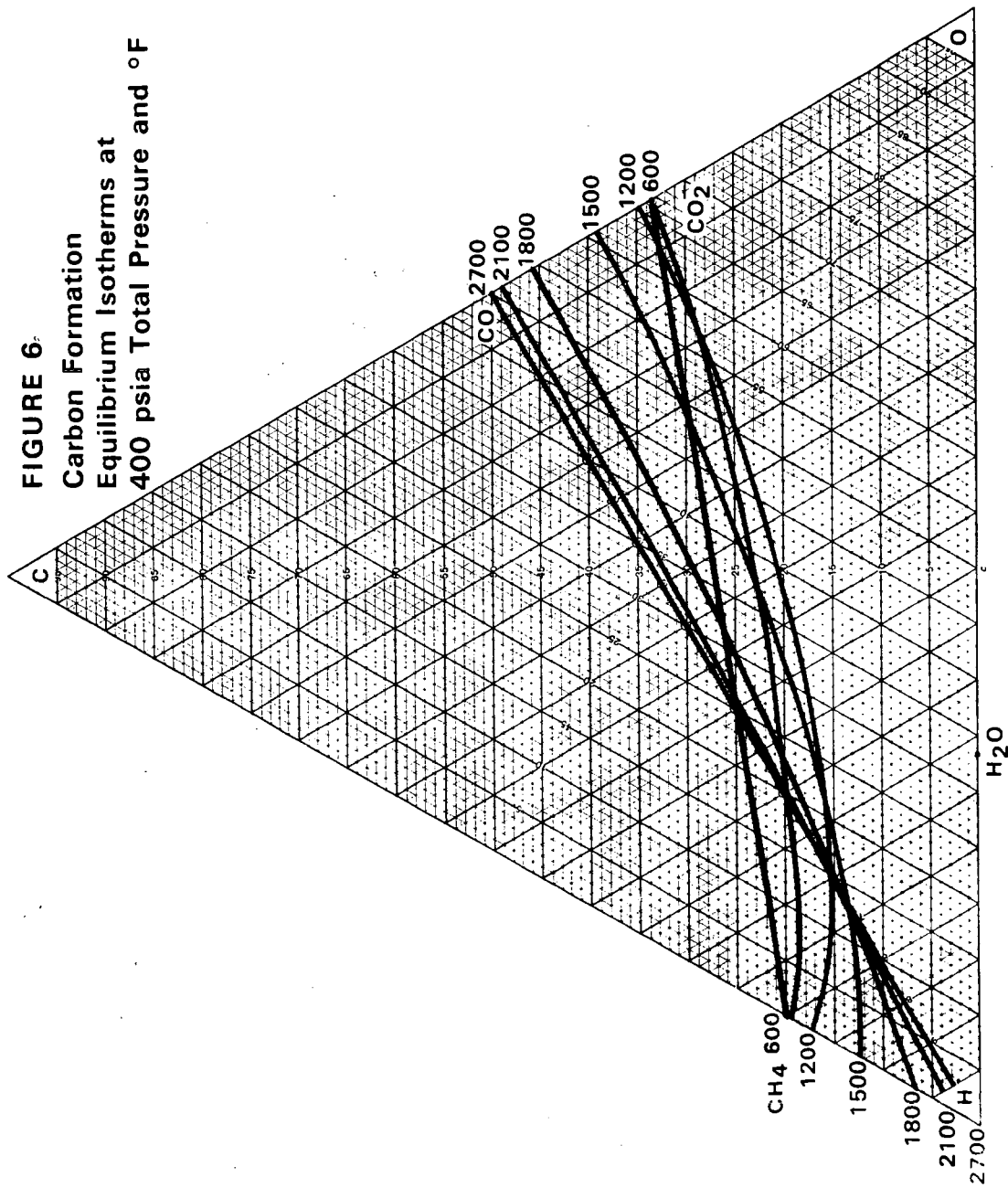


**FIGURE 7**  
**Carbon Formation Isotherms at**  
**400 psia Total Pressure and °F**  
**▽ RMPProcess**

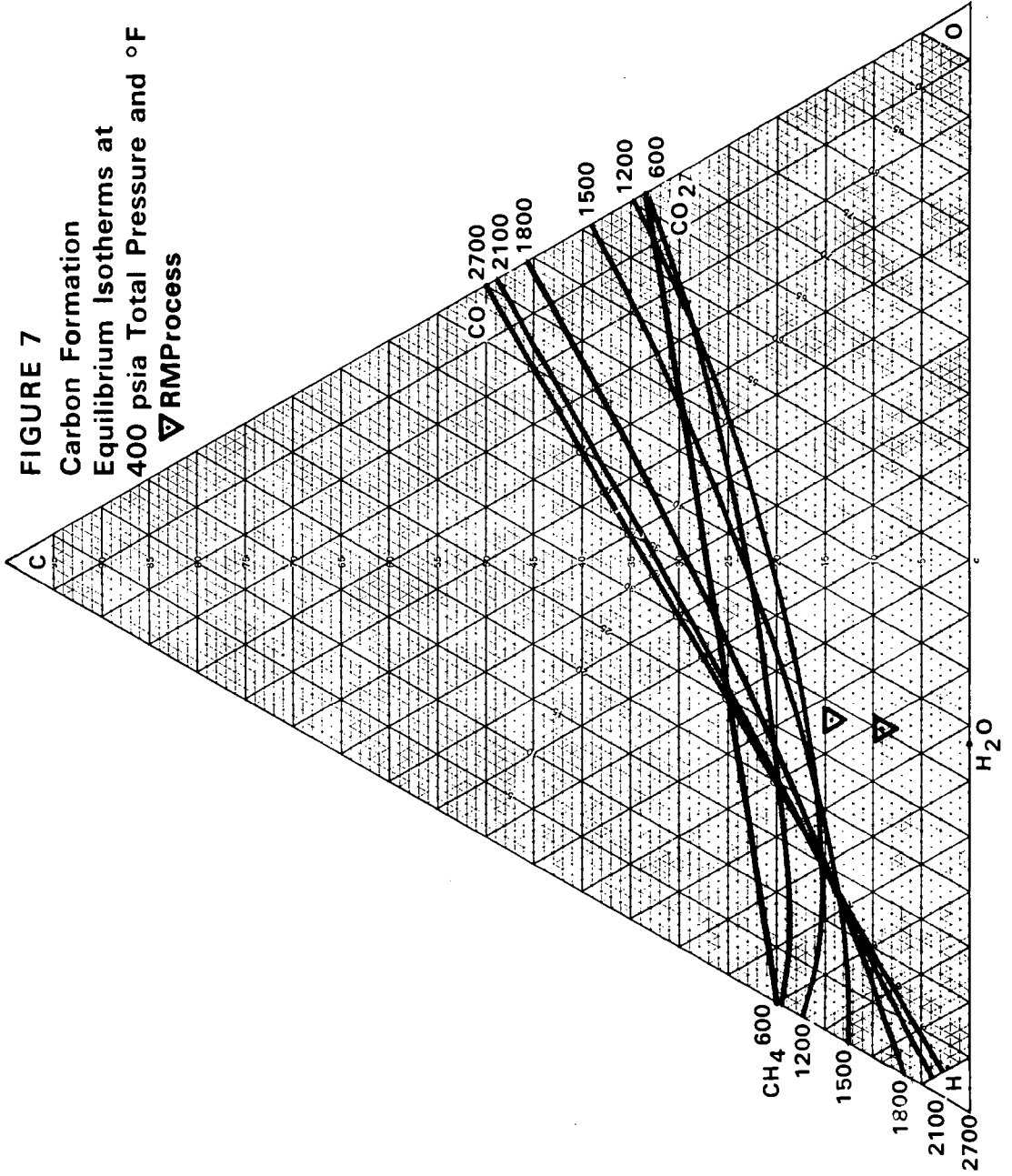


**FIGURE 8**  
**Carbon Formation Isotherms at**  
**Partial Equilibrium Pressure of Hydrogen,**  
**270 psia Partial Pressure of Hydrogen,**  
**Carbon Monoxide, Carbon Dioxide and**  
**Steam and °F**

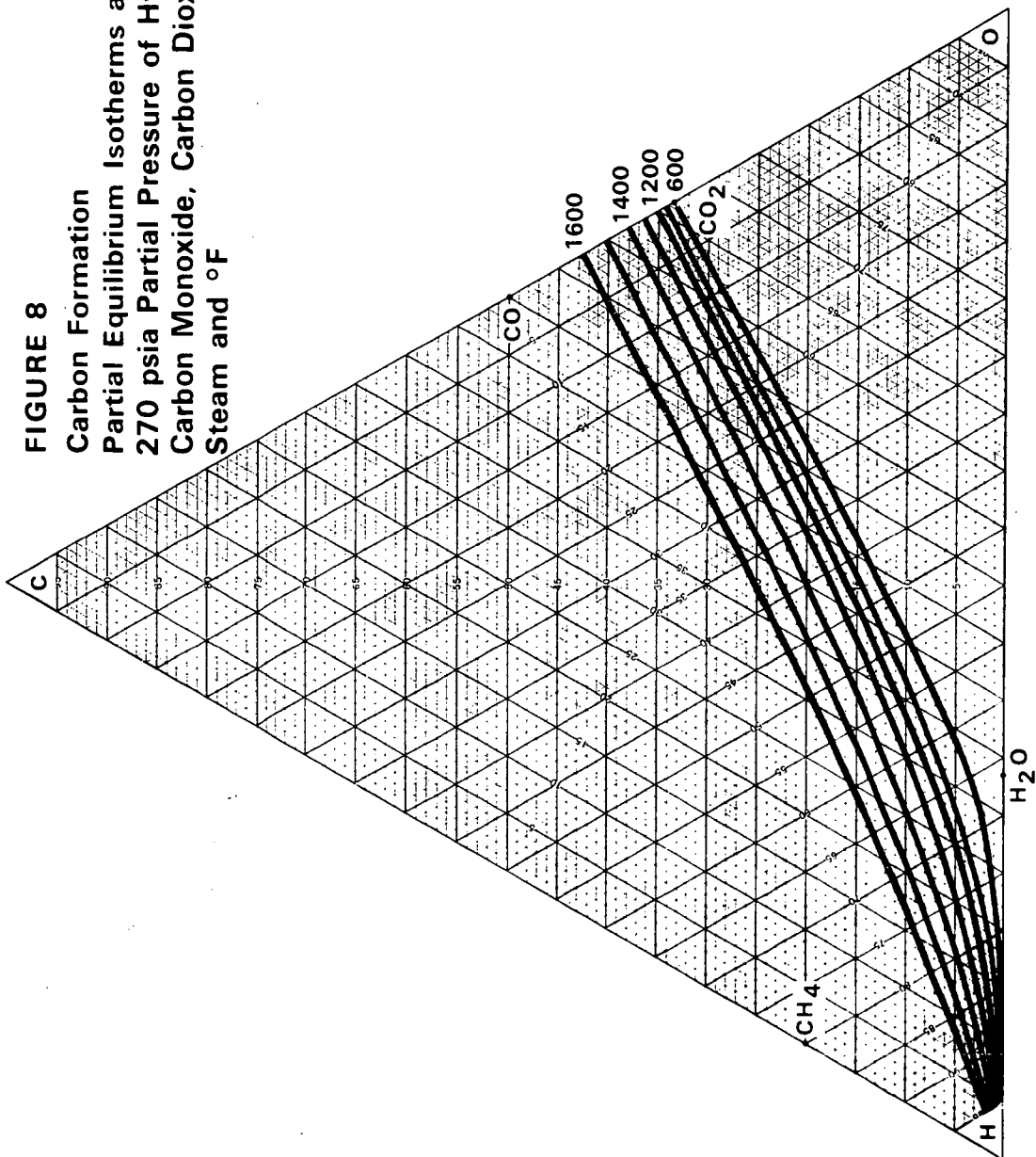
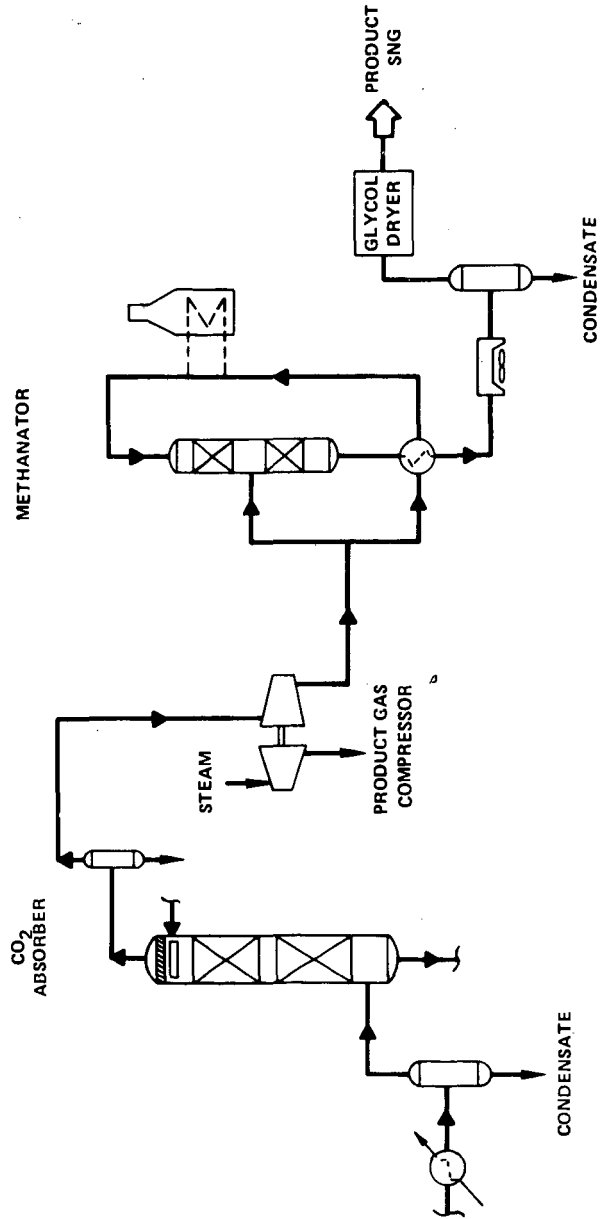


FIGURE 9 - FINAL STAGE OF METHANATION



DEVELOPMENT OF METHANATION CATALYSTS  
FOR THE SNG PROCESSES

70

ABSTRACT

Laboratory work has continued since late 1970 on developing catalysts for commercial methanation of synthesis gas, produced from coal or naphtha gasification, to a high BTU synthetic gas. Over 160 bench-scale tests, involving over 40 different catalysts have been made to determine the most desirable catalysts. Tests were initially made on commercially available catalysts but results indicated a whole new series of catalysts were required for this application. Tests showed the required catalyst loading, operating conditions, effect of particle size, thermal stability, and resistance to poisoning by trace constituents in the feed gas. The literature on the kinetics of the methanation reactors was reviewed in depth to determine the suitability of previous work on the methanation process conditions which are now planned. The initial kinetic system involving CO and CO<sub>2</sub> methanation along with CO shift was revised after analyzing the data utilizing previously published kinetics. A condensed summary of all the tests made to develop a commercial catalyst and an applicable kinetic system are presented.

## DEVELOPMENT OF METHANATION CATALYST FOR SNG PROCESSES

### SUMMARY

In the laboratory studies it was shown that methanation activity increases with increasing nickel content of the catalyst while the activity decreases with increasing catalyst particle size. Increasing steam to gas ratio of the feed gas results in increased carbon monoxide shift conversion but does not influence the rate of methanation.

Trace impurities in the process gas such as  $H_2S$  and  $HCl$  poison the catalyst. The mechanism is different because the sulfur remains on the catalyst while the chloride does not. Hydrocarbons at low concentrations do not affect methanation activity significantly and reform into methane. At higher levels hydrocarbons inhibit methanation and can result in carbon deposition.

A pore diffusion kinetic system was adopted which correlates the laboratory data and defines the rate of reaction.

## INTRODUCTION

In late 1970, Catalysts and Chemicals Inc. began a research and development program on methanation catalysts for the production of a high BTU synthetic natural gas from either coal or naphtha gasification. In 1971, Catalysts and Chemicals Inc. entered into an agreement with the El Paso Natural Gas Company to demonstrate the commercial feasibility of the methanation step in the process for the production of synthetic natural gas from coal. The pilot plant was designed in late 1971 and started up in early 1972. Because of the wide spread interest and concern about the methanation step in the over all production of SNG from coal, this project was opened to other participants in 1972. At that time, the Western Gasification Company and COGAS Development Company decided to participate in the pilot plant program.

This paper is a report on the basic work which was done in the laboratory to develop the catalysts for the methanation of synthesis gas from coal and the development of an applicable kinetic system. This report does not include any of the subsequent pilot plant test work which was carried out.

In the laboratory, over 160 bench-scale tests involving over 40 catalysts have been made to determine the optimum catalysts and process conditions for this application. Tests were initially made on commercially available catalysts but early results indicated that a whole new series of catalysts would be required for this application.

The comprehensive research program included all facets necessary for the development of these catalysts. Laboratory tests were conducted to determine the necessary catalyst loading, the design operating conditions, the effect of particle size, the effect of various trace constituents on catalyst performance and finally, resistance of the catalyst to thermal upsets. In this paper only those results which have direct significance to the kinetic model which was selected will be presented.

The laboratory studies which were particularly important to our development of the most active catalyst and the kinetic model for this new methanation application included the following.

TABLE 1

## LABORATORY STUDIES

Effects on Catalyst Activity by the:

- Nickel Content of the Catalyst
- Particle Size of the Catalyst
- Steam/Gas Ratio in the Process Gas
- Trace Impurities in the Process Gas

In this paper we have included an extensive discussion of the kinetic system we used and the basis for the selection of this system. During our development work, we frequently referred to the literature and the kinetics reported by previous workers. As a part of this program an extensive literature search was made. The complete bibliography of this literature search is presented for future reference by others.

## EFFECT OF NICKEL CONTENT ON CATALYST ACTIVITY

For the methanation reaction, in the process to convert coal to a high BTU gas, various catalyst compositions were evaluated to determine the optimum type catalyst. From this study a series of catalysts were developed to study the effect of nickel content on catalyst activity. This series includes both silica and alumina based catalysts and the nickel content was varied as outlined in Table 2.

TABLE 2

CATALYST DESIGNATIONS FOR  
VARIOUS NICKEL CONTENT CATALYSTS

<u>Nickel Content</u>	<u>Silica Support</u>	<u>Alumina Support</u>
50%	C150-1-02	C150-1-03
40%	C150-2-02	C150-2-03
30%	C150-3-02	C150-3-03

This study was run in a laboratory bench-scale unit with 3/4" reactor tubes. The catalysts were sized to 10 x 12 mesh and diluted 9 to 1 with SiO<sub>2</sub> to spread the reaction out through the bed and allow for the measurement of temperature profiles, the profile being an excellent indicator of the catalyst activity. The space velocities were also varied in an attempt to move away from equilibrium CO leakages, so the relative activity of the catalysts could be obtained.

The catalysts were reduced with 100 percent hydrogen at 700°F and an inlet space velocity of 1000 hour<sup>-1</sup>. Because of the carbon forming potential of a dry gas recycle composition and the cost of reheating the recycle if the water produced by the methanation reaction is removed, this study was made using a wet gas recycle composition. The catalyst loading gas composition and test conditions for these tests are in Table 3 below.

TABLE 3

COAL GASIFICATION PRIMARY METHANATION  
TEST CONDITIONS FOR NICKEL CONTENT STUDY

## Catalyst Loading

Volume (cc's)	5.0
Size (mesh)	10 x 12
Bed (L/D)	7.31
Bed Dilution	9/1

## Gas Composition

% CO	3
% CO <sub>2</sub>	4
% H <sub>2</sub>	12
% CH <sub>4</sub>	81
S/G	.35

## Test Conditions

Temperature, °F	500
Pressure (psig)	370
Space Velocity (v/v/hr)	25,000-95,000
Superficial Linear Velocity (ft/sec)	.343-1.302

A brief comparison is given in Table 4.

TABLE 4

NICKEL CONTENT VERSUS H<sub>2</sub> AND CO LEAKAGE

<u>Catalyst</u>	<u>Percent Nickel</u>	<u>Space Velocity (V/V/Hr Outlet Dry Gas)</u>	<u>% CO Leakage</u>	<u>% H<sub>2</sub> Leakage</u>
C150-1-02	50	93,000	0.18	6.93
C150-2-02	40	96,000	0.80	13.10
C150-3-02	30	96,000	3.35	22.30
C150-1-03	50	88,600	0.66	10.70
C150-2-03	40	96,000	0.27	16.88
C150-3-03	30	96,000	1.24	16.40

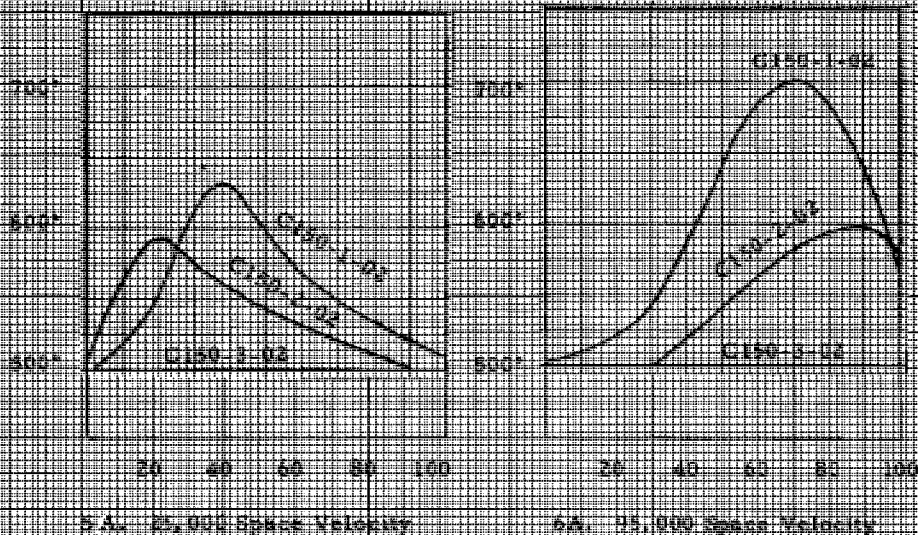
The temperature profiles for each catalyst at two different space velocities are given in Figures 5 and 6.

The lower nickel catalysts demonstrate a reasonable activity but the activity obviously decreases with nickel content. In Figures 5A, 5B, 6A and 6B it can be seen that at approximately 25,000 space velocity the 30% nickel on alumina catalyst uses 50% of the bed to obtain the maximum temperature while at 50% nickel the reaction only uses 30% of the bed. Each of these tests was extended for 300 hours or more. At various times during this study a test condition would be repeated and the percentage of the bed used for reaction indicated the catalyst had not aged.

Carbon analysis indicated that no carbon deposition occurred at the conditions of these tests.

## TEMPERATURE VS PERCENTAGE OF BED DEPTH

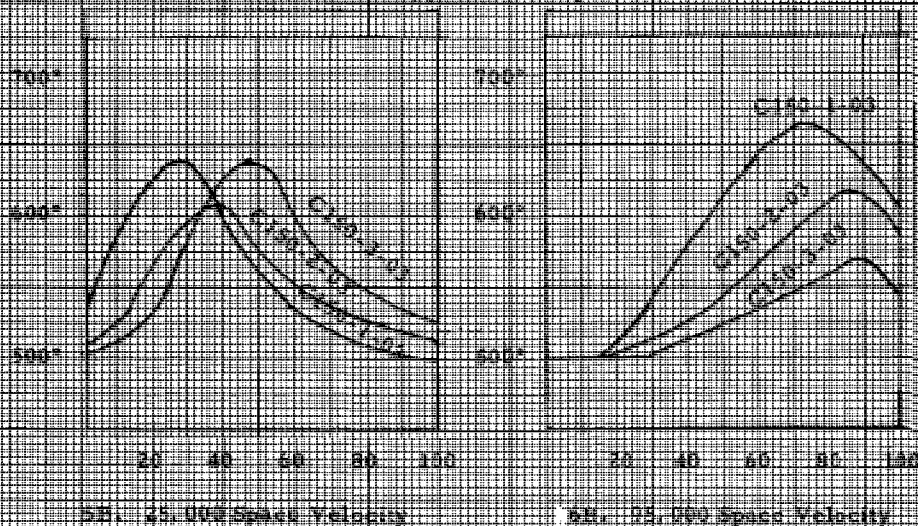
## Silica Supported Catalysts



25,000 Space Velocity

75,000 Space Velocity

## Alumina Supported Catalysts



25,000 Space Velocity

75,000 Space Velocity

## EFFECT OF PARTICLE SIZE ON CATALYST ACTIVITY

The particle size study was made on the C150-1-02 catalyst. The C150-1-02 oxide mixture was tabletted in three different sizes: 1/8" x 1/16", 3/16" x 3/32" and 3/16" x 3/16".

The catalyst was reduced by the procedure described previously and tested at the conditions of the primary wet gas recycle methanation. The catalyst loading, gas composition and test conditions are outlined in Table 7.

TABLE 7

## PARTICLE SIZE STUDY CONDITIONS

## Catalyst Loading:

Type	C150-1-02
Volume, cm <sup>3</sup>	10.0
Form	Tablets
Size, inch	3/16 x 3/16", 3/16 x 3/32", and 1/8 x 3/32"
Bed Length/Diameter	1.46

## Gas Composition:

% CO	5.0
% CO <sub>2</sub>	4.0
% H <sub>2</sub>	23.0
% CH <sub>4</sub>	68.0
S/G	0.35-0.40

## Test Conditions:

Inlet Temp., °F	500-550
Pressure, psig	350
Space Velocity, v/v/hr. (1)	20,000; 40,000; 60,000
Superficial Linear Velocity, ft/sec. (2)	.075-.250

- (1) The space velocity is the volume of outlet dry gas per volume of catalyst per hour.
- (2) The linear velocity is based on 700°F temperature and outlet flow rate.

The results are summarized in Table 8.

TABLE 8

## CATALYST PARTICLE SIZE STUDY

Temperature, °F			Space Velocity V/V/Hr.	Outlet Analyses		Activity Constant Kw CO
Inlet	Hot Spot	Outlet		% CO	% H <sub>2</sub>	
C150-1-02, 3/16" x 3/16"						
558	793	742	20,000	<.03	7.3	40,674
556	740	720	40,000	<.03	10.4	36,659
554	728	680	60,000	<.03	14.8	<u>39,407</u>
Avg.						38,713
C150-1-02, 3/16" x 3/32"						
562	778	735	20,000	<.03	7.3	59,788
563	797	730	40,000	<.03	9.9	<u>51,052</u>
Avg.						55,420
C150-1-02, 1/8" x 1/16"						
564	814	730	20,000	<.03	6.8	78,902
565	785	748	40,000	<.03	8.7	66,045
562	807	755	60,000	<.03	12.2	<u>73,464</u>
Avg						72,804

As the particle size decreases, the hydrogen leakage decreases. Also, the hot spot temperature is higher in the bed as the particle size decreases. Both show that the smaller particle size has greater activity. A kinetic system which defines the reaction in terms of CO and CO<sub>2</sub> methanation and CO shift conversion was used to determine the activity as shown in the last column of the table. The relative activity, based on particle size, is given as follows:

Particle Size	CO Methanation	Kw <sub>x</sub> /Kw <sub>o</sub>
	Kw	
3/16" x 3/16"	38,713	1.00
3/16" x 3/32"	55,420	1.43
1/8" x 1/16"	72,804	1.88

If we assume that the activity is inversely proportional to particle size

$$\frac{Kw_o}{Kw_x} = \left( \frac{D_x}{D_o} \right)^n$$

then n approximately equals 0.9 or Kw is proportional to  $\left( \frac{1}{D} \right)^{0.9}$  where D is the

equivalent sphere diameter. Since the kinetics are based on diffusion control it had been assumed that  $K_w$  was proportional to  $1/D$ . This data gives fairly good agreement since the packing and flow in the small diameter laboratory tubes would also cause some error.

## EFFECT OF STEAM TO GAS RATIO ON CATALYST ACTIVITY

In the various laboratory studies where the outlet gas composition was not at equilibrium, it was observed that the steam to gas ratio significantly affected the hydrogen leakage while the carbon monoxide still remained low.

Assuming that various reactions will proceed at different rates a study was made to determine the effects of the steam to gas ratio on the rate of reaction. The conditions for this test are presented in Table 9. Results of the test are tabulated in Table 10.

In varying the steam/gas ratio from .15 to .40 significant differences were observed. At the lower steam to gas ratios there is no CO shift conversion. At higher steam to gas ratios there is CO shift conversion.

When evaluating the data as summarized in Table 10 and obtaining activity constants for CO and CO<sub>2</sub> methanation and CO shift conversion, the activity for methanation remains the same regardless of the steam to gas ratio. However, with the high steam to gas ratio, shift conversion is occurring at about 25 percent of the rate of CO methanation. At low steam/gas ratios no shift conversion is observed.

TABLE 9

## CONDITIONS FOR STEAM TO GAS RATIO STUDY

## Catalyst Loading:

Type	C150-1-03, C150-4-03
Volume, cm <sup>3</sup>	10.0
Size, inch	3/16 x 3/32"
Bed, Length/Diameter	1.46

## Gas Composition:

% CO	5.0
% CO <sub>2</sub>	4.0
% H <sub>2</sub>	23.0
% CH <sub>4</sub>	68.0
S/G	.15-.40

## Test Conditions:

Temperature, °F	500-850
Pressure, psig	350
Space Velocity, v/v/hr.	20,000
Superficial Linear Velocity, ft./sec.	.078

TABLE 10  
EFFECT OF STEAM TO GAS RATIOS

Catalyst	Hours On Stream	Temperature, °F				Inlet				Outlet				Equilibrium				
		Inlet		Hot		S/G	Inlet	Spot	Outlet	%CO	%CO <sub>2</sub>	%H <sub>2</sub>	%CO	%CO <sub>2</sub>	%H <sub>2</sub>	%CO	%CO <sub>2</sub>	%H <sub>2</sub>
		On Stream	S/G	Inlet	Spot													
C150-1-03 50% Nickel on Alumina	33	.365	498	688	518	4.34	4.13	20.14	.247	5.26	6.45	.007	3.54	2.73				
	79	.368	499	680	518	3.42	6.25	14.60	.183	6.34	4.81	.016	6.50	2.46				
	93	.308	500	637	514	3.12	1.54	14.30	.165	3.01	4.97	.001	.933	2.35				
	35	.15	502	765	512	7.31	4.52	16.90	.459	8.75	2.80	.022	7.21	1.52				
	40	.15	501	773	513	7.31	4.52	16.90	.503	8.50	2.24	.022	7.21	1.52				
	51	.182	502	704	513	4.28	4.26	14.70	.255	6.10	2.34	.020	4.86	2.10				
C150-4-03 60% Nickel on Alumina	58	.02	500	824	518	4.18	5.52	17.70	.167	4.31	1.69	.080	5.44	1.83				
	61	.02	500	804	517	4.18	5.52	17.70	.159	4.43	1.69	.037	5.36	1.25				
	65	.02	500	808	515	4.18	5.52	17.70	.170	4.51	1.82	.061	5.41	1.60				
	33	.365	498	672	514	4.34	4.13	20.14	.223	4.53	4.68	.007	3.54	2.73				
	79	.368	498	666	518	3.42	6.25	14.60	.114	6.10	3.64	.016	6.50	2.46				
	93	.308	499	637	512	3.12	1.54	14.30	.124	2.70	3.36	.001	.933	2.35				
C150-1-03	35	.15	500	731	510	7.31	4.52	16.90	.138	8.77	2.69	.022	7.21	1.52				
	40	.15	499	748	514	7.31	4.52	16.90	.228	8.50	2.27	.022	7.21	1.52				
	51	.182	500	680	512	4.28	4.26	14.70	.139	6.00	1.65	.020	4.86	2.10				
C150-4-03	40	.15	49,564	39,645	29,734	0	0	0	42,336	23,814	0	0	0					
	51	.18	49,564	39,645	29,734	0	0	0	42,336	23,814	0	0	0					
	65	.02	49,564	39,645	29,734	0	0	0	42,336	23,814	0	0	0					
79	.37	37,173	29,734	29,734	13,011	13,011	13,011	13,011	13,011	13,011	13,011	13,011	13,011					
C150-4-03	40	.15	49,564	39,645	29,734	0	0	0	51,216	28,809	0	0	0					
	51	.18	49,564	39,645	29,734	0	0	0	51,216	28,809	0	0	0					
	65	.02	49,564	39,645	29,734	0	0	0	51,216	28,809	0	0	0					
79	.37	54,520	43,610	43,610	13,630	13,630	13,630	13,630	13,630	13,630	13,630	13,630	13,630					

## EFFECT OF TRACE CONSTITUENTS IN THE PROCESS GAS ON CATALYST ACTIVITY

In the process to make SNG from coal the methanation feed gas can contain various trace constituents which could affect performance. The coal can contain various amounts of sulfur, chloride and nitrogen. These will mostly be converted to  $H_2S$ ,  $HCl$ ,  $NO_x$  and  $NH_3$ , the last of which can be scrubbed or condensed out of the gas. These components can then be potential catalyst poisons. In addition to these inorganic compounds, various hydrocarbon compounds will be formed in the gasifier. Most of the heavier components can be separated. However, the  $C_2$  and  $C_3$  hydrocarbons are expected in the methanator feed gas.

Two other components, methanol and benzene, were added to the study. Methanol was included for processes using Rectisol systems for  $CO_2$  removal prior to methanation. Benzene was considered to determine the effect of aromatics on the catalyst activity and potential carbon formation.

In summary, Table 11 shows the components included in this study. The general conditions are tabulated in Table 12.

TABLE 11

### COMPONENTS OF TRACE IMPURITIES STUDY

$H_2S$	$RSH$ and $COS$ were not included since they are expected to hydrogenate to $H_2S$ over the nickel catalyst.
$HCl$	
$NO_x$	$NH_3$ was not included since it can be separated by condensation or scrubbing.
$CH_3OH$	$MeOH$ is included because of anticipated use of a Rectisol System.
$C_2, C_3$	Ethane, ethylene, propane and propylene are the expected light hydrocarbons in the process gas.
Benzene	Benzene was included to study the effect of aromatics on the catalyst in the event of catalytic sulfur removal as opposed to Rectisol.

TABLE 12

## GENERAL CONDITIONS FOR TRACE IMPURITIES STUDY

## Catalyst Loading:

Type	C150-1-03
Volume, cm <sup>3</sup>	10.0
Size	10 x 12 mesh

## Gas Composition:

%CO	5-7
%CO <sub>2</sub>	4-6
%H <sub>2</sub>	20-25
%CH <sub>4</sub>	62-71

## Test Conditions:

Temperature, °F	600
Pressure, psig	350
Space Velocity, V/V/Hr.	10,000
Steam/Gas Ratio	.35

1. Sulfur - Each impurity was added separately to the gas mixture and passed over C150-1-03 to determine its effect on catalyst activity.

These tests were run at the primary methanation conditions, but were run in a small 3/8" tube reactor on sized, 10 x 12 mesh, catalyst. The first test involves the addition of H<sub>2</sub>S in the 1-3 ppm range to the dry feed gas. The effect of the H<sub>2</sub>S on the catalyst activity is summarized in the following table.

TABLE 13  
EFFECT OF SULFUR POISONING

	Initial %-CO Conv.	Initial Kw-CO Meth.	Final %-CO Conv.	Final Kw-CO Meth.	% S Added to Catalyst	Ppm S in Feed	Calculated Inlet Sulfur ppm
Test 1	99.8	81,500	6.4	1,000	0.295	2-3	3.1
Test 2	98.6	65,500	85.5	25,500	0.274	0	0.93
Test 3	98.2	65,000	84.3	25,000	0.125	0	0.26

Tests 2 and 3 were made in the same reactor as Test 1. The catalyst was started up with no sulfur addition to confirm the initial activity. As can be seen from the table in the second and third tests, the catalysts picked up sulfur in both tests and deactivated even though no sulfur was added to the feed indicating that sulfur had remained in the reactor after Test 1. This is a common problem working with sulfur in laboratory test reactors. The sulfur will react with the steel walls of the reactor. Then even though sulfur is removed from the feed sulfur will evolve from the walls of the reactor and either be picked up by the catalyst or appear in the effluent from the reactor. With continuous addition of sulfur the CO leakage continues to increase.

In Test 1 with 3 ppm sulfur in the feed gas the catalyst showed continuous deactivation; it did not maintain some intermediate level of activity. For Tests 2 and 3, the calculated inlet sulfur concentration is shown and this value is calculated based upon the amount of sulfur found on the catalyst and the time on stream. With .13 to .30 percent sulfur on the catalyst, 60-90 percent of the activity was lost. Although Tests 2 and 3 were never conducted as originally planned, feeding 1 ppm sulfur in the feed gas, it was felt that the results of Tests 2 and 3 satisfactorily proved the severe poisoning effect of sulfur on C150-1-03.

RSH or COS as the source of sulfur was not studied because at the conditions of the test they are expected to hydrolyze or hydrogenate to H<sub>2</sub>S and poison the catalyst the same as if they were H<sub>2</sub>S.

2. Chloride - C150-1-03 was tested at primary wet gas conditions to determine the effect of chloride on catalyst performance. Chloride was expected to be very detrimental to catalyst activity, but the manner of deactivation was uncertain. The chloride was added to the system as hydrogen chloride in the feed water, up to 14 ppm, dry gas basis.

The test was conducted in a single reactor unit with an electric furnace heater. The feed water served as the source of steam and chloride for this test.

Table 13 provides a synopsis of test results as the chloride level was changed. Table 14 shows the change in the hot spot location caused by increased chloride levels.

Analysis of the discharged catalyst is presented in Table 15. New catalyst analyzed less than 0.01 percent chloride.

The chloride level was raised to greater than 5 ppm in the feed gas because the hot spot had moved down to the 69 percent level and remained there. Note that the percent conversion changed significantly only when the hot spot had reached the bottom of the bed. When the chloride was removed, neither the hot spot location nor the percent conversion improved.

Hydrogen chloride is a permanent irreversible poison to the methanation activity of C150-1-03 even though the majority of it is not picked up by the catalyst and is observed in the effluent gas. Only 0.02-0.04 percent was found on the discharged catalyst, but any amount of chloride in the feed gas is detrimental to catalyst activity.

TABLE 13

## CHLORIDE POISON TEST

Days		
1 - 5	No Chloride added.	Steady 99.1% conversion of CO with constant hot spot location 31% into the bed.
6 - 21	0.52 ppm Cl added on dry gas basis.	Seemed to be a slight decrease in percent conversion (Avg. = 98.7%). Hot spot moved down into bed to 69% level.
22 - 29	2-4 ppm Cl added on dry gas basis.	The overall average percent conversion was 98.5 during this period. The hot spot remained at the 69% level.
30 - 33	All chlorides were removed from feed.	The conversion did not change when chlorides were removed (98.6%). The hot spot also remained unchanged.
34 - 47	11-14 ppm Cl added on dry gas basis.	The percent conversion steadily decreased during this period of high chloride levels until on the 47th day the conversion was only 84.0%. The hot spot also decreased down into the bed at the 94% level. On the 37th day, the unit had to be shut down to repair a leak on the inlet to the reactor. The catalyst was kept under CO <sub>2</sub> during this period.
48 - 51	All chlorides were removed from feed again.	The percent conversion continued to decrease. On the 51st day the conversion was 75.8% when the test was stopped. The hot spot remained at the 94% level, nearly at the very bottom of the bed. (See Figure 1)

Chloride Poison Study: TABLE 14  
Hot Spot Location Vs. Days on Stream

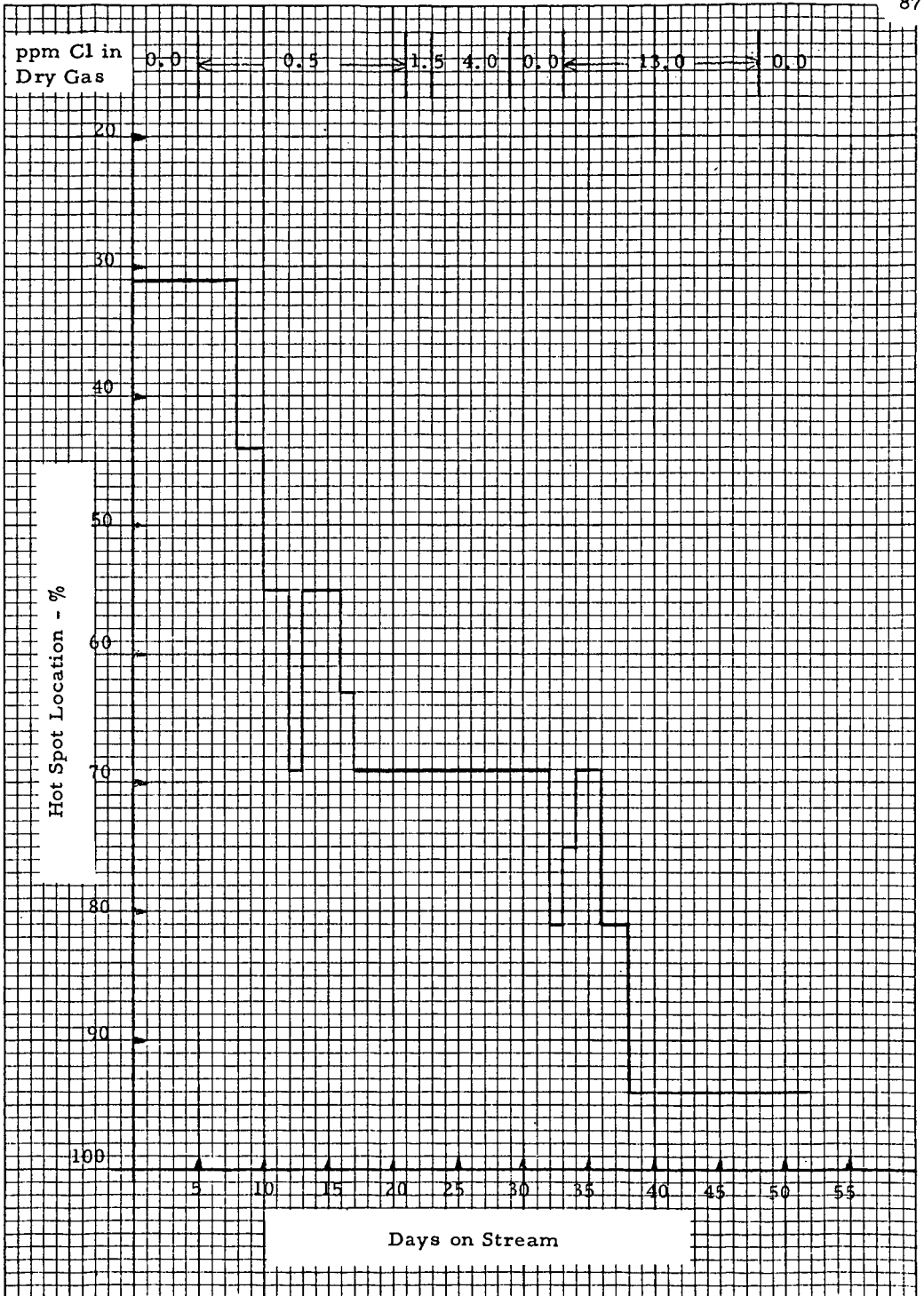


TABLE 15

## ANALYSIS OF DISCHARGED CATALYST

	Wt. % Chloride	
	<u>Wet Method</u>	<u>XRF Method</u>
Top 1/3	0.051	0.04
Middle 1/3	0.039	0.02
Bottom 1/3	<u>0.039</u>	<u>&lt;0.01</u>
Average	0.043	0.023

3. Nitrogen Dioxide - Nitrogen dioxide can be formed in the gasifier from the nitrogen present in the coal. Since it is an acid gas it was included in the study as a potential poison. This study was conducted with C150-1-03 in the electrical furnace reactor unit. The catalyst was tested at primary wet gas conditions with up to 8 ppm nitrogen dioxide in the dry feed gas. Table 16 provides a synopsis of test results as the NO<sub>2</sub> level was changed.

TABLE 16

RESULTS OF NO<sub>2</sub> ON CATALYST ACTIVITY

<u>Days</u>	<u>Condition</u>	<u>Result</u>
1-8	No NO <sub>2</sub> Added	Average 99.1% conversion of CO with hot spot location between 31-44% into bed.
9-13	1-2 ppmv NO <sub>2</sub> Added	Average 99.1% conversion with hot spot location at steady 31%. No change.
14-28	2-7 ppmv NO <sub>2</sub> Added	Average 99.2% conversion with hot spot location between 31-44% into bed.

Nitrogen dioxide up to 8 ppmv concentration in the inlet gas did not poison C150-1-03 catalyst.

The location of the hot spot fluctuated between 31 and 44 percent levels during this test. The hot spot did not drop sharply down into the catalyst bed as did previous poisoning studies with H<sub>2</sub>S and HCl.

4. Alkanes and Alkenes - For this study, C150-1-01 and C150-1-03 were tested at primary wet gas conditions with ethylene, ethane, propylene and propane added to the feed gas. The purpose in testing these hydrocarbons as a possible catalyst poison was to determine whether they would deposit carbon on the catalyst, reform, or pass through without reaction. The test was conducted using the dual-reactor heat sink unit and a water pump and vaporizer as the source of steam. All gas analyses were performed by gas chromatography. The test was stopped with the poisons still in the feed gas in order to preserve any carbon buildup which may have occurred on the catalysts.

The gas analyses, Table 17, show that the catalysts are not visibly affected by these alkanes or alkenes. The CO and H<sub>2</sub> leakages remained low throughout the test, rising slightly after hour 181 when the jacket temperature was raised. The disappearance of the ethane, ethylene, propane and propylene is attributed to reforming reactions taking place, even though a continuous trace ethane leakage was observed. Reforming of such small amounts of hydrocarbons would not create a discernible difference in the gas analyses. There was no downward movement of the hot spot during the test, and carbon deposition did not occur. These observations support our conclusion that ethylene, ethane, propylene and propane undergo reaction over the catalyst but do not poison it.

5. Methanol - In another series of tests, the effect of methanol, which can be carried over from the Rectisol scrubber system, on catalyst activity was determined by adding methanol to the water before vaporizing into the unit. The methanol was added to give .01% to 1.0% on a dry gas basis. Methanol up to 1000 ppm had no effect on activity as evidenced by no change in the H<sub>2</sub> and CO leakages. On increasing the methanol to 1% the temperature profile moved down through the bed but with no noticeable effect on H<sub>2</sub> and CO leakage. On removing the methanol the hot spot returned to its original location in the catalyst bed. The effluent H<sub>2</sub>O showed no methanol during the test, indicating that the methanol has reformed to methane.
6. Benzene - Although benzene would ordinarily be scrubbed out by a Rectisol system before the methanators, the possibility of a different H<sub>2</sub>S removal system resulted in the inclusion of benzene with our poison study. Benzene could pass through the system, hydrogenate, plug up the catalyst pores or reform.

C150-1-03 and C150-4-03 were loaded into the small dual-tube reactor. The unit was equipped with inlet saturators used as the source of benzene, of which poison levels of 0-5 percent were tested. The results are summarized in Table 18.

The test results show that benzene at low levels had no noticeable effect on activity and was reforming to methane, carbon oxides and hydrogen. At higher levels, greater than 0.5 percent, the activity of the catalyst declined which is demonstrated by the hot spot moving down the catalyst bed and the increase in CO and H<sub>2</sub> leakage. In addition, benzene and cyclohexane were observed in the effluent. At very high levels carbon formation was observed over the C150-1-03 catalyst.

Although benzene is not a poison in the sense that H<sub>2</sub>S and HCl are, it is depressing activity by reforming and adsorption on the catalyst, and at high levels can produce carbon.

Poisons not taken into account in kinetics system.

TABLE 17

## EFFECT OF LIGHT HYDROCARBONS ON CATALYST ACTIVITY

INLET	Outlet S/G	Temperature of, °C		% of Catalyst Bed Above Hot Spot	GAS COMPOSITION																
		Top	Bottom		INLET, %				OUTLET, %												
Stream	S/G	Hot Spot	Bottom	Hot Spot	CO	CO <sub>2</sub>	H <sub>2</sub>	CH <sub>4</sub>	C <sub>2</sub> H <sub>4</sub>	C <sub>2</sub> H <sub>6</sub>	C <sub>3</sub> H <sub>8</sub>	C <sub>3</sub> H <sub>6</sub>	C <sub>4</sub> H <sub>10</sub>	C <sub>4</sub> H <sub>8</sub>	C <sub>5</sub> H <sub>12</sub>	C <sub>5</sub> H <sub>10</sub>	C <sub>6</sub> H <sub>14</sub>	C <sub>6</sub> H <sub>12</sub>	C <sub>7</sub> H <sub>16</sub>	C <sub>7</sub> H <sub>14</sub>	
150-1-01																					
15	.531	696	597	11.5	5.07	5.13	26.73	63.07	—	—	—	—	<.01	4.70	3.46	91.84	—	—	—	—	—
23	.538	751	589	11.5	5.17	5.43	28.71	60.69	—	—	—	—	.0125	4.76	3.15	92.09	—	—	—	—	—
73	.536	702	591	11.5	4.27	4.77	24.38	67.37	.186	.473	<.01	4.31	2.99	88.06	<.01	.066	<.01	.0021			
95	.538	730	592	11.5	4.92	4.23	24.57	69.67	.235	.061	.276	.548	<.01	4.04	2.81	94.86	<.01	.072	<.01	.0041	
111	.537	834	620	11.5	4.73	6.68	24.90	64.17	.326	.051	.338	.475	.005	7.21	2.81	90.62	<.01	<.01	<.01	<.01	
161	.530	826	674	11.5	4.05	6.77	24.55	69.75	.333	.059	.481	.556	<.01	6.32	3.66	85.49	<.01	.0101	<.01	<.01	<.01
150-1-03																					
6	.507	728	593	0.0	5.07	5.13	26.73	63.07	—	—	—	—	.0025	4.50	2.45	93.05	—	—	—	—	—
23	.484	760	600	6.9	5.17	5.43	28.71	60.69	—	—	—	—	.008	4.56	2.67	92.77	—	—	—	—	—
51	.505	762	600	6.9	5.06	5.19	25.28	69.01	.447	.088	.491	.162	<.01	5.17	2.21	104.6	<.01	.0695	<.01	<.01	<.01
56	.485	695	604	20.7	4.91	4.16	21.95	71.80	.443	.093	.608	.669	<.01	5.01	2.36	88.35	<.01	.014	<.01	<.01	.0015
95	.483	683	608	20.7	4.92	4.23	24.57	69.67	.235	.061	.276	.548	<.01	4.20	2.79	95.48	<.01	.021	<.01	<.01	.0037
111	.505	787	644	20.7	4.73	6.68	24.90	64.17	.326	.051	.338	.475	.005	7.24	2.05	91.03	<.01	<.01	<.01	<.01	<.01
121	.506	798	680	6.9	4.91	10.99	26.31	64.35	.353	.045	.321	.547	.0373	11.7	2.71	86.32	<.01	.0018	<.01	<.01	<.01
161	.497	789	688	20.7	4.05	6.77	24.55	69.75	.333	.059	.481	.556	<.01	6.29	3.20	99.42	<.01	.0039	<.01	<.01	<.01

## Discharged Catalyst Properties

	% C	% S	% Reduction
150-1-01	3.08 (New 2.58)	.048 (New .06)	62.0
150-1-03	6.14 (New 5.84)	.066 (New .09)	76.3

TABLE 18

EFFECT OF BENZENE ON CATALYST ACTIVITY

Hours Onstream	Catalyst	% Catalyst Bed Above Hot Spot	Gas Composition						C <sub>6</sub> H <sub>12</sub>		
			% Inlet			% Outlet					
			CO	CO <sub>2</sub>	H <sub>2</sub>	C <sub>6</sub> H <sub>6</sub>	CO	CO <sub>2</sub>	H <sub>2</sub>	C <sub>6</sub> H <sub>6</sub>	
32	C150-1-03	0.0	5.91	5.90	23.11	-	.0025	5.45	2.13	-	-
58		16.7	5.57	5.76	23.36	.161	.0025	6.99	2.61	-	-
123		33.3	3.81	6.34	23.73	.410	.0025	6.32	3.58	.053	-
251		33.3	4.31	4.63	26.24	1.86	.01	5.31	7.38	1.281	.04589
304		100.0	4.47	7.26	25.79	3.64	.01	6.83	18.93	5.74	.29693
335	50.0	3.55	4.98	21.75	-	.01	5.69	12.50	-	-	
32	C150-4-03	0.0	5.91	5.90	23.11	-	.0025	5.49	1.96	-	-
51		16.7	5.98	5.59	24.53	.102	.0025	5.82	2.71	.095	.00037
84		33.3	3.81	5.65	23.02	1.09	.0025	5.82	3.05	.297	-
89		41.7	3.81	5.65	23.02	.361	.005	6.56	3.22	.720	.00015
145		50.0	3.44	5.06	24.5	.404	.005	5.77	4.57	.139	-
251		66.7	4.31	4.63	26.24	1.19	.01	5.18	9.06	1.018	.00279
304		83.3	4.47	7.26	25.79	5.53	.02	6.02	11.13	7.211	.1443
335	66.7	3.55	4.98	21.75	-	.01	5.18	9.35	-	-	

## DISCUSSION OF KINETIC SYSTEM

In various fields of commercial catalyst practice it has been customary for over thirty years (58) to use a very simple first order, or psuedo first order, equation in preliminary converter design where very great changes of conditions are not made. This equation, for constituent X may be written as

$$\begin{aligned}
 KW &= SVW \log_{10} \left( \frac{\text{Lb. mols/hr. of X in} - \text{Lb. mols/hr. of X}_{\text{eq.}}}{\text{Lb. mols/hr. of X out} - \text{Lb. mols/hr. of X}_{\text{eq.}}} \right) \\
 &= SVW \log_{10} A
 \end{aligned} \tag{1}$$

In equation 1, KW is a rate constant at a specific pressure and temperature, SVW is total wet gas space velocity, expressed as SCF of total gas per hour per cubic foot of bulk catalyst. X in refers to the lb. mols/hr. of constituent entering the section of catalyst for which the space velocity is measured, whereas X out indicated the lb. mols/hr. leaving the section. X<sub>eq.</sub> indicates the lb. mols/hr. which would pass through the section under equilibrium conditions. For reactions with large heats, it is necessary to divide a catalyst bed into a number of sections, so that each section is essentially isothermal.

Equation 1 almost necessarily has as its basis the concept that diffusion, either through pores or to the gross surface of the catalyst particle, controls the reaction rate.

Where the control is strictly by the gas film surrounding the catalyst, one would have to convert equation 1 to  $KW \sqrt{L} = SVW \log_{10} A$

where L is the catalyst bed depth in feet. This is required because the controlling film thickness is reduced as gas velocities are increased. In general equation (1) is satisfactory for commercial reactors. The differential equation from which (1) may be derived is:

$$- \frac{dX}{dV} = 6.07 \times 10^{-3} KW \left( \frac{\text{Lb. mols/hr. of X}}{\text{Lb. mols/hr. of Gas Flow}} - \frac{\text{Lb. mols/hr. of X}_{\text{eq.}}}{\text{Lb. mols/hr. of Gas Flow at equilibrium}} \right) \tag{3}$$

This may also be given as

$$- \frac{dX}{dV} = 6.07 \times 10^{-3} KW (N_x - N_x \text{ eq.}) \tag{4}$$

This refers to the total gas flow, through a plane of catalyst, where  $N_x$  is the mol fraction of X in the gas passing through the plane, and  $N_x \text{ eq.}$  is the mol fraction of X at equilibrium under conditions at this point in the catalyst bed.

Another equation which is helpful for computer use is:

$$\begin{aligned} & \text{lb. mols/hr. of X in} - \text{Lb. mols/hr. of X out} \\ & = \left(1 - 10 \frac{-K_w}{SVW}\right) \left(\text{lb. mols/hr. of X in} - \text{lb. mols/hr. of X}_{\text{eq.}}\right) \end{aligned} \quad (5)$$

In cases where there is no volume change in the reaction, (1) and (5) may be readily derived from (3) or (4).

The solution of equation (3) is complicated when there is a volume change in the reaction which removes constituent X.

For these reactions equation (3) may be used, with  $dX$  replaced by  $\Delta X$ , and  $dV$  by  $\Delta V$ . This may be made as accurate a solution as one wants, if the increments are sufficiently small.

However, equation (5) may be used as is, but a more accurate solution is:

$$\begin{aligned} & \text{lb. mols/hr. of X in} - \text{Lb. mols/hr. of X out} \\ & = \left(1 - 10 \frac{-K_w}{SVW}\right) \left(\text{lb. mols/hr. of X in} - \text{lb. mols/hr. of X}_{\text{eq.}} \times \frac{\text{Flow}}{\text{Flow}_{\text{eq.}}}\right) \end{aligned} \quad (6)$$

Equation (6) has been used in correlating the data of this paper; however, a more accurate approximation solution of (3) is

$$\begin{aligned} & \text{lb. mols/hr. of X in} - \text{Lb. mols/hr. of X out} \\ & = \left(1 - 10 \frac{-K_w \text{ Flow}^*}{SVW \text{ Flow}_{\text{eq.}}}\right) \left(\text{Lb. mols/hr. of X in} - \text{lb. mols/hr. of X}_{\text{eq.}}\right) \end{aligned} \quad (7)$$

Where  $\text{Flow}^*$  is the volume of gas which would pass if 100% of constituent X were reacted.

Finally, a fairly complicated exact solution of (3) may be derived. It must be noted, however, that equation (3) itself cannot be strictly accurate, since only the diffusion of a single constituent has been considered.

The application of equation (3) to the methanation of CO by the reaction  $\text{CO} + 3\text{H}_2 = \text{CH}_4 + \text{H}_2\text{O}$ , starting with a mixture of say 90% CO and 10%  $\text{H}_2$ , using CO as X, would lead to the erroneous conclusion that methanation is impossible under these conditions. The requirement is that equation (3), operating on one constituent, can only be accurate (even when diffusion is strictly controlling) if X is present at a low concentration. To solve the 90% CO - 10%  $\text{H}_2$  case previously mentioned, it would be necessary to consider the diffusion of constituents other than CO.

In view of the above, and the fact that all of the various approximate solutions of equation (3) give about the same answer when the reactant concentration is low, it did not seem worthwhile to work on obtaining better accuracy in the solution of (3).

Equation (7) is, however, of interest when one does comparisons of various kinetic equations. It may be rewritten as

$$\begin{aligned} & \text{lb. mols/hr. of X in} - \text{lb. mols/hr. of X out} \\ & = (1 - 10 \frac{-K_w}{SVW} xQ) \left( \text{lb. mols/hr. of X in} - \text{lb. mols/hr. of X eq.} \right) \end{aligned} \quad (8)$$

Thus, (7) is a special case of (8) where

$$Q = \text{Flow}^*/\text{Flow eq.} \quad (9)$$

In computer operations with other kinetic systems equation (8) may be used, and all of the unique features of the kinetic system may be incorporated into the value of Q, which may, of course, be a very complex expression. This technique is only of interest in that it simplifies the work necessary to analyze data using any specific kinetics for a chemical reaction. The technique requires sectioning of the catalyst bed; in most cases with normal space velocities 50 to 100 sections, involving two or three minutes of time on a small computer, appear to be sufficient even when very complex equations are used.

$K_w$  in the foregoing equations is a function of pressure and temperature. Although the effect of pressure and temperature on strictly diffusion controlled processes is small, the effect of these variables on surface reactions is generally quite large. Thus, although diffusion may be the major contributor to the mathematical form of the kinetic equations, a residuum of influence from the basic process taking place at the end of the catalyst pores will also affect the rate constant. The usual balance achieved with respect to pressure is a rate increasing with the square root of the total pressure. Since essentially all of the experimental work in this project was at essentially the same pressure, this study gives no information on the pressure dependence of rate. It should be noted, however, that the form of several proposed kinetic equations (25, 57) would give this type of pressure - rate relationship. Data are available from commercial ammonia plant methanators, and laboratory studies relative to them, which show this type of pressure dependence.

For this reason a square root of pressure term has been introduced into the equation for  $K_w$ . Further experimental work would be desirable if pressures greatly different from 25 atm were to be used.

The effect of temperature on  $K_w$  has been introduced through an activation energy term. This follows the normal form for this type of reaction, with a very high activation energy below the "threshold" temperature, and a lower value, tending to diminish with increasing temperature, at higher temperatures. This reflects an increasing dependence of reaction rate on diffusion as the temperature is

raised. Activation energies for rate data derived from experiments (7, 28, 30, 32, 48, 50) on the hydrogenation of CO and CO<sub>2</sub> at low pressures and low temperatures using small catalyst particles of .01 to .03 in. diameter generally run from 15,000 to 30,000 cal/g mol. On the other hand, for work at higher pressures and temperatures, with commercial size catalyst (1/8 to 1/4 in. diameter), values of 0 to 10,000 cal/g mol are obtained (32, 33, 25, 50, 57).

In the early phases of study, temperature surveys were run on various catalyst with the object of finding the "threshold" temperature for CO methanation. The following rather typical results were calculated for 1/4 in. C150-1-02 catalyst.

<u>Average Temperature, °F</u>	<u>Kw</u>	<u>Activation Energy, cal/g mol, calc. from previous temperature value</u>
320	170	-
362	710	24,000
389	6020	61,000
416	11850	21,000
529	24300	6,100

In general, considering that these tests are on catalyst which has not been aged, a Kw value below several thousand is indicative of a catalyst not practical for commercial use, so from a utilitarian standpoint these data show a "threshold" temperature slightly below 400°F. Because of the small amount of reaction at the lower temperatures, and the effect of small temperature errors on the activation energy calculation, the three values at low temperatures are not very consistent; however, the average of 35,000 cal/g mol is not in bad agreement with the results of other investigators. The value of 6100 cal/g mol is typical for the diffusion control region.

An examination of laboratory data on C150-1-01 and C150-1-02 catalysts for CO hydrogenation tends to show essentially no change in Kw value between 500, 600 and 700°F. This would suggest an activation energy of zero. Although these data show a small, essentially zero, temperature dependence from 500-700°F (33) the difficulties in unraveling the relationship between the rates of CO and CO<sub>2</sub> methanation, and the water-gas shift reaction ( $\text{CO} + \text{H}_2\text{O} = \text{CO}_2 + \text{H}_2$ ) prevent one from getting a good value for the activation energy for any one reaction. Considering these tests, as well as various literature studies (32, 33, 25, 50, 57) an activation energy of 5,000 cal/g mol was used below 700°F, and 2,000 cal/g mol above 700°F. One must bear in mind that below the "threshold temperature" any predicted performance would be virtually meaningless. It may be noted that a kinetic equation which in practice is very close to the simple Kw expression (25, 57) uses a 6900 cal/g mol over the entire temperature range (525 - 900°F).

Finally, one needs to know the effect of catalyst particle size on Kw. For a pore diffusion controlled reaction activity should be inversely proportional to catalyst particle diameter; that is, directly proportional to external catalyst surface area.

Several studies (48, 50, 51) show that above 400°F, pore diffusion will control catalyst activity if the particle diameter is above .02 to .03 in. This is far below any practical commercial catalyst particle diameter.

In this investigation (Table 8) values of Kw for CO hydrogenation were found to be dependent on the 0.9 power of the reciprocal of the particle diameter. In view of this, and the literature results, a linear (first power) dependence on reciprocal of particle diameter was used in the Kw expression. Measurement accuracy is certainly insufficient to distinguish between a 0.9 and 1.0 power dependence.

If KWS is a standard value of Kw at a base temperature in °Rankine (TB), a base absolute pressure, PB, and a base catalyst particle diameter, DB, then, at other values of temperature (°R=T), and pressure, P, and catalyst diameter D,

$$K_W = K_{WS} \sqrt{\frac{P}{P_B}} \times \frac{D_B}{D} \times F_W \times 10^{-.3934 \Delta H \left( \frac{1}{T} - \frac{1}{T_B} \right)} \quad (10)$$

FW in commercial reactors is near one; it is the ratio of number of catalyst tablets per cubic foot to the number per cubic foot one would have in a reactor of infinite diameter. P and PB, and D and DB must be in consistent units.

Where two activation energies are used, TB should be the temperature at which the change is introduced. Thus, in our system TB is 1159.67 (700°F), and 2000 is used for Delta H if T > 1159.67, and 5000 if T < 1159.67.

The value used for PB is one atmosphere, and since activity calculations are made by computing the square feet of catalyst area per cubic foot of catalyst, this amounts to using a standard DB of 45.144 inches in a reactor of infinite diameter.

Where DV is vessel diameter (in the same units as D),

$$F_W = 1 - .4912 D/DV \quad (11)$$

A characteristic of most equations for surface controlled kinetics, as opposed to diffusion controlled kinetics, is a number of partial pressure terms, often to high powers. When large changes in partial pressures are made, differences between observed and calculated reaction can easily equal a factor of 1000 or more. Where diffusion type kinetics are used, one seldom finds differences of more than a factor or two or three. While this may not seem very accurate, the comparison between the two methods can be rather startling.

Table 19 compares activities of two catalysts, C150-1-01 and another commercial catalyst. First, from literature data, a catalyst activity is obtained using their kinetics, and another by using equation (5). Then, from typical data taken on the C150-1-01 catalyst, the same procedure is followed. Table 19 reports the activity ratios that are obtained.

It is evident that the equation for reference 1 has broken down completely for CO hydrogenation. The other equations for CO hydrogenation give correlations similar to those obtained by the simple kinetics. These equations are all, however, of relatively simple form. They use low activation energies, and in general, would show an activity dependence on the square root of the pressure, similar to that of the simple kinetics.

For the CO<sub>2</sub> kinetics, the literature kinetics gives more reasonable correlation than the simple, though the difference is not great. However, reference 4 involves methanation of over 50% CO<sub>2</sub> in H<sub>2</sub>, under conditions where equation (3) would break down, and 12 involves only the initial hydrogenation (less than the first one or two percent) of the CO<sub>2</sub> present. Furthermore, there is a possibility that the reverse shift would produce enough CO to poison the CO<sub>2</sub> methanation in these experiments, which would make it difficult to obtain agreement between various runs.

TABLE 19

## RATIO OF C150-1-01/OTHER COMMERCIAL CATALYST

Reference	Reactant	Literature Equation	Activity Ratio, Literature Equation	Activity Ratio, Equation 3, Approximation Equation 5
1	CO	$r = \frac{pCOpH_2^3}{(A+BpCO+DpCO_2^4 + EpCH_4)}$	9000	5.8
33	CO	$r = \frac{1.1pCOpH_2}{1 + 1.5pH_2}$	$1/2$ 1.2	2.3
2	CO	$r = \frac{KpCOpH_2}{1+K_2pH_2+K_3pCH_4}$	$1/2$ 2.3	2.6
4	CO <sub>2</sub>	$r = \frac{C_1pCO_2pH_2^2}{(pH_2^{1/2}+C_pCO_2+C_3)}$	2.2	3.9
12	CO <sub>2</sub>	$r = \frac{kpCO_2pH_2^4}{(1+K_1pH_2+K_2pCO_2)^5}$	6.2	13.1

A number of measurements made on the methanation of  $\text{CO}_2$  may be correlated using equations (5) and (10), with the same values of  $\Delta H$  as for the CO hydrogenation. Based on diffusion considerations, the value of KWS for  $\text{CO}_2$  hydrogenation was taken as 0.8 of that for CO.

Attempts were made to correlate data where both CO and  $\text{CO}_2$  were methanated, using simple diffusion for both, with the  $\text{CO}_2$  rate set at 80% of the CO rate. In order to get good agreement with experimental data it is necessary to introduce a variable water-gas shift reaction activity.

An examination of some laboratory runs with diluted C150-1-02 catalyst can illustrate this problem. In one run, with 579°F inlet, 598°F exit, 97297 outlet dry gas space velocity, the following results were obtained after minor corrections for analytical errors. 99.9885 percent of the CO present (out of an inlet 2.04 mol %) disappeared in reaction, while the  $\text{CO}_2$  present (from an initial 1.96%), increased by over 30%. Equilibrium carbon oxides for both methanation reactions was essentially zero, while the equilibrium CO based on the water-gas shift reaction at the exit composition, was about one-third of the actual CO exit of 0.03 mol %. From these data activities for the various reactions may be estimated, based on various assumptions. Table 20 shows the effect of two differing assumptions.

TABLE 20

Water-Gas Shift Kw	350000	50000
$\text{CO}_2$ Methanation Kw	56000	0
CO Methanation Kw	70000	150000

For the first assumption, the value of Kw for shift appears too high. It must be this high because of the necessity of making  $\text{CO}_2$  appear while both  $\text{CO}_2$  and CO are being consumed rapidly by methanation. The data may be tested to see if the indicated rate appears unreasonable from the standpoint of mass transfer to the gross catalyst surface.

Regardless of the rate of diffusion in catalyst pores, or the surface reaction rate, it is unlikely that reaction can proceed more rapidly than material can get to the gross pill surface unless the reaction is a homogeneous one, catalyzed by free radicals strewn from the catalyst into the gas stream.

The following equation has been derived for testing mass transfer limitation to the gross catalyst particle (56).

$$Kw = \frac{8100}{D} \sqrt{\frac{L \times SVW}{M \times D \times T}} \quad (12)$$

Here M is average molecular weight of the gas, T is temperature in °Rankine, D is catalyst particle diameter, inches, and L is bed depth in feet. For this calculation, involving a diluted bed, SVW and L must be computed as if all of the active catalyst were gathered into one place. In this experiment L is then .02 feet, SVW is 130000 (counting the steam present), D is .078 in., M is about 16, and T is 1048. This leads to a limiting Kw of about 150000.

Although 150000 is somewhat of an average value of expected maximum Kw, and uncertainties in the computations make the minimum Kw about 15000, below which no mass transfer to gross surface could be expected to be limiting, whereas the maximum possible Kw might be over 1000000, assumption 2 certainly gives the more reasonable explanation of the data.

Many references discuss the inhibition of CO<sub>2</sub> methanation by CO (15, 30, 37, 42, 48, 49, 51). At 320°F, and 300 psig, there is indication that as little as 65 ppm of CO would stop CO<sub>2</sub> methanation (51). Under atmospheric pressure, with .015 inch catalyst (48) CO poisoning of CO<sub>2</sub> methanation was shown with 200 ppm of CO, at up to 446°F.

It is to be expected that the poisoning of the CO<sub>2</sub> methanation by CO will be observed at lower CO concentrations when catalyst particle diameters are smaller. This is because the smaller particle will be poisoned throughout, whereas at some depth in the pores of larger sized catalyst the poisoning effect will drop off, and some significant methanation of CO<sub>2</sub> be permitted to take place. It is noteworthy that the only results in this investigation, such as those considered in Table II, where poisoning was likely at very low CO concentrations, were obtained with very small catalyst particles.

It is concluded that a fully satisfactory system for calculating simultaneous reactions of CO and CO<sub>2</sub> with H<sub>2</sub> and H<sub>2</sub>O will require a schedule of the effect of CO on CO<sub>2</sub> methanation as a function of temperature. This effect will probably be different with different particle sizes. From a commercial standpoint the possible size range may be too small to require much difference in the treatment, but in laboratory somewhat lower than the CO methanation rate. A simple kinetics system, such as that derived from equation (3), may be satisfactory for all the reactions. It is unlikely that reliable data will soon be collected for the shift reaction (since it is of a somewhat secondary nature and difficult to study by itself) to justify a more complicated treatment.

For CO methanation one of the simple literature kinetic systems (25, 57) should be as reliable or better than the one used in this study. With CO<sub>2</sub> methanation it is less certain that a simple system is indicated. It is probably of more urgency to elucidate the quantitative effect of the CO on the CO<sub>2</sub> methanation than to find a complex kinetic expression for the CO<sub>2</sub>-H<sub>2</sub> reaction itself.

It is expected that the actual rate of CO methanation will always be high, at least under industrial conditions, whereas the CO<sub>2</sub> methanation rate will vary from about the same as the CO rate down to zero, depending on the operating pressure, temperature, CO content of the gas, and catalyst particle size. Meanwhile a water-gas shift (or reverse shift) reaction will be going on at all times at a fairly high rate.

1. Akers, W. W., and White, R. R. "Kinetics of CH<sub>4</sub> Synthesis," Chem Eng. Progress, Vol. 44, No. 7, pp 553-556, (July, 1948)
2. Bienstock, D. et al, 1 "Pilot Plant Development of the Hot Gas Recycle Process for The Synthesis of High Btu Gas," U.S. Bureau of Mines. R. I. 5841 (1961).
3. Bienstock, D. et al, American Gas Journal, 189, 47-49, 52, 58, 60. (March, 1962).
4. Binder, G. C., and White, R. R. "Synthesis of CH<sub>4</sub> From CO<sub>2</sub> and H<sub>2</sub>", Chem Eng. Progress, Vol 46, pp 563-74. (Nov. 1950) American Documentation Institute, 1719 N. Street, N.W. Washington, D. C. Document 2834
5. Booth, N. "Catalytic Synthesis of CH<sub>4</sub>," Communication GRB21, The Gas Research Board, London, England (Aug. 1948).
6. Boudart, M. "Kinetics on Ideal and Real Surfaces," AICHE Journal 2, No. 1, (March, 1956).
7. Bousquet, J.L., and Teichner, S.J. "Methanation of CO by H<sub>2</sub> in Contact with Catalysts Prepared From Ni Hydroaluminat." Ball Soc. Chem Fr., 2963-2971 (Sept. 1969) (Conoco Library Trans. TR 71-15
8. Cherryshev, A.B., and Gudkov, S.F. "The Mechanism of CH<sub>4</sub> Synthesis on a Fluidized Nickel Catalyst," Isbrannye Trudy, 1956, 307-10, Ibid, 311-18.
9. Demeter, J.J. and Youngblood, A.J., Field, J.H. Bienstock, D. "Synthesis of High Btu Gas in a Raney Nickel Coated Tube Wall Reactor," U.S. Bur. Mines, R. I. 7033, (1967)
10. Dent, F. J. and Hebden, D. "The Catalytic Synthesis of Methane as a Method of Enrichment for Town Gas Manufacture," Communication GRB51. The Gas Research Board, Bechemham, England, (Nov. 1949)
11. Dent, F.J. et al. "An Investigation into the Catalytic Synthesis of Methane for Town Gas Manufacture," Communication GRB 20/10, The Gas Research Board, London, England. (Feb. 1948)
12. Dew, J.N., and White, R. R. and Slipevich, C.M. "Hydrogenation of CO<sub>2</sub> on Nickel-Kieselghur Catalyst," Ind. Eng. Chem. Vol 47, 140-146 (Jan. 1955). Ph.D. Thesis, University of Michigan, Ann Arbor, (1953).
13. Dirksen, H. A. and Linden, H.R., "Pipeline Gas by Methanation of Synthesis Gas over Raney Nickel Catalyst," Ind. Eng. Chem. Vol 52, pp. 584-89, (July, 1960) IGT Research Bulletin, No. 31, (July, 1963).
14. Field, J.H. et al, "Development of Catalysts and Reactor Systems for Methanation," Ind. Eng. Chem. Prod. Res. Develop. Vol 3, pp 150-153 (June, 1964)
15. Fisher, F., and Pichler, H. Brennst. Chem. Vol 14, 306-10 (1933)

16. Forney, A. J., Bienstock, D., and Demski, R. J. "Use of Large Diameter Reactor in Synthesising Pipeline Gas and Gasoline by The Hot Gas Recycle Process," U.S. Bureau of Mines, R.I. 6126, (1962).
17. Gilkerson, M. M., White, R. R. and Sliepcevich. "Synthesis of  $\text{CH}_4$  by Hydrogenation of CO in a Tubular Reactor," Ind. Eng. Chem. 45, pp 460-67, (Feb. 1953).
18. Greyson, M. "Methanation," Catalysis IV, P.H. Emmett, ed. pp 473-511, Reinhold, N. Y., N. Y. (1956).
19. Greyson, M., Dementer, J. J., Schlesinger, N.D., Johnson, G. E., Jonakin, J., and Meyers, J.W. "Synthesis of  $\text{CH}_4$ " U.S. Bur. Mines R.I. 5137 (1955).
20. Goldberger, W. M. and Othmer, D.F. "The Kinetics and Thermodynamics of Ni (CO) Formation are Discussed," Ind. Eng. Chem. Process Design Development, Vol 2., pp 202-209, (July, 1963).
21. Gudkor, S.F. and Chernyshev, A. B. "A Study of  $\text{CH}_4$  Synthesis with a Fluidized Catalyst," Invest, Akad, Nauk, S.S.S. R., Otdel. Tekn. Nauk. 1555, N. 5, 154-6.
22. Horiuti, Y. First International Conference on Catalysis. In K. A. Library.
23. Karn, F.S., Schultz, J.F., and Anderson, R.B. "Hydrogenation of CO and  $\text{CO}_2$  on Supported Ruthenium at Moderate Pressures," Ind. Eng. Chem. Prod. Res. Develop., Vol 4, pp 265-269. (Dec. 1969).
24. Kurita, H., and Tsutsuni, Y. "Hydrogenation of CO in the Presence of Borides of Nickel, Cobalt, and Iron," Nippon Kagaku Zasshi, 82, pp 1461-3 (1961)
25. Lee, A. L., Feldkirchner, and Tajbl, D. G. "Methanation for Coal Hydrogasification," ACS Div. Fuel Chem. Preprints, 14, No. 4 Part 1, 126-142, (Sept. 1970).
26. Linden, H.R. "Conversion of Solid Fossil Fuels to High Heating Value Pipeline Gas," Chem, Eng. Progr. Symposium., 61 No. 54, 76-103, (1965).
27. Lobo, P.A. Slieperich, C.M. and White, R. R. "Steel Catalyst and Hydrogenation of CO and  $\text{CO}_2$ ," Ind. Eng. Chem. 48, No. 5., 906 (1956)
28. Luyten, L and Jungers, J.C. "The Kinetics of the Catalytic Synthesis of  $\text{CH}_4$  in Nickel," Bulletin Soc. Chin. Belg. 54, 303-18 (1945)
29. McKee, D. W. "Interaction of  $\text{H}_2$  and CO on Pt Group Metals," J.Cotel, 8, pp 240-249 (July, 1967)
30. Nicolai, J., d'Hont, U. and Jungers. J.C. "Methanation of  $\text{CO}_2$ ," Bulletin. Soc. Chin. Belg. 55, pp 160-176 (1946).
31. PEDU Studies, Engineering Mass Transfer Effects. Methanation Studies, (1970 or later)

32. Pour, V. "Hydrogenation of CO<sub>2</sub> on Nickel Catalysts, I. Kinetics and II. Effectiveness Factor," Collect Csech Commun. 34, 45-56, (Jan. 1969) and 34, 1217-1228, (April, 1969).
33. Pursley, J.A., White, R. R. and Slipeovich, C. "The Rate of Formation of CH<sub>4</sub> From CO and H<sub>2</sub> with a Nickel Catalyst at Elevated Pressures," Chem, Eng. Progress Symp. Ser., 48, No. 4, 51-58 (1952).
34. Pursley, J. A. Ph.D Thesis, University of Michigan, Ann Arbor (1951).
35. Randhava, S.S., Camara, E. H., and Rehmat, A. "Methanation of Low Levels of CO over Nickel Catalysts," Ind. Eng. Chem Prod. Res. & Dev. 8, No. 4 (Dec. 1969)
36. Randhava, S. S. and Rehmat, A. "The Hydrogenation of CO<sub>2</sub> in Parts Per Million Level," ACS Div. Fuel Chem. Preprint, 14, No. 3, 1 - 9, (Sept. 1970)
37. Rehmat, A., and Randhava, S.S. "Selective Methanation of CO," Ind. Eng. Chem. Prod. Res. Develop. 9, No. 4. (1970)
38. Rosenberg, S.D. Guter, G.A., Miller F. E. and Jameson, G.R. Catalytic Reduction of CO with H<sub>2</sub>. Aerossett General Corp. (July 1964) NASA Contractor Report CR-57.
39. Satterfield, C.N. and Sherwood, T.K. The Role of Diffusion in Catalysts. Addison-Wesley Publishing Co., Reading, Mass. (1963)
40. Schlesinger, M.D., Demeter, J.J. and Greyson, M. "Catalyst for Producing CH<sub>4</sub> from H<sub>2</sub> and CO," Ind. Eng. Chem. 48, 68-70. (Jan. 1956)
41. Schultz, J.F., Karn, F.S. and Anderson, R. B. "Methanation Over Noble Metal Mo and W." U.S. Bureau of Mines, R.I. 6974, p.20. (1967)
42. Schuster, F., Panning, G. and Buelow, H. Brennst. Chem. 16, 368 (1935)
43. Smith, P.D. and White, R. R. "Catalytic Hydrogenation of CO and CO<sub>2</sub> Over Steel," AIChE Journal 2, No. 1, 46 (1956)
44. Tajbl, D. G., Feldkirchner, H.L. and Lee, A. L. "Cleanup Methanation for Hydrogasification Process" Fuel Gasification, R.F. Gould, Pd. pp. 166-172. ACS Advances in Chemistry Series 69, Washington D.C. (1967)
45. Tajbl, D.G., Feldkirchner, H.L. and Lee, A. L. "Cleanup Methanation for Hydrogasification Process," ACS Gasification, Symposium, NYC. Sept. 1966; Vol 10; No. 4.
46. Thompson, E. B. Jr. "Investigation of Catalytic Reactions for CO<sub>2</sub> Reduction," Technical Documentary Report No. FDL TDR-64-22, I, II, III, IV, V., 1964-67

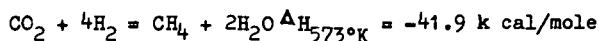
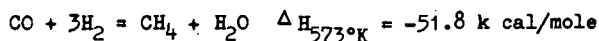
47. Vahala, J. "Methanation Catalysts. III Thermally Stable Catalysts," Chem. Prum. 1971, 161, 270-277.
48. Van Herwijnen, T. Van Doesburg, H. and DeJong, W. A. "Kinetics of the Methanation of CO and CO<sub>2</sub> on a Nickel Catalyst," Journal of Catalysis 28, 391-402. (1973)
49. Vlasenko, V.M. and Yuzefovich. "Methanation of the Catalytic Hydrogenation of Oxides of Carbon to CH<sub>4</sub>," USP Khim. 38, 1622-1647, (Sept. 1969). Translation: Russian Chem. Rev. 38, 728 -739 (Sept. 1969)
50. Vlasenko, V. M. Rusan, M.T., and Yuzefovich. "Kinetics of CO<sub>2</sub> Hydrogenation on Nickel Catalyst," Kineti Katul 2 , 525-528, (July, Aug. 1961)
51. Vlasenko, V.M. and Yuzefovich. "Hydrogenation of CO and CO<sub>2</sub> over Nickel Catalyst," Kineti Katul. 6, 938-941. (Sept. Oct. 1965).
52. Wainwright, H.W. Egleson, G.C., and Brock, C.M. "Laboratory Scale Investigation of Catalytic Conversion of Synthesis Gas to Methane," U.S. Bureau of Mines, R. I. 5046, (April 1959).
53. Wakao, N. and Smith, J. M. "Diffusion in Catalyst Pellets Deals with Diffusion through a Macropoic-Micropore System," Chem Eng. Science, Vol 17, pp. 825-35 (1962)
54. Weller, S. "Analysis of Kinetic Data for Heterogeneous Reactions," AIChE Journal 2, No. 1, (March 1956)
55. Wen, C.Y., Chen, P. W., Kato, K., and Galli, A.F. "Optimization of Fixed Bed Methanation Processes," ACS Fuel Chem Preprints, 14 No. 3, 104-163. (Sept. 8-13, 1964).
56. Wheeler, A. Emmett, Catalysis, Vol. 12, pp. 140-150. Reinhart Publishing Company, N. Y. (1955)
57. Lee, A.L., "Methanation for Coal Gasification," "Clean Fuel for Coal Symposium," Chicago (Sept., 1973)
58. Laupichler, F.G., Ind. Eng. Chem. 30, 578-86 (1938)

George W Bridger and Colin Woodward

Research Department, Imperial Chemical Industries Limited, Agricultural Division,  
P O Box 6, Billingham, Teesside, TS23 1LE, England

### Introduction

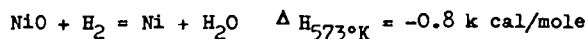
Methanation is the final stage in the purification of synthesis gas in which small concentrations of CO and CO<sub>2</sub> (0.1 - 0.5%) are removed catalytically by reaction with hydrogen:-



The methanation process commonly operates at pressure up to 30 atms and, with the nickel catalyst which is almost universally used for the process, the inlet temperature is about 300°C (570°F). Almost complete conversion of the oxides of carbon occurs giving a product synthesis gas containing less than 5 ppm CO + CO<sub>2</sub>. The temperature rise for the exothermic methanation reactions is typically 35°C (60°F).

### Catalyst Formulation

The catalysts used in the process are essentially nickel metal dispersed on a support material consisting of various oxide mixtures such as alumina, silica, lime, magnesia and compounds such as calcium aluminate cements. When the catalyst is made the nickel is present as nickel oxide which is reduced in the plant converter with hydrogen, usually the 3:1 H<sub>2</sub>:N<sub>2</sub> synthesis gas:-



The heat of reaction is negligible and there is no significant change in temperature in the catalyst bed during reduction. Design limitations in most modern plants require that the catalyst should preferably be reduced at its normal operating temperature, around 300°C (570°F). Once some metallic nickel has been formed, however, methanation begins with the corresponding temperature rise which accelerates reduction of the catalyst further down the reactor. Clearly, the reduction process will continue after the reactor is on-line so that it is common for the activity of the catalyst to continue to increase for some time until an equilibrium state, corresponding to a particular degree of reduction of the nickel, is reached. If engineering considerations permit, the reduction process can be accelerated without detrimental effect upon the catalyst by increasing the temperature to ~660°F.

A good methanation catalyst is one which is physically strong, reducible at 300°C (570°F) and has a high activity. In order to provide a long life, it must retain these properties in use. Commonly lives of 3-5 years are obtained from charges of ICI catalyst 11-3, depending on the temperature of operation and the presence of poisons in the synthesis gas, factors which are discussed later relative to catalyst life. These properties can be obtained by careful attention to the formulation and manufacture of the catalyst.

Methanation activity is related to the surface area of the nickel metal obtained when the catalyst is reduced. The highest surface area of metal and the highest activity are obtained when the nickel is produced as very small crystallites, usually below 100 Å in diameter. One of the functions of the other oxides in the catalyst is to support this fine dispersion of nickel crystallites so that they are available for reaction. The oxides mixed with nickel also retard growth or

sintering of the metal to form large crystallites with a lower surface area and lower activity. The nickel can be dispersed among the other oxides in various ways producing different degrees of mixing e g by impregnation of a preformed oxide support with a soluble nickel compound, or by coprecipitating a nickel compound together with the other materials such as aluminium or magnesium as hydroxides or carbonates. These materials are worked up by drying, decomposing etc and pelleting or extruding precipitated materials, to produce the final catalyst.

Intimate mixing of the components can lead to the formation of compounds or of solid solutions of the components which are difficult to reduce at 300°F but which, when reduced, contain well dispersed and well stabilised nickel. Methanation catalysts in practice therefore are compromises which achieve an optimum reducibility with activity and stability.

An example of compound formation is provided by alumina which, with nickel oxide, readily forms spinel compounds of the type  $\text{NiO} \cdot \text{Al}_2\text{O}_3$ . A temperature around 1000°C (1800°F) is necessary for combination when NiO is mixed with  $\alpha$ - $\text{Al}_2\text{O}_3$  but with finely divided NiO and  $\gamma$ - $\text{Al}_2\text{O}_3$  temperatures around 500°C (930°F) are sufficient. When the oxides are coprecipitated "spinel precursors" can be detected in the dried precipitate and such catalysts have to be reduced at temperatures as high as 500°C (930°F). They are, therefore, unsuitable for use in conventional ammonia synthesis methanation units.

Magnesia forms solid solutions with NiO. Both MgO and NiO have face-centred cubic lattices with NaCl - type structures. The similarity between the ionic radii of the metals ( $\text{Ni}^{2+} = 0.69\text{Å}$ ,  $\text{Mg}^{2+} = 0.65\text{Å}$ ) allows interchangeability in a crystal lattice and thus the formation of solid solutions of any proportions of the two oxides is possible. Such solid solutions are more difficult to reduce than separate NiO. Thus Takemura et al (Ref 1) showed that NiO reduced completely in the range 230° - 400°C (440° - 750°F) while a 10% NiO - 90% MgO solid solution reduced in two stages, one in the range 230° - 400°C and the other in the range 500° - 600°C (930° - 1100°F). For ease and completeness of reduction in a methanation catalyst, therefore, excessive solid solution formation should be avoided. As indicated above however solid solution formation is beneficial in retarding crystal growth of NiO during manufacture and of reduced Ni during operation. During manufacture a precipitated nickel compound such as the carbonate has to be converted into nickel oxide and, in order to obtain small NiO crystallites, it is desirable that the calcination temperature should be the minimum compatible with efficient conversion of  $\text{NiCO}_3$  to NiO. Differential thermal analysis (Figure 1) shows that this endothermic process occurs in two main stages with maxima around 150°C (300°F) and 340°C (640°F) and that the presence of a proportion of magnesia in a solid solution raises the required temperature by only about 15°C (25°F).

This presence of MgO, however, does retard the growth of NiO during calcination as shown in figures 2, 3 and 4. Figure 2 shows, for example, that calcination at 500°C (920°F) for 4 hours results in an increase in NiO crystallite size to 300 - 400 Å whereas, after the same treatment, the crystallite size of an NiO-MgO solid solution (60 - 40 w/w) would be only about 80 Å. Figures 3 and 4 show the effect of duration of calcination on crystal growth at different temperatures. Crystallite size is proportional to  $T^{0.25}$  for NiO alone, and proportional to  $T^{0.12}$  for NiO-MgO and for MgO alone.

Figure 5 shows the effect of calcination temperature on the subsequent activity of the catalyst after reduction at 300°C (570°F). These activity measurements are made in laboratory tubular reactors operating at 1 atmosphere pressure, inlet gas composition CO 0.40%,  $\text{N}_2$  25%,  $\text{H}_2$  74.6% and inlet temperature 300°C. Conversion of CO is measured and the catalyst activity expressed as the activity coefficient, k, in the first order equation :

$$\text{rate} = k p_{\text{CO}} P^{0.3} \left(1 - \frac{K}{K_p}\right) e^{-\frac{e}{RT}}$$

The reducibility of the catalyst is demonstrated in Figure 6 which shows the activity of catalysts, measured as described above, after reduction to constant activity at temperatures in the range 280° - 350°C (530° - 660°F). It will be seen that catalyst 11-3 compares favourably with other catalysts which contain larger amounts of alumina and consequently are more difficult to reduce at acceptable temperatures.

In summary, therefore, we have found it beneficial to include a small amount of MgO (2 - 3%) in ICI methanation catalyst 11-3. This provides the ideal compromise between ease of reducibility and sintering resistance. By this means, a catalyst is produced which is readily reduced at 300°C - 350°C (570° - 660°F) but with which loss of activity caused by sintering is not a problem during several years' normal operation at temperatures up to 350°C (660°F). This good performance has been confirmed by experience in many plants including ICI's three 1000 ton/day ammonia plants at Billingham, England.

#### Poisons

With a well constituted catalyst of this type, at normal operating temperatures sintering is not an important cause of loss of activity even if the catalyst is occasionally overheated. The principal cause is poisoning. Sulphur compounds are virulent poisons for nickel catalysts but in the synthesis gas purification stream the methanation catalyst is protected by the LT shift catalyst in the preceding stage which is an efficient sulphur-guard. Therefore in normal operation the methanation catalyst is unlikely to be exposed to sulphur. The exception to this would be if the LT shift converter were partially by-passed in which instance sulphur could reach the methanation catalyst. Serious deactivation of the catalyst can occur; for example one containing about 30% NiO (before reduction) shows significant loss of activity when the sulphur content exceeds ~0.1%.

The poisons most likely to be encountered on an ammonia plant are those originating in the CO<sub>2</sub>-removal system which precedes the methanator. Carry-over of a small amount of liquid into the methanator, which is almost inevitable, is not normally serious. Plant malfunction, however, can sometimes result in large quantities of CO<sub>2</sub>-removal liquor being pumped over the catalyst and this can be very deleterious. Table 1 shows the effect of common CO<sub>2</sub> - removal liquors on methanation catalyst activity.

Table 1 Poisoning effects of CO<sub>2</sub> removal systems

Process	Chemicals	Effect
Benfield process	Aqueous potassium carbonate	Blocking of pores of methanation catalyst by evaporation of potassium carbonate solution
Vetrocoke process	Aqueous potassium carbonate-arsenious oxide	As Benfield. Also As <sub>2</sub> O <sub>3</sub> is poison - about one-half of activity is lost when As = 0.5%
Benfield DEA	Aqueous potassium carbonate plus 3 per cent diethanolamine	As Benfield. DEA is harmless
Sulphinol	Sulpholane, water, di-isopropanolamine	Sulpholane will decompose and give sulphur poisoning
MEA, DEA	Mono- or diethanolamine in aqueous solution	No poisoning effect
Cold Rectisol	Methanol	No poisoning effect

## Prediction of Catalyst Life

In the operation of a methanator, it is important to be able to estimate the remaining future useful life of a catalyst charge at any moment. The question to be answered is "should this catalyst charge be changed during the shut-down planned for x weeks time or is it good enough to last until the next shut-down planned for a year hence?". Strictly, therefore, the requirement is for a Yes/No answer rather than a precise prediction, the assumption being that changing a catalyst alone will never be the reason for a shutdown. This is reasonable because, if the cost of plant down-time is compared with the cost of a catalyst charge, it is clearly economic to change catalyst rather than to run the risk of a catalyst failure causing an additional shut-down.

Methanation converters on most ammonia plants are over-designed, both for safety reasons and as a result of increases in catalyst activity since plants were built. Consequently at the beginning of the catalyst's life most of the methanation is virtually completed in the first 25% of the bed and monitoring exit gas composition gives no information about die-off of the catalyst. Catalyst deactivation occurs normally by a poisoning mechanism and, as poisoning continues, the volume of active catalyst remaining will eventually be insufficient to meet the required duty. Although the thermodynamic exit levels of CO and CO<sub>2</sub> are about 10<sup>-4</sup> ppm, in practice these are not attained because of kinetic and other limitations and the actual exit concentrations, during normal operation, are of the order of 1-2 ppm.

A technique has been devised for calculating when exit carbon oxides will exceed any given design level and hence predicting the future useful life of the catalyst charge. The method is based upon accurate measurement of the temperature profile in the bed using a moveable thermocouple or a series of fixed thermocouples. A point on the profile is selected at which conversion is nearly complete. This point can, for example, be taken as the point at which 5°F temperature rise remains; the total temperature rise across a methanator is typically 60°F. The 5°F point provides a good compromise between selecting a point near the top of the temperature rise, so that pressures and temperatures can be regarded as nearly constant for the remainder of the bed, and minimising inaccuracies in temperature measurements. Obviously, if the method is valid, any selected point will give the same result. The method also assumes that CO methanates before CO<sub>2</sub>, which is commonly accepted (Ref 2), so that over the last part of the catalyst bed, only the completeness of CO<sub>2</sub> methanation need be considered.

The temperature profile obtained by means of a moveable thermocouple is of the form shown in Figure 7. For highest accuracy, the maximum possible number of readings should be made in the region of the 5°F point. Interpretation of this profile to obtain a catalyst life prediction is made graphically and the mathematical derivation of the technique appears in the Appendix. The method assumes first order reaction kinetics with respect to CO<sub>2</sub> (Ref 2). If the gradient of the temperature profile at the 5°F point is drawn, i.e. the tangent to the curve at this point, this is a measure of the rate of reaction at this point in the bed. If catalyst activity is assumed to be constant in the remainder of the bed, this can be used to estimate the further depth of bed required for reaction to reach any selected carbon oxides level. Design limits may be imposed by the requirement to have total CO + CO<sub>2</sub> low enough to avoid poisoning ammonia synthesis catalyst (e.g. CO + CO<sub>2</sub> < 10 ppm). More commonly, however, the main objective is to minimise ammonium carbamate, NH<sub>4</sub>COONH<sub>2</sub>, in the synthesis gas loop for which a limit of CO<sub>2</sub> < 2 ppm appears desirable.

The last 5°F rise of temperature at the end of the bed corresponds to methanation of about 465 ppm CO<sub>2</sub>; typically methanation of 1% CO<sub>2</sub> produces a temperature rise of 108°F; 1% CO produces 133°F. It can be shown (see Appendix) that an exit level of 2 ppm CO<sub>2</sub> corresponds to the point at which the tangent intersects a horizontal line drawn 28°F above the 5°F point. The graphical constructions are therefore as shown in Figure 8. This permits identification of the present position of the "effective end of the bed" and hence of the amount of reserve

catalyst remaining. In our experience, the "effective end of the bed" is usually located by this method as 1-1.5 ft below the point at which, within measurement accuracy, maximum temperature is attained. This figure obviously depends upon the shape of the profile, i.e. on the activity of the catalyst, and should be regarded as not more than an indication. It is then necessary to study the previous history of the charge in order to estimate the rate of profile movement and likely future useful life of the charge.

The main disadvantage of this technique is that it relies upon very accurate temperature measurement, particularly near the top of the temperature profile so that the position of the 5°F point can be established and the tangent accurately constructed. Also, the end of the bed is predicted from only kinetic considerations when, in fact, other factors may be more important. In practice, however, although this introduces some scatter into successive measurements - as does variation in duty required of the methanator - the technique has proved very satisfactory. Typical findings are represented in Figure 9 where, if the present rate of catalyst die-off continues, the end of useful catalyst life is reached when the current end of the bed reaches the actual end of the bed, in this instance after about 6 years on line.

#### Conclusion

In summary, therefore, we can say that methanation catalysts for these applications are very satisfactory in terms of activity, strength and stability. In the absence of detrimental mal-operations, one can expect favourable operating experience and we have demonstrated a simple and convenient method by which the future useful life of a catalyst on-line can be estimated.

#### Acknowledgements

We are pleased to acknowledge our indebtedness to colleagues Dr P J Baldock and Mr A Parker for the X-ray crystallographic studies, to Dr P Snowden who devised the life prediction technique and to Imperial Chemical Industries Ltd. for permission to publish this paper.

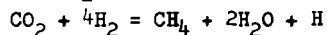
#### References

- 1 Y Takemura, Y Morita and K Yamamoto, Bull. Jap. Petrol. Inst., 9, 13, (1967)
- 2 T Van Herwijnen, H Van Doesburg and W A De Jong, J Catal., 28, 391, (1973)

#### Appendix

##### Derivation of Graphical Method

The CO<sub>2</sub> methanation reaction is:-



where H = heat of reaction

The rate of conversion of CO<sub>2</sub> in a short section of the catalyst bed of length dl can be calculated from the first order rate equation:-

$$dX = k_{op} P^a \left[ 1 - f\left(\frac{K}{K_p}\right) \right] e^{-\frac{E}{R} \left( \frac{1}{T} - \frac{1}{T_0} \right)} \dots \dots \dots 1)$$

where dX = moles CO<sub>2</sub> converted per second per unit volume of bed

- $k_o$  = rate constant at  $T_o$
- $p$  = partial pressure of  $CO_2$
- $P$  = total pressure
- $T$  = temperature of section of bed, °K
- $a$  = total pressure coefficient
- $K_p$  = equilibrium constant for the reaction
- $K = \frac{(p_{CH_4})(p_{H_2O})^2}{p(P_{H_2})^4}$

Since the system is far from equilibrium, (the actual  $CO_2$  concentration even at the exit of the bed is about 2 ppm compared with an equilibrium concentration of  $10^{-4}$  ppm),  $K$  is small compared with  $K_p$  and the term  $\left[1 - f\left(\frac{K}{K_p}\right)\right]$  becomes unity

i.e. the effect of the reverse reaction can be ignored. Equation (1) then becomes:-

$$dX = k_o p P^a e^{-\frac{E}{R}\left(\frac{1}{T} - \frac{1}{T_o}\right)} \dots \dots \dots 2)$$

Considering the small section of bed of length  $dl$  and cross-sectional area  $A$ :-  
 Heat from reaction =  $dX.HA.dl$  cals/second  
 Therefore the temperature rise  $dT$  across the section of bed is given by:-

$$dT = \frac{dX.HA.dl}{CG} \dots \dots \dots 3)$$

where  $G$  = gas flow rate in moles/second  
 $C$  = specific heat of gas per mole at  $T$  and  $P$

Rearranging (3) and combining with (2):-

$$dX = \frac{C}{H} \frac{G}{A} \frac{dT}{dl} = k_o p P^a e^{-\frac{E}{R}\left(\frac{1}{T} - \frac{1}{T_o}\right)}$$

The temperature gradient at a point in the bed where the temperature is  $T$  is therefore:-

$$\frac{dT}{dl} = \frac{HA}{CG} \cdot k_o P^a p e^{-\frac{E}{R}\left(\frac{1}{T} - \frac{1}{T_o}\right)}$$

Now for a point  $A$  near the top of the profile (see Fig 8) at temperature  $T_1$ , the temperature gradient  $\left(\frac{dT}{dl}\right)_1$  is given by:-

$$\left(\frac{dT}{dl}\right)_1 = \left(\frac{HA}{CG}\right)_1 k_o P_1^a p_1 e^{-\frac{E}{R}\left(\frac{1}{T_1} - \frac{1}{T_o}\right)}$$

Now substituting for  $k_o$  in equation (2),

$$dX = \left(\frac{dT}{dl}\right)_1 \left(\frac{CG}{HA}\right)_1 \frac{P^a p e^{-\frac{E}{R}\left(\frac{1}{T} - \frac{1}{T_o}\right)}}{P_1^a p_1 e^{-\frac{E}{R}\left(\frac{1}{T_1} - \frac{1}{T_o}\right)}}$$



FIGURE 1. D.T.A. CURVES OF BASIC CARBONATES

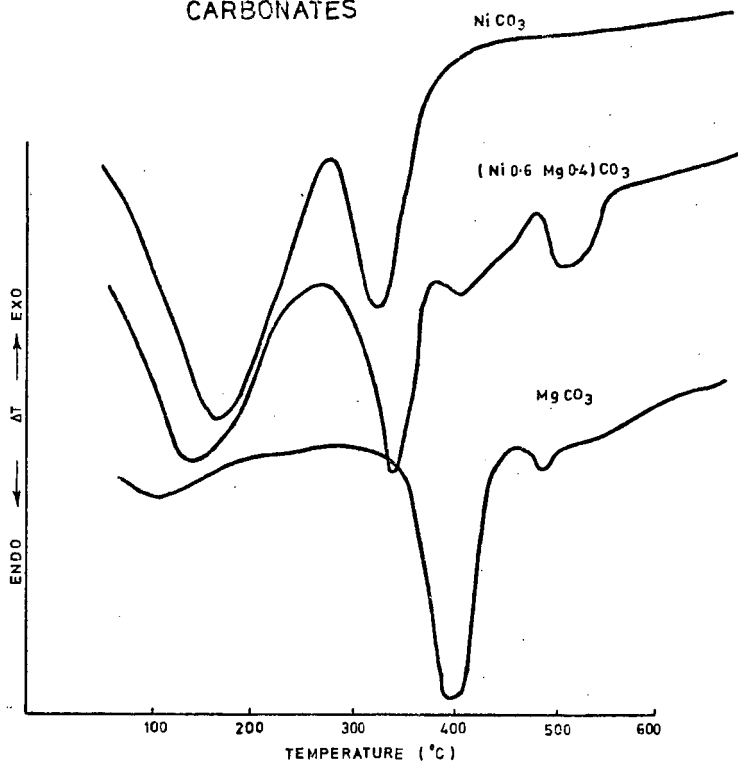


FIGURE 2. VARIATION OF CRYSTALLITE SIZE WITH CALCINATION TEMPERATURE

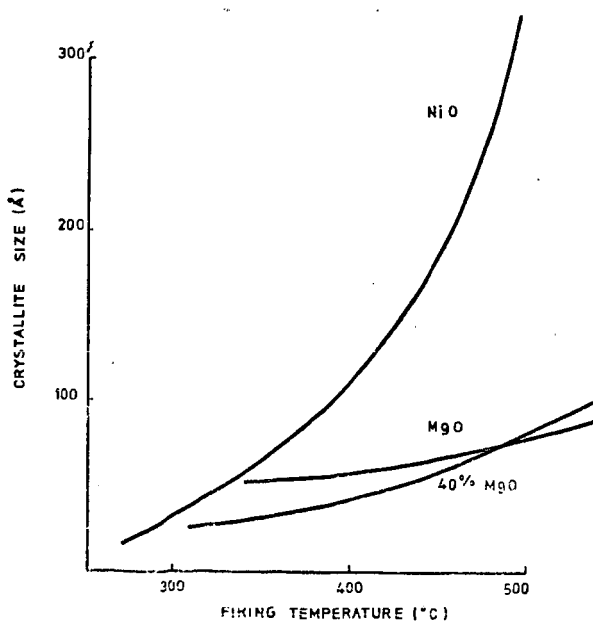


FIGURE 4. VARIATION OF NiO-40% MgO CRYSTALLITE SIZE WITH TIME

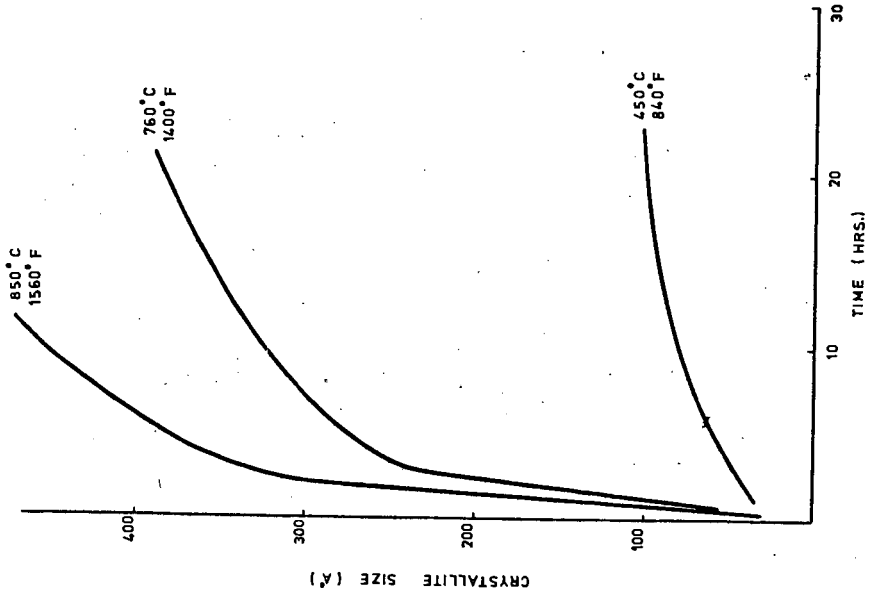


FIGURE 3. VARIATION OF NiO CRYSTALLITE SIZE WITH TIME

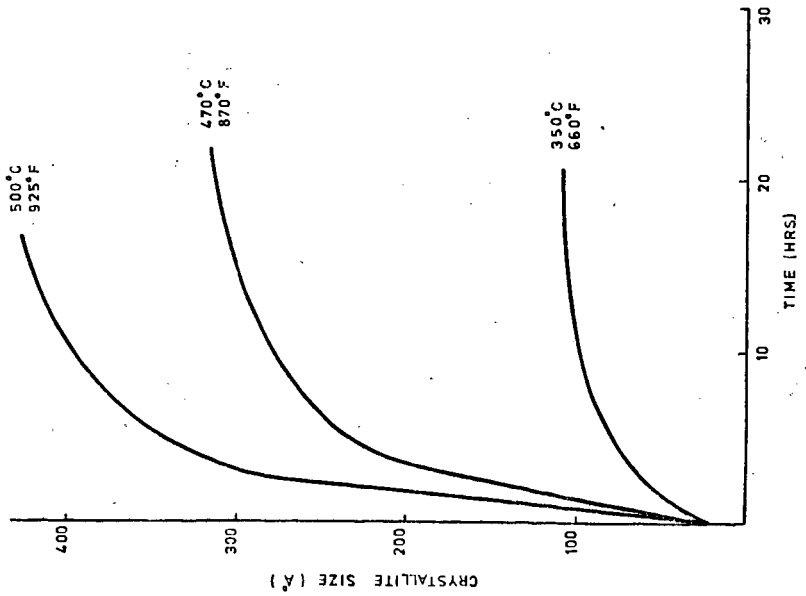


FIGURE 5. ACTIVITY vs CALCINATION TEMPERATURE

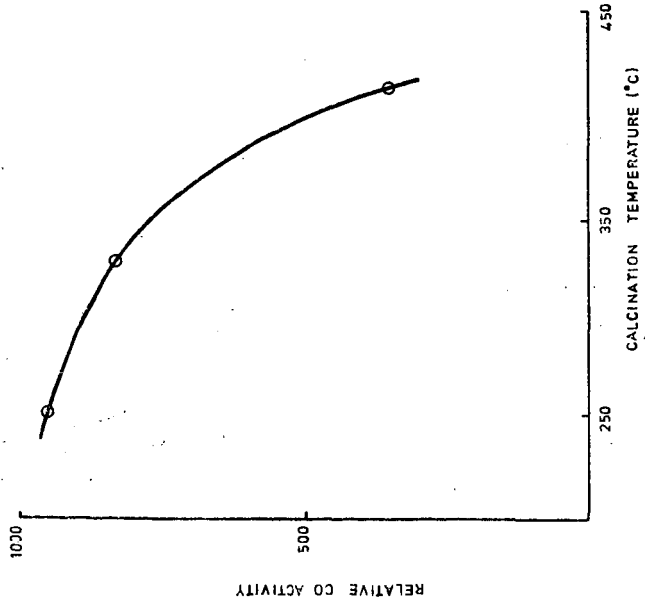


FIGURE 6. ACTIVITY vs REDUCTION TEMPERATURE

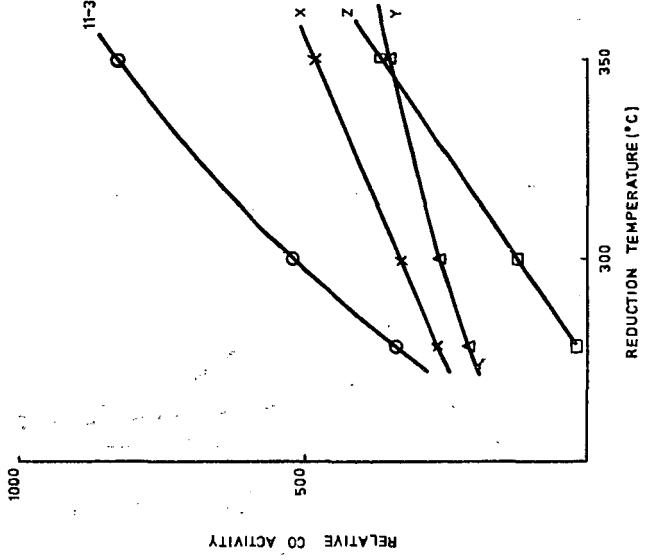


FIGURE 7. TYPICAL METHANATOR TEMPERATURE PROFILE

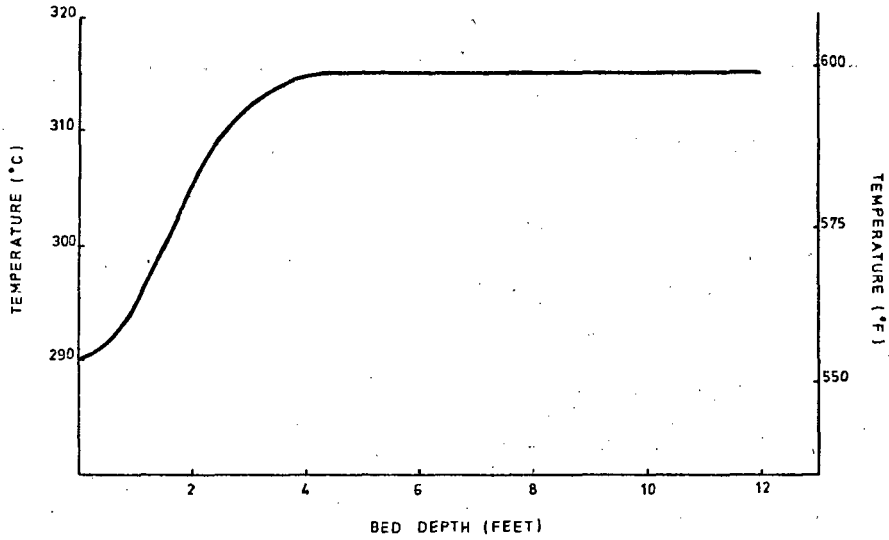


FIGURE 8. LOCATION OF EFFECTIVE END OF BED

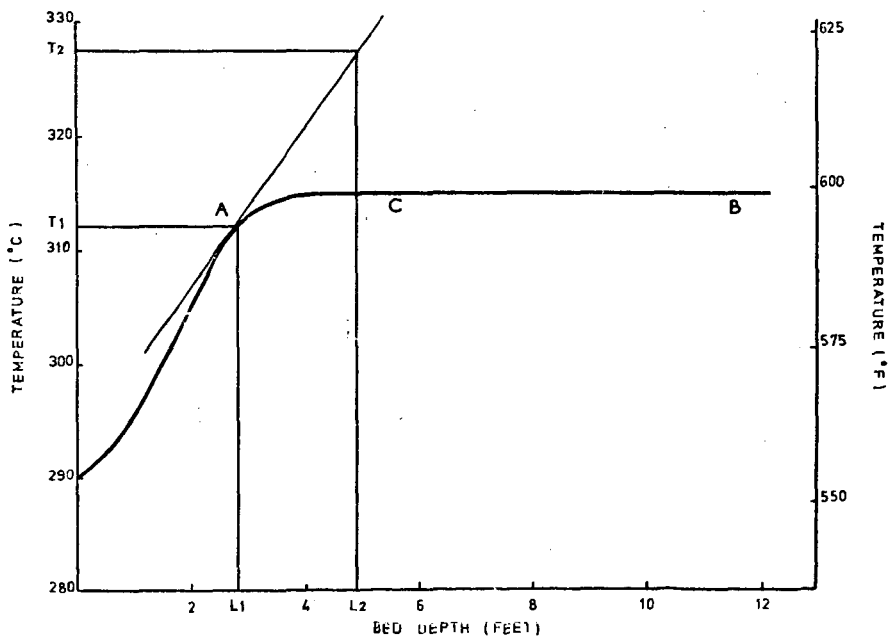
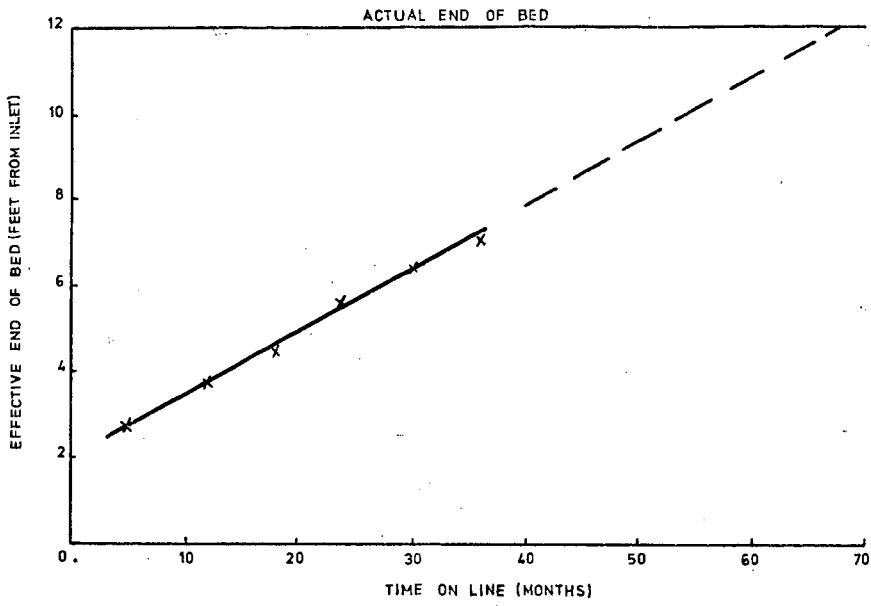


FIGURE 9. FUTURE USEFUL LIFE PREDICTION



## Equilibrium Considerations in the Methane Synthesis System

Gerald Gruber

FMC Corporation, Princeton, N. J.

### Summary

An investigation was made into the equilibria of the methanation reaction, coupled with the shift reaction and the carbon deposition reaction. Of particular interest is the exploration of regions where carbon deposition is possible according to thermodynamic criterion, assuming that carbon is deposited as graphite or "Dent" carbon.

The carbon laydown curves are plotted on a unique coordinate system which corresponds to starting composition variables that are commonly used. The effects of pressure, temperature and starting composition on carbon laydown are investigated over a wide range of practical interest, and beyond. All possible starting compositions are considered over a temperature range of 600°K (625°F) to 2000°K (3140°F) and a pressure range of 30 atm (426 psig) to 300 atm (4395 psig). In addition, the effects of pressure, temperature and starting composition on equilibrium composition and product gas heating value are examined. The figures presented provide a useful tool for the rapid scanning of the effect of possible starting gas composition, pressure and temperature on product gas quality and useful operating regions. The utility of the graphs are not limited to a single stage reaction, but can be used for multiple stage reactors with arbitrary amounts of diluents ( $H_2O$ ,  $CO_2$ ,  $CH_4$ ) and recycle gas, which may change from stage to stage. Additionally, the pressure and temperature of each stage may be considered independently.

## Equilibrium Considerations in the Methane Synthesis System

Gerald Gruber

FMC Corp., Princeton, N. J.

Introduction

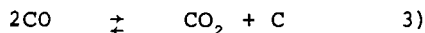
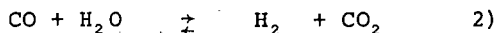
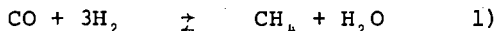
Considering the synthesis of methane from carbon monoxide and hydrogen, it is desired to operate a reactor, or reactors, in such a way as to avoid the deposition of carbon on catalyst surfaces and to produce a high quality product gas. Since gas compositions entering the reactor may vary considerably because of the use of diluents and recycle gas in a technical operation, it is desirable to estimate the effects of initial gas composition on the subsequent operation. Pressure and temperature are additional parameters.

It is a simple enough matter to calculate the equilibrium composition for any given starting composition, pressure and temperature. It is no more difficult to do it for a range of starting compositions, pressures and temperatures, except that it takes longer. Since the calculations are done on a computer, many parameters can be closely examined. However, faced with the great mass of calculated results, it is important to have them presented in a concise, informative manner.

By using a particular type of triangular diagram, it is possible to represent all possible starting compositions of CO, CO<sub>2</sub>, H<sub>2</sub>, H<sub>2</sub>O and CH<sub>4</sub> on a single coordinate system which is easy to use.

Chemistry

Consider the following reactions which are sufficient to describe the system:



In addition, it will be convenient to make reference to another reaction:



which is not independent of reactions 1-3.

Reactions 1 and 3 are highly exothermic and therefore have equilibrium constants that decrease rapidly with temperature. Reaction 2 is moderately exothermic, and consequently its equilibrium constant shows a moderate decrease with temperature. Reaction 4 is moderately endothermic and its equilibrium constant increases with increasing temperature.

The relationship between temperature and equilibrium constant for these four reactions is indicated in Figure I, where carbon is assumed to be graphite. Thermodynamic data were taken from JANEF (1) and Rossini (2).

If we allow for the fact that carbon may be deposited in a form other than graphite, the equilibrium constants of reactions 3 and 4 must reflect the different state. This behavior has in fact been observed by Dent (3).

Dent and his coworkers found that the observed equilibrium constant for reaction 3 was less than the theoretical equilibrium constant for deposition of graphite based on measurements made between 600°K and 1200°K. The departure was greatest at 600°K, and the observed and theoretical equilibrium constants approached each other as the temperature increased, becoming equal at about 1100°K to 1200°K. The difference in free energy between graphite and the actual form of carbon deposited was also determined by decomposing pure  $\text{CH}_4$  and by depositing carbon from a  $\text{CO}$  and  $\text{H}_2$  mixture. These results confirmed the measurements made by decomposing pure  $\text{CO}$ . These experiments were performed over a nickel catalyst and it is speculated that the anomalous free energy of the deposited carbon may be due to the fact that it forms a carbide or a solid solution.

Whatever the exact form of the carbon deposition is, it must be recognized and taken into account in future calculations. The deposited material is called "Dent" carbon, and equilibrium constants based on its free energy are also indicated in Figure I. The fact that carbon deposits as "Dent" carbon has been qualitatively confirmed by Pursley (4).

Other recent equilibrium calculations (5, 6, 7) found in the literature assume carbon deposition to be in the form of graphite. In this paper, calculations are based on both cases, graphite and "Dent" carbon.

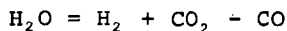
#### Calculation of Carbon Deposition

If we consider the system consisting of the six species,  $\text{CO}$ ,  $\text{H}_2$ ,  $\text{H}_2\text{O}$ ,  $\text{CO}_2$ ,  $\text{CH}_4$ , and  $\text{C}$ , together with the three independent reactions 1 through 3, the system can be uniquely defined by specifying three species. As a matter of convenience, we

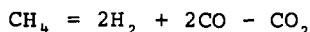
select the three species to be  $H_2$ ,  $CO$ , and  $CO_2$ , and furthermore, by normalizing the composition such that the number of moles of the species sums to unity we only have to specify two species explicitly, which are chosen to be  $H_2$  and  $CO$ . Then, the composition of  $CO_2$  is implied. In order to calculate carbon deposition, for any given starting temperature the procedure is to solve equations 1 and 2 for the equilibrium composition, ignoring carbon deposition. After the equilibrium composition is obtained, a check is made to see if the ratio  $(CO)^2/CO_2$  according to equation 3 would lead to carbon deposition. If no carbon deposition is indicated, then the entire calculation is repeated using equations 1 to 3 if it is desired to calculate the amount of carbon deposited. By using the above procedure, a line is defined which defines the coordinate region into two areas; one where graphite may deposit, and one where graphite may not deposit - based on equilibrium calculations. A sample of this type of graph is shown in Figure II.

#### Coordinate Systems

Before we discuss the curves in Figure II, a short discussion of the coordinate system will be presented. As indicated above, any possible composition of  $CO$ ,  $CO_2$ ,  $H_2$ ,  $H_2O$ , and  $CH_4$  (solid carbon also) may be depicted on the coordinate system shown if the independent species are selected to be  $H_2$ ,  $CO$  and  $CO_2$ . Further, the sum of the species is set to unity and only  $H_2$  (Y coordinate) and  $CO$  (X coordinate) are explicitly plotted. Pure  $H_2$  is indicated as the point (0, 1.0) and pure  $CO$  is indicated at the point (1.0, 0). Similarly, pure  $CO_2$  is at the point (0, 0), and compositions corresponding to pure  $H_2O$  (-1, 1) and pure  $CH_4$  (2/3, 2/3) are also indicated. Water, for example, in terms of the independent species is expressed as



as the point on the graph corresponds to  $X = 1$  and  $Y = 1$ . Similarly,  $CH_4$  may be expressed as



The total number of moles is 3 so that upon normalizing  $Y = 2/3$  and  $X = 2/3$ . In general, for a mixture of arbitrary composition, the coordinates are given by

$$Y = \frac{H_2O + H_2 + 2CH_4}{H_2O + H_2 + CO_2 + CO + 3CH_4} \quad 5)$$

$$X = \frac{CO - H_2O + 2CH_4}{H_2O + H_2 + CO_2 + CO + 3CH_4} \quad 6)$$

Furthermore, compositions may be found graphically by a lever rule. All mixtures of pure  $\text{CO}_2$  and pure  $\text{H}_2$  fall along the Y axis, the distance from pure  $\text{CO}_2$  being inversely proportional to the amount of pure  $\text{CO}_2$  in the mixture. Similar rules hold for any pair of pure components or, in fact, for any pair of mixtures, with the exception of methane, or mixtures containing methane. Since one mole of methane is equivalent to 3 moles of independent species, methane concentrations must be weighed by a factor of three.

Generally speaking, the area of physical reality corresponds to the region bounded by the straight lines connecting the pure components on Figure II. The region formed to the right of  $\text{CH}_4 - \text{CO}$  line and below the extension of the  $\text{H}_2\text{O} - \text{CH}_4$  line corresponds to mixtures of  $\text{CH}_4$ ,  $\text{CO}$  and solid C, and, although physically realizable, is not considered here.

The two curves shown in Figure II divide the graph into graphite forming and non-graphite forming regions. These curves are for 30 atm pressure and for  $650^\circ\text{K}$  and  $750^\circ\text{K}$ , conditions which are typical of many proposed methanation processes (4, 8, 9, 10). The region below and to the right of the curve is where graphite might be deposited.

Consider the point A on Figure II corresponding to a stoichiometric mixture of  $\text{H}_2$  and  $\text{CO}$ . If pure  $\text{CO}_2$  is added to the mixture, the point C may be reached by moving along the line connecting the point and pure  $\text{CO}_2$ . Similarly, if pure  $\text{H}_2\text{O}$  is added, the composition moves along the line connecting point C and pure  $\text{H}_2\text{O}$  until the point D is reached. Point B can be reached by adding  $\text{H}_2$  and removing  $\text{H}_2\text{O}$ , which point incidently corresponds to a stoichiometric mixture of  $\text{H}_2$  and  $\text{CO}_2$ , or it may be viewed as a stoichiometric mixture of  $\text{H}_2$  and  $\text{CO}$  with an excess of water.

Suppose a starting mixture corresponding to point A, is allowed to react according to equation 1 to produce some  $\text{CH}_4$  and  $\text{H}_2\text{O}$ . The composition of this new mixture is still represented by point A. If water is now removed from the mixture, the composition moves along the line connecting point A and pure  $\text{H}_2\text{O}$  to a point E. The extension of this line intersects the point for pure  $\text{CH}_4$ . If the mixture, whose composition is represented by E, is allowed to react further, and if the water produced is subsequently removed, the point representing the composition will move along the line A - E getting closer to pure  $\text{CH}_4$ .

One objective is to approach pure methane without causing the deposition of carbon or graphite, and these curves provide a rapid picture of how this may be done by operating at different starting compositions and temperatures, even with multiple stages.

Let us now focus attention on the curves in Figure II. Either one will serve as a basis for a qualitative discussion. Consider first mixtures of pure CO and  $\text{CO}_2$ , all points of which lie on the X axis. The equilibrium in this system is fully described by equation 3. As the temperature increases, the equilibrium constant decreases, and CO becomes stable. At the temperature considered here, the mixture will deposit graphite until almost pure  $\text{CO}_2$  is reached. Thus the graphite deposition curve will intersect the X axis at a point which is very close to  $X = 0$  (at  $750^\circ\text{K}$  it is approximately  $X = .01$ ). Pure  $\text{CO}_2$  is stable with respect to carbon deposition, as is pure  $\text{H}_2$ , but there is a large composition range where mixtures of  $\text{H}_2$  and  $\text{CO}_2$  will deposit graphite. Thus the carbon deposition curve intersects the Y axis at two points, as indicated on Figure II. In the region of pure  $\text{CH}_4$ , the equilibrium is governed by equation 4. For this reaction, the equilibrium constant increases with temperature so that at high enough temperatures there will be appreciable dissociation  $\text{CH}_4$  to  $\text{H}_2$  and graphite. In the temperature range considered here, the thermodynamic equilibrium indicates only a very small amount of dissociation so the intersection of the graphite deposition curve and the  $\text{H}_2 - \text{CH}_4$  line occurs at almost pure  $\text{CH}_4$ . As the temperature increases, the point of intersection will move towards pure  $\text{H}_2$  on the  $\text{H}_2 - \text{CH}_4$  line.

So far, we have discussed graphite deposition only in terms of the two reactions 3 and 4. As the temperature increases, graphite deposition by reaction 4 is favored, and is retarded by reaction 3. The net result is that the graphite deposition curves for two temperatures will intersect at some point. This will become clearer when we consider curves at different temperatures than indicated here.

## Carbon and Graphite Deposition

### A. Pressure

In Figure II, curves for two temperatures have been presented that indicate the areas of graphite deposition. Before we consider the effects of higher temperatures, the effect of pressure will be examined.

Figure III shows the graphite deposition curves for 3 pressures at  $700^\circ\text{K}$ . This graph uses the same coordinate system, but is plotted on a larger scale. Again we start by considering the effects of pressure on the two, 2-component systems represented by reaction 3 in one case, and by reaction 4 in the other case.

An increase in pressure favors the reverse of reaction 4 which has the effect of decreasing the graphite formation area in the vicinity of pure methane. Thus the intersection of the graphite deposition curve and the pure  $H_2 - CH_4$  line moves toward pure  $CH_4$ . In considering reaction 3, an increase in pressure enhances the deposition of graphite and the intersection of the graphite deposition curve and the X axis will move closer to pure  $CO_2$ . This behavior again leads to an intersection of the graphite deposition curve for two different pressures. For the temperature indicated ( $700^\circ K$ ), the effect of pressure on the location of the graphite deposition curve is not large, although the effect is more pronounced at higher temperatures.

#### B. Temperature

Attention will now be focused on the effect of temperature on the graphite deposition curve, considering a larger temperature range and the deposition of "Dent" carbon.

Figure IV shows the graphite deposition curves for the temperature range of  $650^\circ K$  to  $2000^\circ K$ . The upper temperature is far above the maximum capability of catalysts which are being proposed to carry out the methanation reaction on a large scale (6); however, it is interesting to carry out the calculations to these high temperatures, assuming that no other reactions will take place.

The behavior previously discussed is now more evident. Along the X axis, as the temperature increases, the intersection of the graphite deposition curve moves towards pure CO, while along the  $H_2 - CH_4$  line the intersection moves towards pure  $H_2$ . Thus, the odd result appears that as the temperature increases, graphite deposition is less likely for starting mixtures which are near stoichiometric, but it is more difficult to produce pure methane by removing water and reacting the mixture further. Due to equilibrium considerations, the final approach to pure methane must be done at a relatively low temperature.

If it is assumed that the solid deposit is not graphite, but has the thermodynamic properties of "Dent" carbon, the situation is quite a bit different. At lower temperatures considered, "Dent" carbon is much less likely to be deposited than graphite, as indicated by the curve for  $600^\circ K$  in Figure V. As the temperature increases, the behavior of "Dent" carbon approaches that of graphite, and the carbon deposition region becomes greater. At approximately  $1100^\circ K$ , the curves for "Dent" carbon and graphite are the same. At higher temperatures, it is assumed that "Dent" carbon and graphite also behave identically in regards to deposition.

Since the effects of temperature on reactions 3 and 4 are in opposite directions, the different temperature curves also intersect, as is the case for graphite.

If it is assumed that the deposition of carbon is governed by the thermochemistry of "Dent" carbon, rather than graphite, it is obvious that there is a much greater region where deposition will not take place.

#### Equilibrium Compositions and Heating Value

The preceding discussion has been mostly confined to the carbon deposition curves as a function of temperature, pressure and initial composition. Also of interest, especially for methane synthesis, is the composition and heating value of the equilibrium gas mixture. It is desirable to produce a gas with a high heating value, which implies a high concentration of  $\text{CH}_4$ , and a low concentration of the other species. Of particular interest are the concentrations of  $\text{H}_2$  and  $\text{CO}$  as these generally are the valuable raw materials. Also, by custom it is desirable to maintain a  $\text{CO}$  concentration of less than 1 percent. The calculated heating values are reported according to the custom in the gas industry, which is based on a cubic foot at 30" Hg and 60°F, saturated with water vapor (11). Furthermore, it is calculated and reported for a  $\text{CO}_2$  and  $\text{H}_2\text{O}$  free gas as these components may be removed from the mixture after the final chemical reaction. Concentrations of  $\text{CH}_4$ ,  $\text{CO}$  and  $\text{H}_2$  are also reported on a  $\text{CO}_2 - \text{H}_2\text{O}$  free basis.

The higher heating value is plotted on the composition coordinate in Figure VI. These curves are for 50 atm and 700°K. The contours of constant heating value increase uniformly in the direction of pure methane. These contours, of course, are very similar to the contours of  $\text{CH}_4$  concentration, which are indicated in Figure VII, for the same conditions, 50 atm and 700°K.

Hydrogen concentration contours for 50 atm and 700°K are shown in Figure VIII. These contours indicate that there is appreciable unreacted hydrogen after equilibrium is obtained, and it is clear that multiple reaction stages are required to approach pure methane.

Carbon monoxide concentration contours are shown in Figure IX for 50 atm and 700°K. These curves indicate that the  $\text{CO}$  leakage will not be high if equilibrium is obtained if the initial composition is near the stoichiometric line.

Figure X shows the effect of temperature on higher heating value,  $\text{CH}_4$ ,  $\text{H}_2$ , and  $\text{CO}$  concentrations for four different starting compositions, which are also indicated on Figure II. The four starting compositions are:

	Y	X	
1	.75	.25	stoichiometric
2	.8	.0	stoichiometric
3	.7	.1	hydrogen deficient
4	.8	.05	hydrogen rich

In this context, "stoichiometric" implies any composition point on the line connecting pure water and pure methane. These mixtures have an  $\text{H}_2/\text{CO}$  ratio of 3.0 and contain either excess water or methane. Thus, they are stoichiometric with respect to hydrogen and carbon monoxide according to reaction 1. Points falling below the line are deficient in hydrogen, and points above the line are hydrogen rich.

In Figure X-A and B, the heating value and methane concentration decrease as a function of temperature for all four starting compositions. Conversely, the hydrogen and carbon monoxide concentrations increase, as seen on Figures X-C and D. The  $\text{CO}$  leakage is about the same for the two stoichiometric points, but is considerably larger for the hydrogen deficient starting composition.

Figure XI shows the effect of pressure on higher heating value and equilibrium composition for the same four starting compositions indicated on Figure X, all for a temperature of  $700^\circ\text{K}$ . Generally, the effect of pressure decreases as the pressure increases, most of the change occurring in the region up to 200 atm. For all of the compositions, as well as the higher heating values, the curves for two stoichiometric and for the hydrogen deficient starting points are similar. A difference is noted for the starting composition which is hydrogen rich. This is more apparent on Figure XI because it is plotted on a larger scale than on Figure X.

#### General Discussion

Various schemes have been proposed in the literature for carrying out the methane synthesis reaction, some of which are in use (6, 12, 13, 14).

A major engineering problem is removing the large amount of heat generated during the synthesis and numerous ways of doing this have been considered. The reactor temperature may be controlled by recycling product gas, with or without the water being condensed, or by otherwise diluting the reacting mixture with an excess of any of the products or reactants. This effectively changes the overall mixture composition. In addition, the fresh feed composition is widely variable depending upon the source of the feed gas. However, the charts presented here are applicable to a gas of any composition and allow one to see immediately if the possibility of carbon deposition exists for any given temperature within the range of interest. On Figure V for example, it indicates that it is not possible to approach pure  $\text{CH}_4$  at a high temperature without depositing carbon, and in fact, that a catalyst with a high temperature capability is not universally useful, but depends on the starting composition of the mixture. In any event, the final stage of the reaction to approach pure  $\text{CH}_4$  must be carried out at a low temperature.

References

- (1) Joint Army-Navy-Air Force Thermochemical Table, 2nd Ed., June 1971.
- (2) Rossini, F. D., et.al., "Selected Values of Properties of Hydrocarbons, Nat. Bur. Standards, Circular C461, 1947.
- (3) Dent, J. F., Moignard, L. A., Blackbraun, W. H., Herbden, D., "An Investigation into the Catalytic Synthesis of Methane by Town Gas Manufacture", 49th Report of the Joint Research Committee of the Gas Research Board and the University of Leeds, GRB20, 1945.
- (4) Pursley, J. A., R. R. White and C. Sliepceovich, Chem. Eng. Prog. Symposium Series, Vol. 48, No. 4, Reaction Kinetics, pp. 51-58, 1958.
- (5) Lunde, P. J. and F. L. Kester, Ind. Eng. Chem., Proc. Des. Develop., 13, No. 1, 1974.
- (6) Mills, G. A. and F. W. Steffgen, Catalysis Reviews, 8, No. 2, 159-210 (1973).
- (7) Greyson, M., in Catalysis, (P. H. Emmet, Ed.), 4, Chapter 6, 1956, Reinhold, N. Y.
- (8) Lee, A. L., H. L. Feldkirchner and D. G. Tajbl, "Methanation of Coal Hydrogasification", ACS Div. Fuel Chem. Preprints, 14, No. 4, Part I, 126-142, September, 1970.
- (9) Wen, C. Y., P. W. Chen, K. Kato and A. F. Galli, "Optimization of Fixed Bed Methanation Processes", ACS Div. Fuel Chemistry Preprints, 14, No. 3, 104-163, September, 1970.
- (10) Forney, A. J. and J. P. McGee, "The Synthane Process", Fourth AGA Pipeline Gas Symposium, Chicago, 1972.
- (11) McClahahan, D. N., Oil & Gas Journal, Feb. 20, 1967, pp. 84-90.
- (12) Greyson, M., et.al., U. S. Bureau of Mines, Rept. of Invest., 6609 (1965).
- (13) Forney, A. J. and W. P. Haynes, "The Synthane Coal to Gas Process: A Progress Report", ACS Div. Fuel Chem. Preprints, September, 1971.
- (14) Schoubye, P. J., Catalysis, 18, (1), 118 (1970).

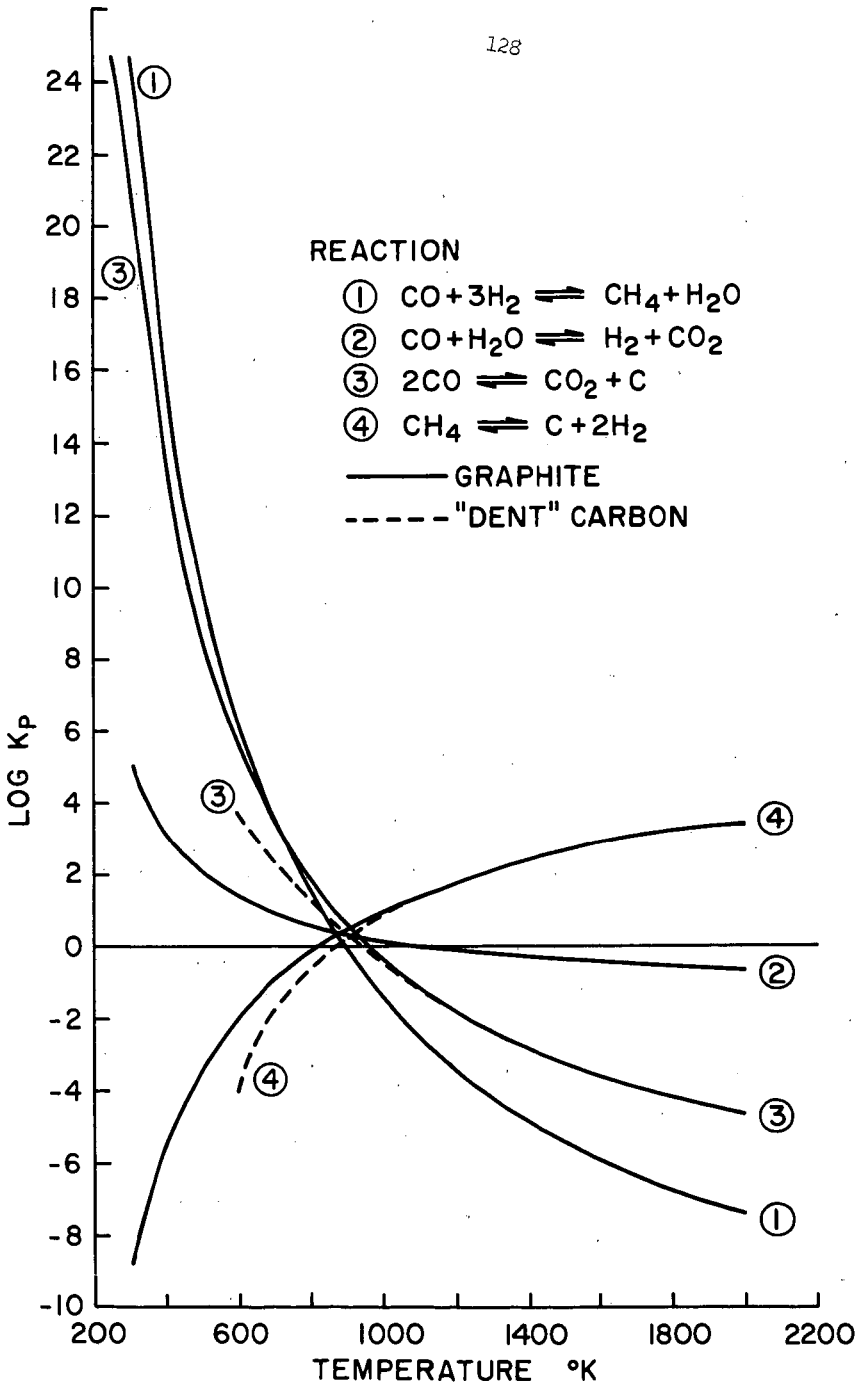


FIGURE I - EQUILIBRIUM CONSTANTS  
AS A FUNCTION OF  
TEMPERATURE

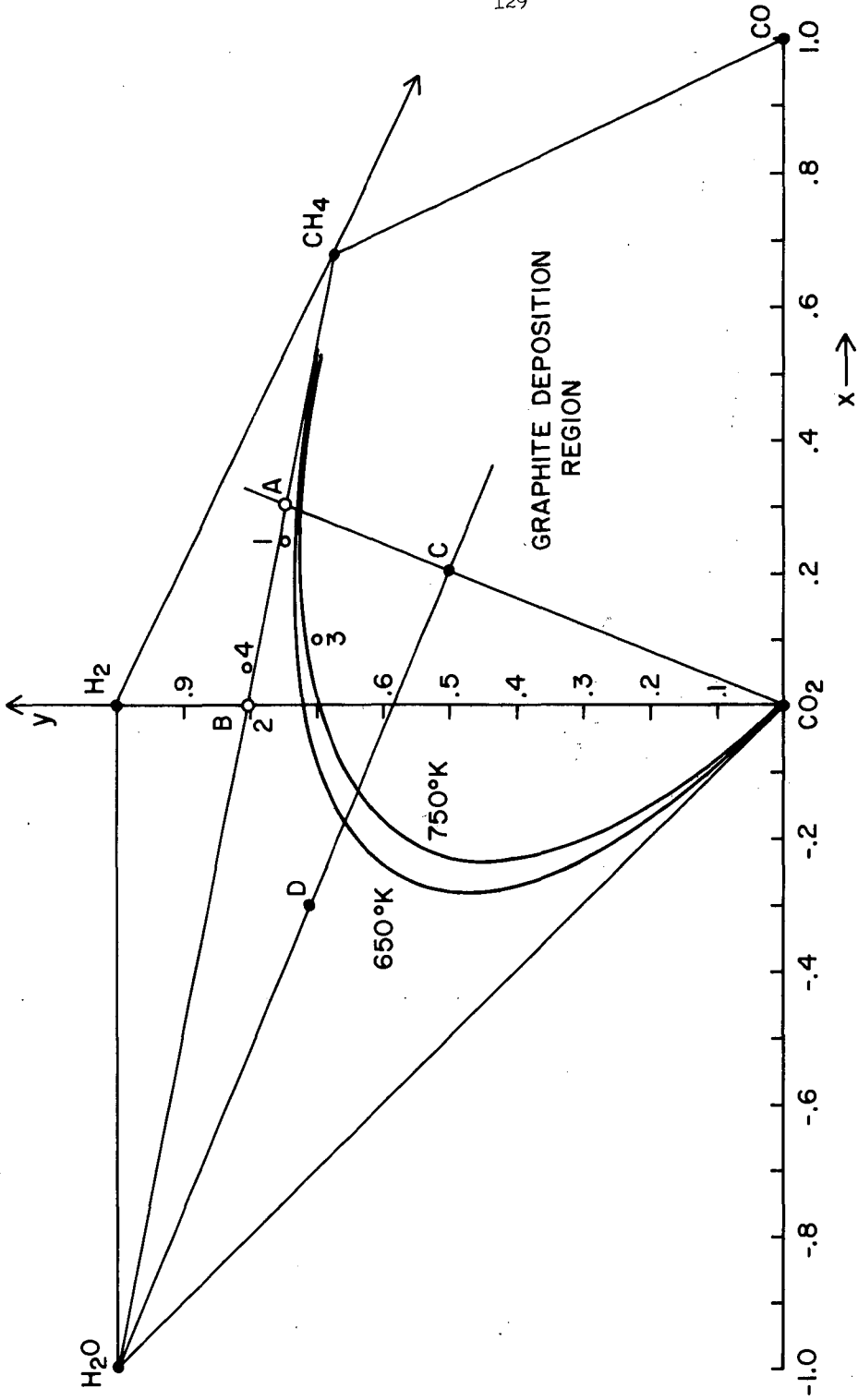


FIGURE II - GRAPHITE DEPOSITION AS A FUNCTION OF COMPOSITION AND TEMPERATURE 30 ATM

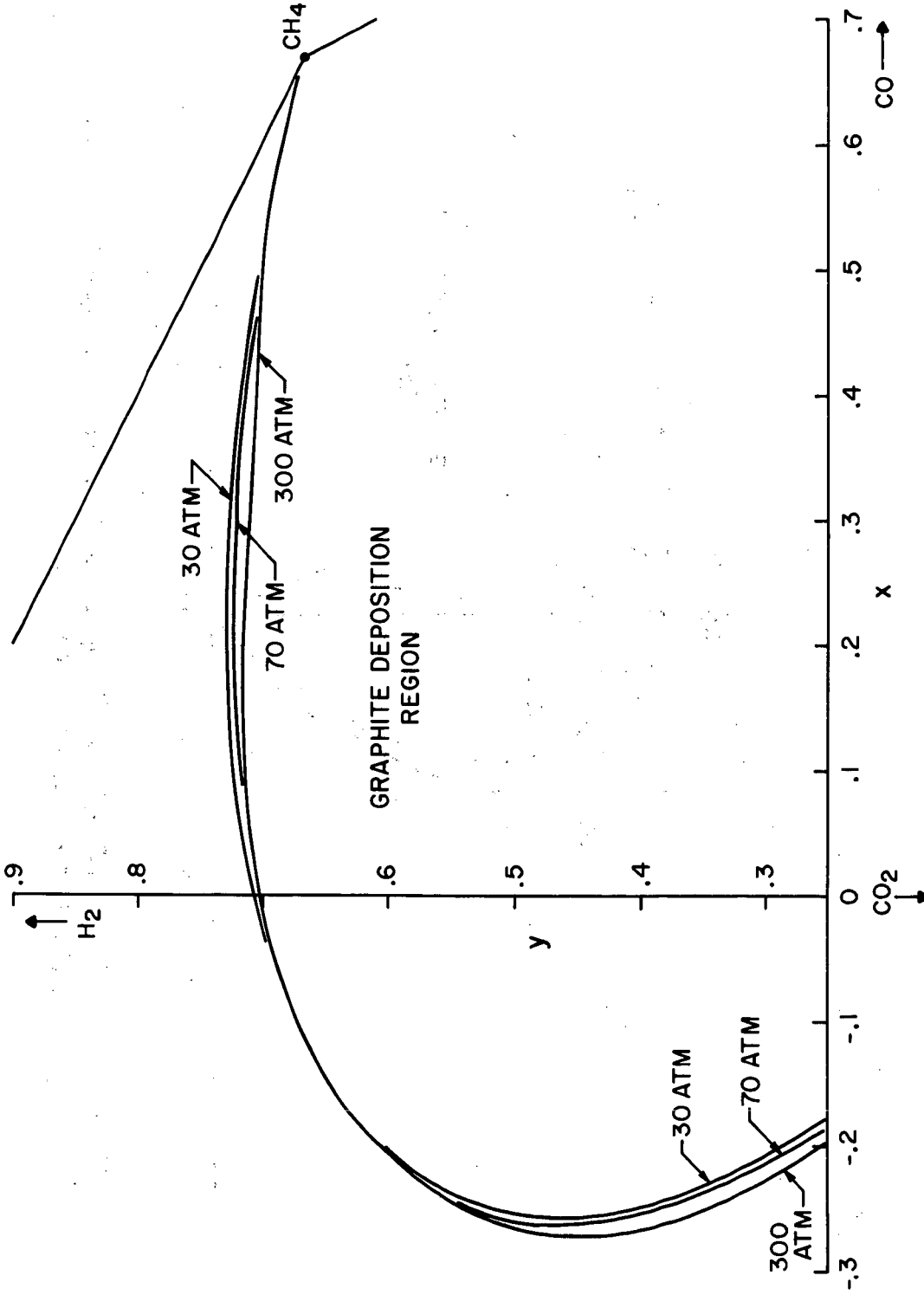


FIGURE III - EFFECT OF PRESSURE & COMPOSITION ON GRAPHITE DEPOSITION 700°K

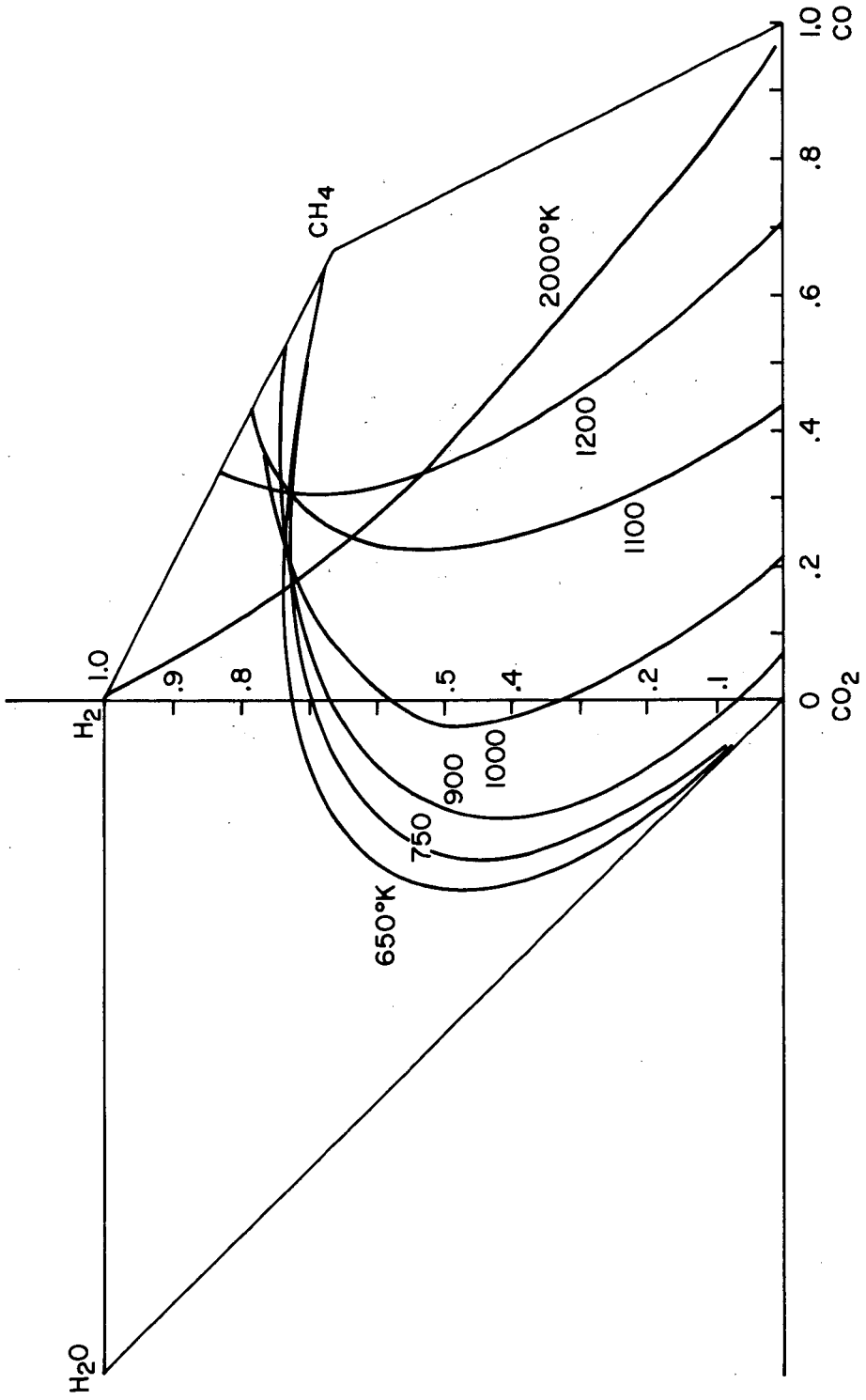


FIGURE IV - GRAPHITE DEPOSITION AT 30 ATM 650°K-2000°K

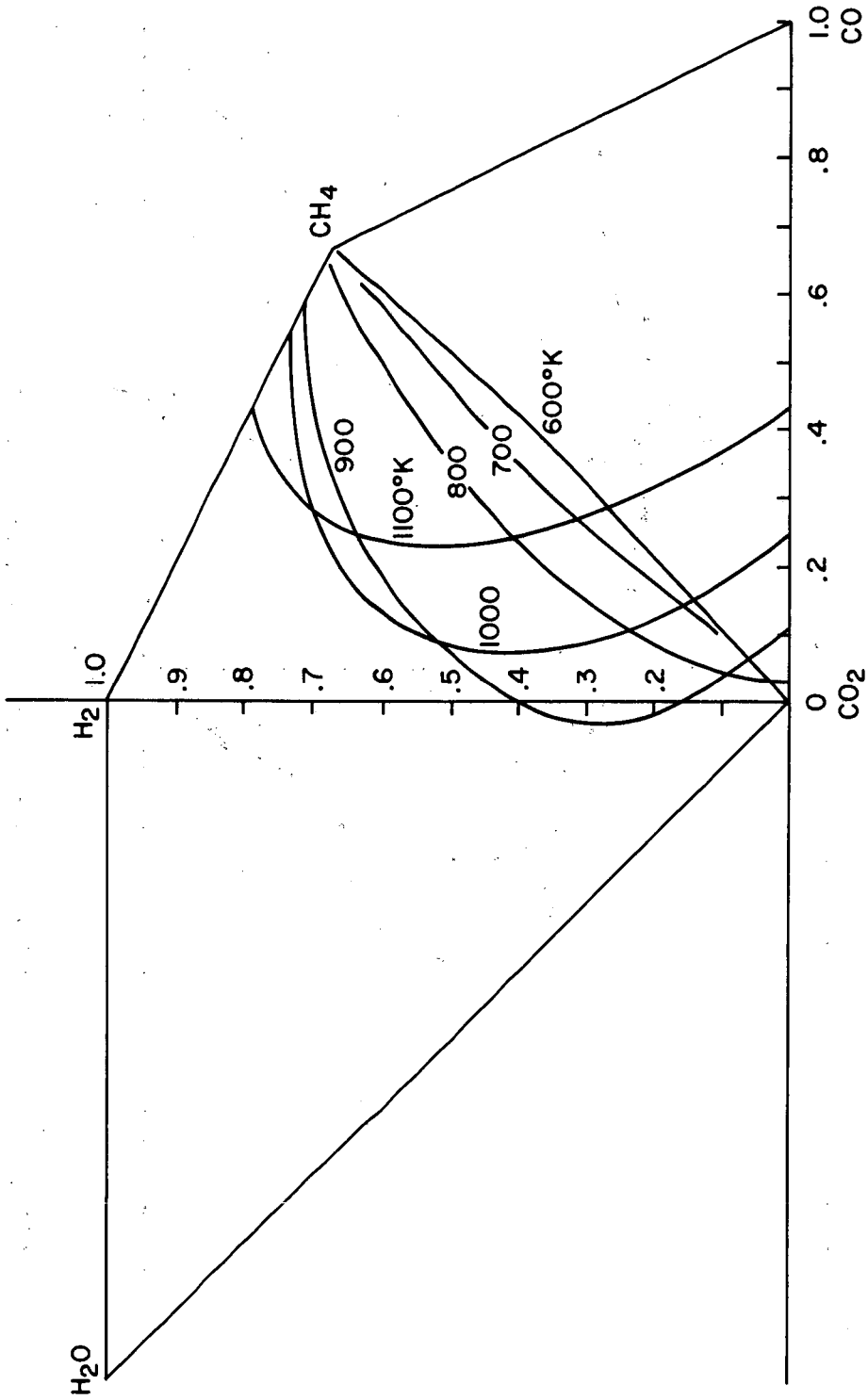


FIGURE V - DEPOSITION OF "DENT" CARBON 30 ATM

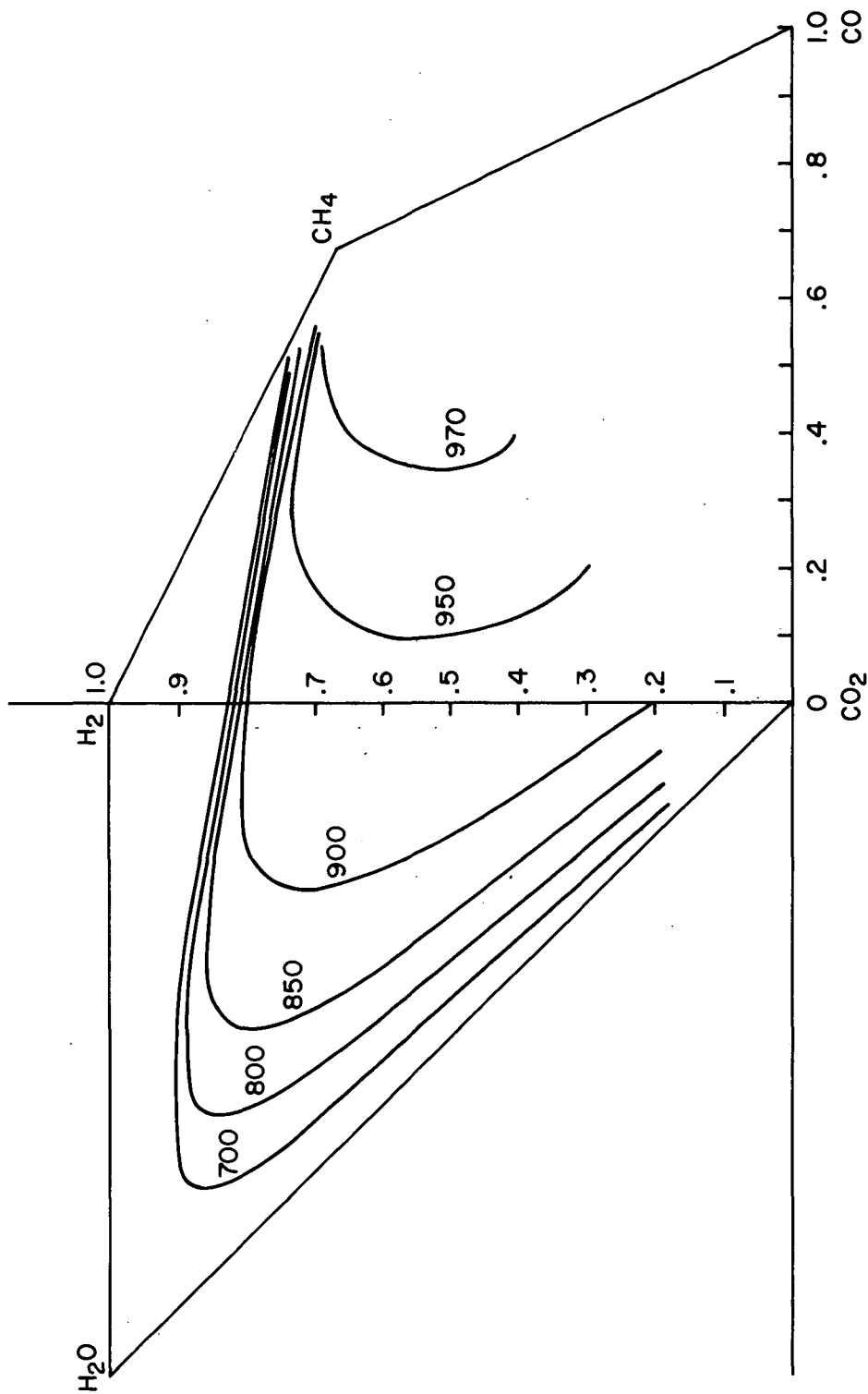


FIGURE VI - HIGHER HEATING VALUE OF  $\text{CO}_2$ ,  $\text{H}_2\text{O}$  FREE EQUILIBRIUM MIXTURES AS A FUNCTION OF STARTING COMPOSITION  
50 ATM, 700°K

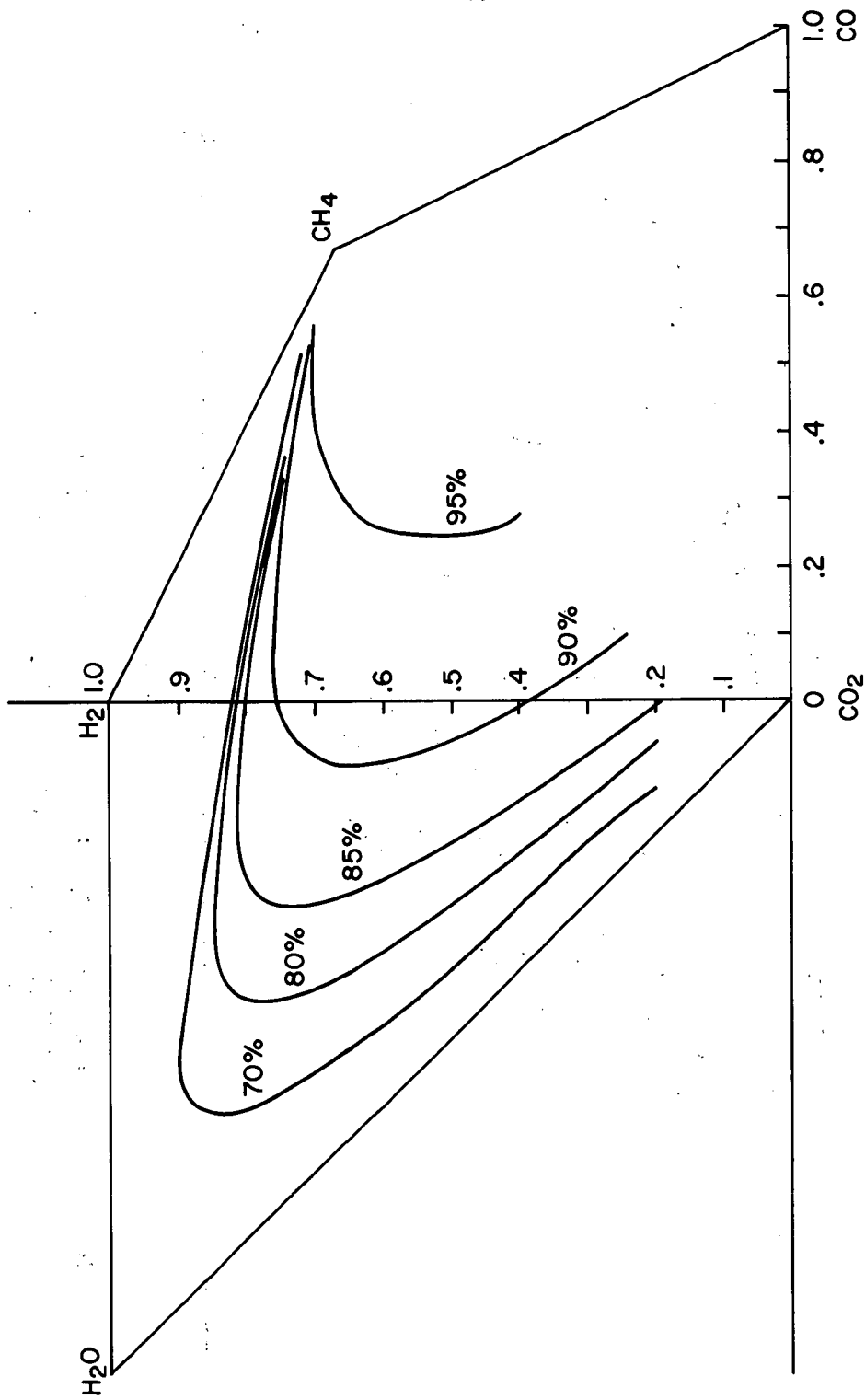


FIGURE VII - CH<sub>4</sub> CONCENTRATION OF EQUILIBRIUM MIXTURES  
50 ATM, 700°K

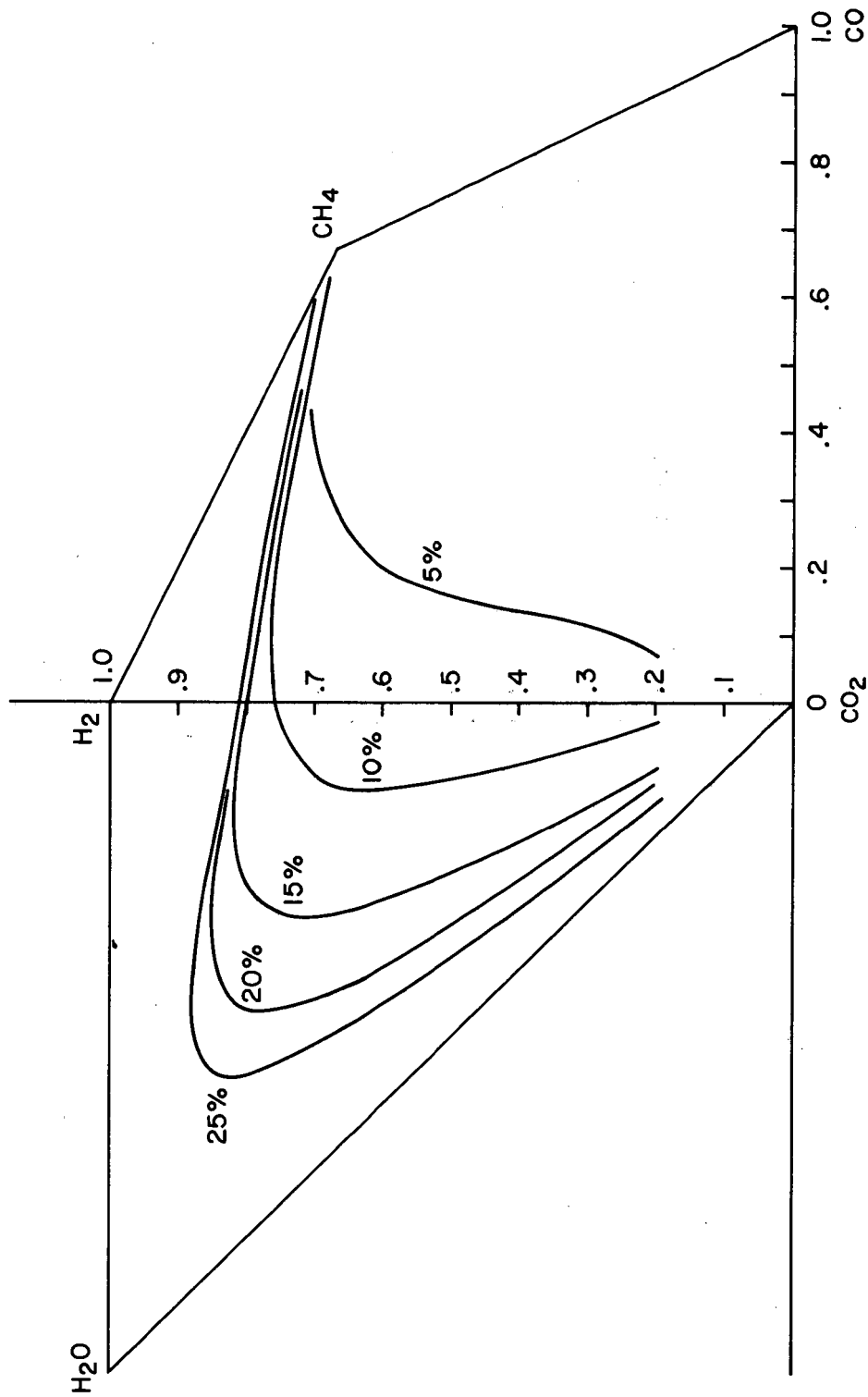


FIGURE VIII -  $H_2$  CONCENTRATION OF EQUILIBRIUM MIXTURES  
 $H_2O$  &  $CO_2$  FREE 50ATM, 700°K

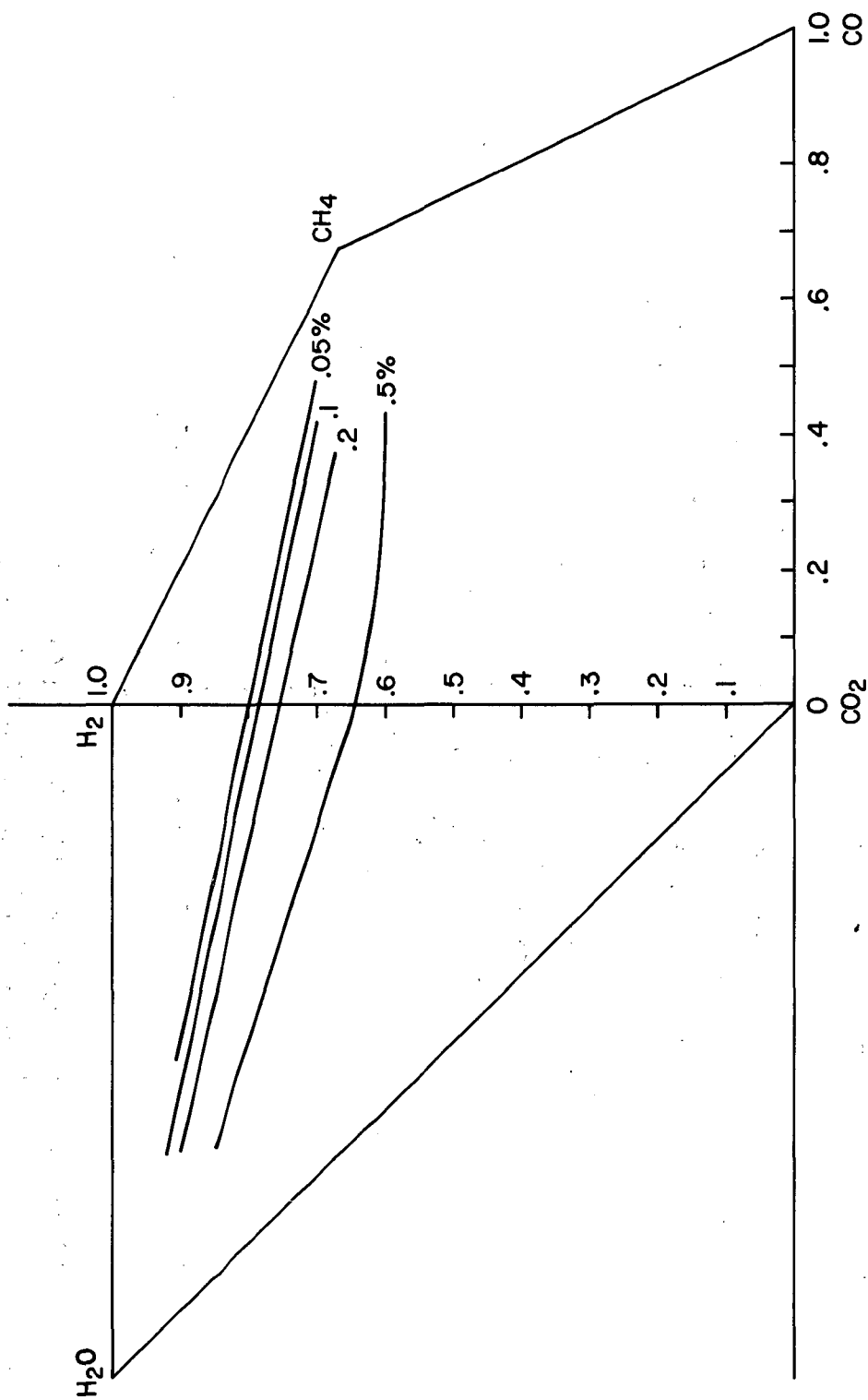


FIGURE IX - EQUILIBRIUM CO CONCENTRATION H<sub>2</sub>O & CO<sub>2</sub> FREE  
50 ATM, 700°K

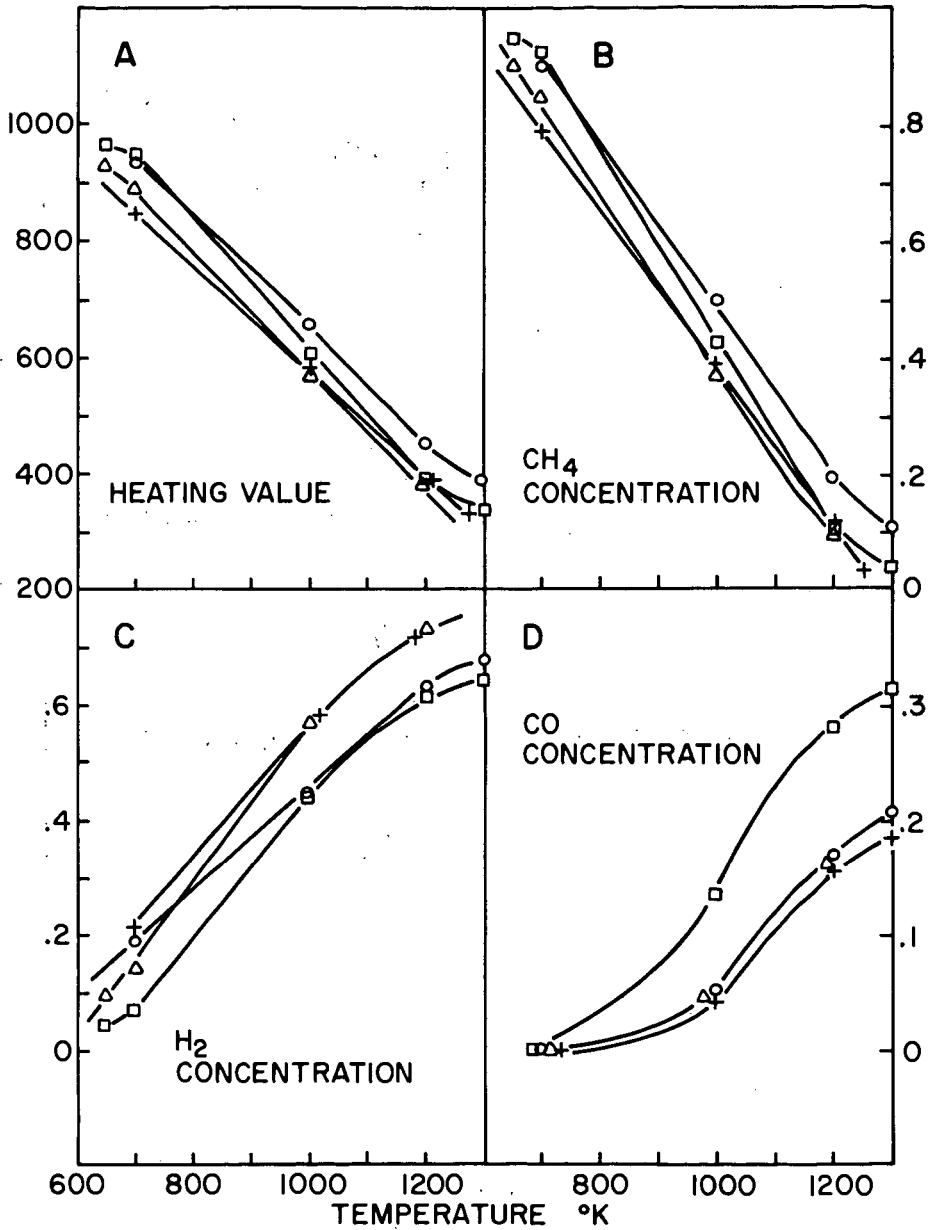


FIGURE X-EFFECT OF TEMPERATURE ON CONCENTRATION AT 50 ATM

	y	x
○	.75	.25
△	.8	0
□	.7	.1
+	.8	.05

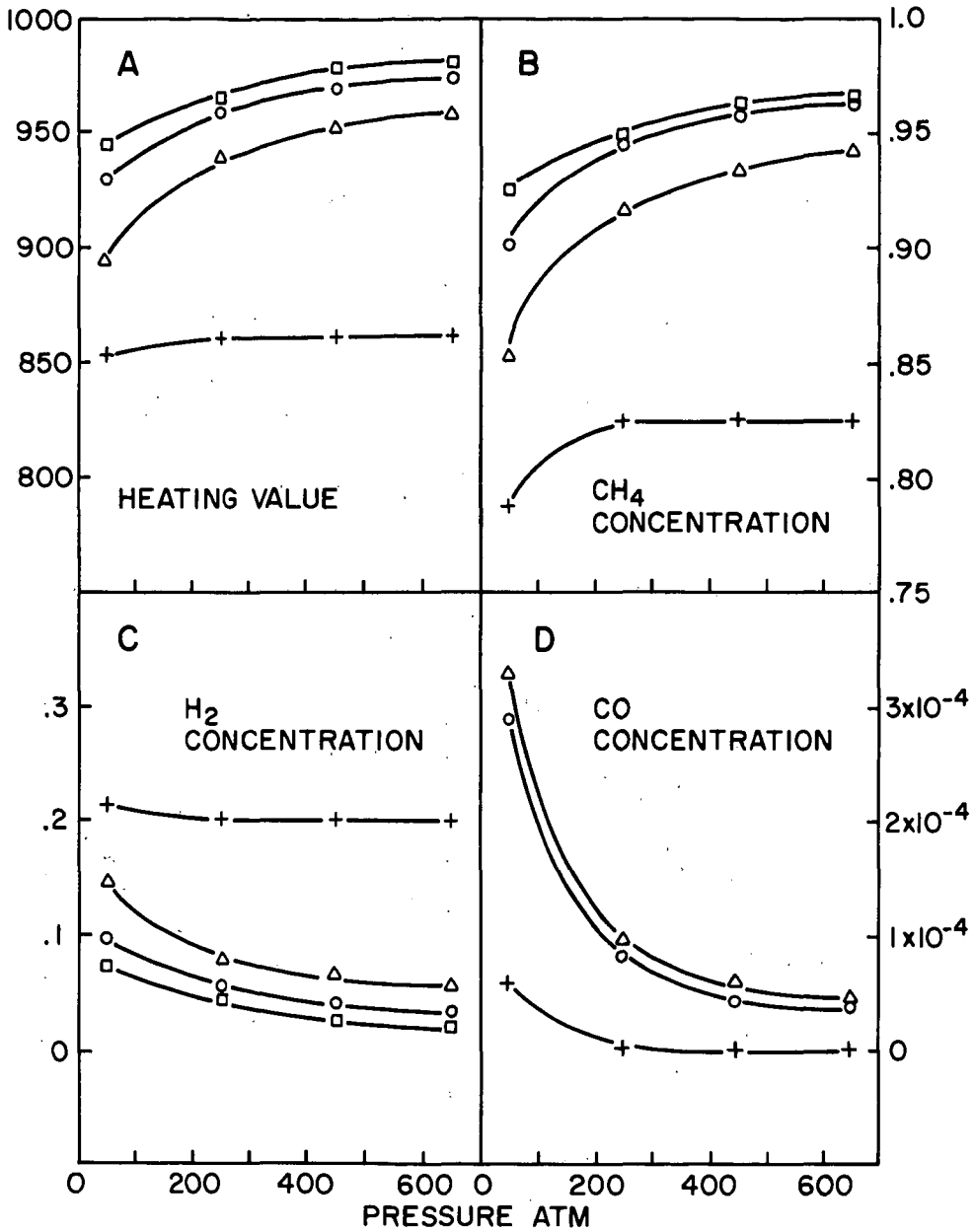


FIGURE XI-EFFECT OF PRESSURE ON CONCENTRATION AT 700°K

	y	x
o	.75	.25
Δ	.8	0
□	.7	.1
+	.8	.05

**MECHANISM OF THE METHANATION REACTION,**

B. R. Franko-Filipasic, FMC Corporation and L. Seglin Bechtel Associates  
Professional Corporation, 485 Lexington Avenue, New York, N. Y. 10017

Various mechanisms proposed for the methanation reaction are discussed, analyzed, and critiqued. Methods for testing the validity of these mechanisms are proposed, and examples are given.